ISSN 0915-6364

NATIONAL INSTITUTE FOR FUSION SCIENCE

Dielectronic Recombination of Be-like Fe Ion

K. Moribayashi and T. Kato

(Received - Jan. 16, 1996)

NIFS-DATA-36 Apr. 1996

RESEARCH REPORT
NIFS-DATA Series

NAGOYA, JAPAN

Dielectronic recombination of Be-like Fe ion

Kengo Moribayashi and Takako Kato

National Institute for Fusion Science, Chikusaku Nagoya 464, Japan

Abstract

Energy level(E), radiative transition probability(Ar), and autoionization rate(Aa) for Be-like Fe^{22+} ion are calculated with use of Cowan's code. Using these atomic data, the dielectronic recombination rate coefficient(α) to the excited states and the intensity factor(Qd) of the dielectronic satellite lines have been calculated. The doubly excited states $1s^2 3lnl'$ as well as the $1s^2 2pnl$ of Fe^{22+} ion are considered. The results are given in tables and figures. The n- and l-dependence for Ar, Aa, and α is studied. With use of it, Aa and Ar at large n are extrapolated. The dielectronic recombination processes from the $1s^2 2pnl$ and those from the $1s^2 3lnl'$ dominate at low and at high temperature, respectively. The qualitative different behaviors for E, Ar, and α between Be-like ions and He-like ions are discussed with use of atomic nuclear charge scaling.

Keywords

dielectronic recombination rate coefficient, Beryllium-like ion, Fe XXIII ion, energy level, radiative transition probability, autoionization rate, atomic nuclear charge scaling, autoionzation state, Cowan's code, dielectronic satellite spectra

1. Introduction

The dielectronic recombination(DR) process plays an important role in high temperature plasma such as tokamak plasma and solar corona[1, 2]. The process is composed by the two step transitions, the dielectronic capture and the radiative decay,

$$A^{z}(i_0) + e^- \rightarrow A^{(z-1)**}(i) \rightarrow A^{(z-1)*}(f) + h\nu. \qquad (1)$$

Here $A^{(z-1)**}$ expresses the autoionization state of $A^{(z-1)}$ ions. Dielectronic recombination rate coefficient(α) from the initial state (i_0) to the final state (f) in Eq.(1), which provides us the population of the excited states, is represented by

$$\alpha(i_0, f) = \frac{C(T_e)}{g_0} \sum_i \frac{g(i)Aa(i, i_0)Ar(i \rightarrow f)}{\sum\limits_{all\ i_0'} Aa(i, i_0') + \sum\limits_{all\ f'} Ar(i \rightarrow f')} \exp(-\frac{\Delta E_i}{kT_e}) \qquad (2)$$

with

$$C(T_e) = \frac{1}{2}(\frac{h^2}{2\pi mkT_e})^{3/2}. \qquad (3)$$

Here Ar, Aa, T_e, g_0 and ΔE_i represent radiative transition probability, autoionization rate, electron temperature, statistical weight of the initial state (i_0), and the energy difference between the autoionization state (i) and the initial state (i_0), respectively. Therefore in order to estimate α, the atomic data such as the energy levels, Ar and Aa are required.

The Ar and Aa values are also useful for understanding double-electron charge transfer processes by ion-atom collision as well as the DR processes. Recently the double-electron charge transfer processes between I^{10+} ion and multi-electron atoms (A) such as Ne, Ar, Kr, Xe were measured[3, 4, 5]. The following process,

$$I^{10+} + A \rightarrow I^{8+**} + A^{+2} \rightarrow I^{8+*} + A^{+2} + h\nu, \qquad (4)$$

is similar to the DR process as in Eq.(1). The second step is the radiative transition process, which is the same as that in the DR process.

The spectral lines of L-shell ions have been often measured (eg.[6, 7]) and the dielectronic recombination of the Fe^{22+} ion have been often studied[8-11]. However, as long as we know, there are few papers which give us enough data of the dielectronic recombination rate coefficient to each final bound state. These data are necessary to estimate the population of the excited states by a collisional radiative model[12]. Our purpose is to calculate the data for the dielectronic recombination to the excited states of Fe^{22+} ion.

We treat the $1s^2 3l_1 nl_2$ states, which are important for the DR process around the 1 keV temperature, as well as the $1s^2 2l_1 nl_2$ states. Here $l_1(l_2)$ expresses the angular momentum of inner (outer) electron. The calculations are executed with the use of Cowan's code[13, 14] in which configuration interaction(CI) method is employed. Full number of configurations must be considered for small principal quantum number n. However, as the value of n increases, the number of configuration can be restricted because electron correlation becomes weaker. After we test the convergence of Ar and Aa for the number of the states, we selected the configurations necessary for the calculation. We calculated the Ar and Aa values up to n =20. Further extrapolation is used for n >20.

The aims of this paper are (i) to estimate α for each final state as well as the intensity of the dielectronic satellite spectra, and (ii) to understand the atomic nuclear charge dependence as will be mentioned in Sec.2 for Ar, Aa, and α.

2. Atomic nuclear charge scaling for radiative transition probability and autoionization rate

In this section, we describe Z-scaling for Ar and Aa values following the discussion in Ref.[15], where Z represents the atomic effective nuclear charge of ions, in order to understand the behavior of Fe^{22+} ion and the phenomena of the dielectronic recombination more clearly. The Z value is the quantity removed the number of the inner electrons from the real atomic nuclear charge. For example, in the case of $1s^2 2pnl$ state in Fe^{22+} ion, it is 24 for the $2p$ electron and 23 for the nl electron, respectively.

Ar for the process from state A to state B is given by

$$Ar = N\sigma^3 S. \tag{5}$$

Here N and σ are the normalization constant and the energy difference between the states A and B, respectively and S is the line-strength given by

$$S = | < \psi_B | \vec{r} | \psi_A > |^2, \tag{6}$$

where $\psi_{A(B)}$ is the wave function of the state A(B). The Z value of Fe^{22+} ion is so large that the independent particle model is suitable for them in discussing qualitatively. Firstly S decreases according to Z^{-2} because the atomic radius $< r > \propto Z^{-1}$. On the other hand, in order to estimate the Z-scaling for σ, Z-expansion method[16] is useful. With the use of this method, the energy for large Z can be written as

$$E \cong Z^2(E_0 + E_1/Z), \tag{7}$$

because second and over order expansion can be neglected for large Z. Here $E_{0(1)}$ is the 0(1)-th expansion coefficient. The E_0 values are the same for the state A and the state B in the case when the principal quantum numbers n are the same between the states A and B. Therefore σ can be approximated by

$$\begin{aligned} \sigma &\propto Z^2 \qquad \text{for} \quad \Delta n \neq 0 \\ \sigma &\propto Z \qquad \text{for} \quad \Delta n = 0, \end{aligned} \tag{8}$$

where Δn expresses the difference between the principal quantum number of the transition electron in the state A and that in the state B. From Eqs.(5) and (8), Ar can be given by

$$\begin{aligned} Ar &\propto Z^4 \qquad \text{for} \quad \Delta n \neq 0 \\ Ar &\propto Z \qquad \text{for} \quad \Delta n = 0. \end{aligned} \tag{9}$$

Then, Aa is given by

$$Aa \sim \frac{2\pi}{\hbar} | < \Psi_{j_1} \Psi_{j_2} | \frac{1}{r_{12}} | \Psi_{j_3} \Psi_i > |^2, \tag{10}$$

where the states j and i express discrete and continuum states, respectively and r_{12} is the distance between two electrons. In Cowan's code[13, 14], a free electron state is assumed to be separable from the bound state. Then the wave function of a free electron, which is of the same form as that for a bound electron, is given by

$$\Psi_{i,\epsilon l m_l m_s}(\vec{r}) = \frac{1}{r} P_{\epsilon l}(r) Y_{l m_l}(\theta, \phi) \Sigma_{m_s}(s_z). \tag{11}$$

with

$$P_{\epsilon l} \sim (\frac{2}{\pi p_c})^{1/2} \frac{1}{r} \sin(p_c r + \delta(r)). \tag{12}$$

Here p_c equals to $\epsilon^{1/2}$ where ϵ is the free electron energy. That is, p_c increases according to

$$\begin{aligned} p_c &\propto Z \qquad \text{for} \quad \Delta n_c \neq 0 \\ p_c &\propto Z^{1/2} \qquad \text{for} \quad \Delta n_c = 0. \end{aligned} \tag{13}$$

Namely,

$$\begin{aligned} \Psi_i &\propto Z^{1/2} \qquad \text{for} \quad \Delta n_c \neq 0 \\ \Psi_i &\propto Z^{3/4} \qquad \text{for} \quad \Delta n_c = 0 \end{aligned} \tag{14}$$

because $< r^{-1} > \propto Z$. Then Ψ_j and $< r_{12}^{-1} >$ increase according to $Z^{3/2}$ and Z, respectively and $dr_1^3 dr_2^3$ decreases according to Z^{-6}. Therefore Aa becomes

$$\begin{aligned} Aa &\propto Z^0 \qquad \text{for} \quad \Delta n_c \neq 0 \\ Aa &\propto Z^{1/2} \qquad \text{for} \quad \Delta n_c = 0. \end{aligned} \tag{15}$$

Here Δn_c expresses the difference of the principal quantum number between the states j_1 and j_3. After all it is found that the Z-dependence for Aa is weaker than that for Ar.

3.Atomic data :Energy level, radiative transition probability, and autoionization rate

We investigate the following dielectronic recombination process of Fe^{22+} ion,

$$\mathrm{Fe}^{23+}(1s^2 2s) + e^- \rightarrow \mathrm{Fe}^{22+**}(1s^2 2pnl, 1s^2 3l_1 nl_2) \rightarrow \mathrm{Fe}^{22+*} + h\nu. \tag{16}$$

In this section, we present the atomic data of Aa and Ar calculated with use of Cowan's code[13, 14]. We use the extrapolation formula of Ar and Aa for $n > 20$ based on n-dependence for Ar and Aa in order to save the CPU time and memory. It is noticed that the autoionization states at large n contribute to the dielectronic recombination significantly at high temperature plasma.

Table I lists the energy levels and weighted transition probabilities summed over all the final states($\sum gAr$) for the $1s^22snl$ and $1s^22pnl$ ($n = 2 \sim 5$) states of Fe^{22+} ion. Here g is the statistical weight of the upper state. The energy levels given by Shirai et.al.[17] are also listed. For $n = 2$ and 3, the differences between the present energy level and the others are less than 5%. On the other hand, for $n = 4$ and 5, the agreement becomes better, that is, the errors are less than 1%. In our table, the two states with the same designation exist, for example, $2p3d\ ^3P_2$ ($^3D_2$). This is because the $2p3d\ ^3P_2$ state mixes with $2p3d\ ^3D_2$ one strongly. Therefore this level can be named as $2p3d\ ^3D_2$ as well.

Table II lists Aa and Ar values for $n = 11$, 13, and 20 levels. The ionization energy from the ground state $1s^22s^2$ of Fe^{22+} ion is about 15730000 cm^{-1} (1950eV). The autoionization takes place only when the energy for the doubly excited states is above the threshold energy. For the $1s^22pnl$ ($n < 11$) states, the energies are less than that of the threshold. Therefore, $1s^22pnl$ ($n < 11$) states are not autoionization states although these states are the doubly excited states. The energy difference between the threshold $1s^22s$ and the $1s^22snl$ states increases according to Z^2 because the threshold corresponds to the $1s^22snl$ ($n \to \infty$). On the other hand, the energy difference between the $1s^22snl$ and $1s^22pnl$ is proportional to Z as mentioned in Eq.(8) in Sec.2. Therefore, the $\Delta E/I_p$ value for $1s^22pnl$ becomes smaller as Z increases where I_p is the ionization potential of $1s^22s^2$. Consequently for the ions with larger Z, the $1s^22pnl$ state at the larger n values locates below the threshold. It should be noted that this feature is not seen in He-like and Li-like ions since there is no Δn=0 transition. In these ions, the threshold corresponds to the $1s$ or $1s^2$ states. Then, the transition for dielectronic recombination is only the $np \to 1s$, whose energy difference increases according to Z^2. Therefore, ΔE increases according to Z^2. In the doubly excited $1s^23l_1nl_2$ states, ΔE increases according to Z^2 because only the $3l_1 \to 2l'$ ($\Delta n \neq 0$) transition takes place.

For the $1s^22pnl$ ($n = 11$) states, as is seen in Table II, both autoionization states and bound states exist. This is due to the fact that the two thresholds, $1s^22p\ ^2P_{1/2}$ and $1s^22p\ ^2P_{3/2}$ exist. As n increases, the $1s^22pnl$ states reach either $1s^22p\ ^2P_{1/2}$ or $1s^22p\ ^2P_{3/2}$ state. The energy difference between them is about 130000cm^{-1}, which is almost the same as that between the autoionzation states and the bound states for $1s^22p11l$. From $n = 13$, all of the energies begin to be above the threshold, although the ΔE values are very small (60000 and 185000 cm^{-1}). At $n = 20$, the ΔE values become about 260000 cm^{-1} (32.2eV) and 385000 cm^{-1} (47.7 eV). Although they are far below the second threshold of $1s^22p$ states whose energy is 392000 cm^{-1} (48.6 eV) for $1s^22p\ ^2P_{1/2}$ state and 520000cm^{-1} (64.5 eV) for the $1s^22p\ ^2P_{3/2}$ state measured from the $1s^22s$ state.

Table III lists Ar from the $1s^22snl$ and $1s^22pnl$ ($n \leq 5$) to the $1s^22s^2$, $1s^22p^2$, and $1s^22s2p$ states. The Ar values given by Shirai et.al.[17] are also shown. Our results agree very well with them within 10 % except for a few transitions where n is small values, that is, n=2 or 3. In the table, the radiative transitions with large values take place mainly for the 4 cases, $\{\Delta J = \Delta L = \Delta l_1$ (or Δl_2)=1$\}$, $\{\Delta J = 0, \Delta L = \Delta l_1$ (or Δl_2)=1$\}$, $\{\Delta L = 0, \Delta J = \Delta l_1$ (or Δl_2)=1$\}$, and $\{\Delta J = \Delta L = 0, \Delta l_1$ (or Δl_2)=1$\}$. Here ΔX expresses the difference of X values between the lower state and upper states. For the 4 cases, ΔX=-1 dose not exist. The plus sign and 0 of ΔX mean that the X value of upper state is larger than or equals to that of the lower state.

Figs.1 show gAr from the $1s^22pnl$ of Fe^{22+} ion as a function of n. Here the Ar values are given by

$$gAr = \sum_{S'L'J'} \sum_{SLJ} (2J+1) Ar(1s^22pnl\ ^{2S+1}L_J \rightarrow 1s^22l''n'l'\ ^{2S'+1}L'_{J'}). \qquad (17)$$

The Ar values for the transition from $1s^22pnl$ to the low excited states such as $1s^22p2p$, $1s^22p3p$, are more than or comparable to those for the $1s^22pnl \rightarrow 1s^22snl$ transitions even at $n = 20$. In the case of small Z such as C^{2+} ion, the latter is much larger than the former at $n = 20$[19]. This comes from the fact that the former and the latter increase according to Z^4 and Z as mentioned in Eq.(9) in Sec.2, respectively. In the case of Fe^{22+} ion, we can use the following extrapolation for $n > 20$ because the Ar values for the $1s^22pnl \rightarrow 1s^22snl$ and those for the $1s^22pnl \rightarrow 1s^22pn'l'$ processes keep constant and decrease according to n^{-3} as n increases, respectively.

$$Ar(1s^22pnl\ ^SL_J \rightarrow 1s^22snl\ ^{S'}L'_{J'}) \cong Ar(1s^22p20l\ ^SL_J \rightarrow 1s^22s20l\ ^{S'}L'_{J'}) \qquad (18)$$

and

$$Ar(1s^22pnl\ ^SL_J \rightarrow 1s^22pn'l'\ ^{S'}L'_{J'}) \cong Ar(1s^22p20l\ ^SL_J \rightarrow 1s^22pn'l'\ ^{S'}L'_{J'}) \times (20/n)^3. \quad (19)$$

Fig.2 shows Aa values given by

$$Aa = \sum_{SLJ} Aa(1s^22pnl\ ^SL_J, i_0) \quad (20)$$

from the $1s^22pnl$ ($n \geq 13$) of Fe^{22+} as a function of n. As mentioned before, since the energies of the $1s^22pnl$ (n <13) are below the ionization threshold, Aa is plotted only for $n \geq 13$ in Fig.2. The Aa values for $n > 20$ are also estimated by scaling the values at n =20 as

$$Aa(1s^22pnl\ ^SL_J, i_0) \cong Aa(1s^22p20l\ ^SL_J, i_0) \times (20/n)^3 \quad (21)$$

because the Aa values are expected to decrease according to n^{-3}.

Figs.3 show the Ar values, the same form as in Fig.1 from the $1s^23l_1nl_2$ to the $1s^22l'_1n'l'_2$ state. Even for the small value of n, the Ar values for the transitions $1s^23snl \rightarrow 1s^22pnl$ (n <11), $1s^23pnl \rightarrow 1s^22snl$, and $1s^23dnl \rightarrow 1s^22pnl$ ($n < 11$) are much larger than those for the other transitions such as $1s^23pnl \rightarrow 1s^22l'3l''$. The Ar values for all the transitions from the $1s^23l_1nl_2$ state to the bound states increase according to Z^4 because of the $3l_1 \rightarrow 2l'_1$ transitions. As a result, these Ar values for the $1s^23l_1nl_2 \rightarrow 1s^22l'_1nl_2$, which keep constant for n, are much larger than those for the $1s^23l_1nl_2 \rightarrow 1s^22l'_1n'l'_2$ at large n.

Figs.4 show the Aa values of the $1s^23l_1nl_2$. For $1s^23l_1nl_2$ states, there are three autoionization processes to $1s^22s\epsilon l$, $1s^22p\epsilon l$, and $1s^23s\epsilon l$ where ϵl represents the free electron. However, since the energy for the $1s^23l_1nl_2$ at $n = 20$ is below the threshold $1s^23s$ state, the processes to the $1s^23s\epsilon l$ are ignored. The Aa value from the $1s^23snl$ to the $1s^22s$ is more than or comparable to that to the $1s^22p$. On the other hand, in the processes from the $1s^23pnl$ and $1s^23dnl$, the Aa values to $1s^22p$ are much larger than those to $1s^22s$. Since the Aa values are smaller in comparison with Ar for $1s^23l_1nl_2$ states for $n > 20$, the processes for $n > 20$ give little contribution to dielectronic recombination.

Fig.5 shows l-distribution of the Ar value for $1s^2 2pnl \rightarrow 1s^2 2l''n'l'$ given by

$$Ar = \sum_{n'l'l''} \sum_{S'L'J'} \sum_{SLJ} Ar(1s^2 2pnl\ ^S L_J \rightarrow 1s^2 2l''n'l'\ ^{S'} L'_{J'}). \quad (22)$$

for n=11, 13, 20. Each curve for n=11, 13, and 20 shows the similar features. Namely the Ar values have a peak at $l = 2$ and decrease gradually for large l ($l \geq 4$) values. The transitions $1s^2 2pnl \rightarrow 1s^2 2pn'l'$ give a main contribution to the dielectronic recombination at low temperature and the Ar values for these transitions decrease according to n^{-3}. The Ar values for the $1s^2 2pnl \rightarrow 1s^2 2snl$ keep constant for both l and n as is seen in Ref.[18, 19]. Fig.6 shows the Aa values given in Eq.(20) for n=15 and 20 as a function of l. We find a peak at $l = 1$ and a dip at l=3. For $l \geq 5$, the Aa values decrease rapidly. Since α is proportional to Aa in the case of $Ar \gg Aa$, we can neglect the contribution from large l ($l \geq$7) for high n states.

4. Dielectronic satellite spectra

The dielectronic satellite lines (e.g. $2snl - 3pnl$) of Be-like ions appear near the excitation lines (e.g. $2s - 3p$) of Li-like ions. Table IV shows wavelength (λ), radiative transition probabilities summed over all the final states ($\sum gAr$), autoionization rate (Aa), and the intensity factor (Qd) for the dielectronic satellite lines given by

$$Qd(i_0, i, f) = \frac{g(i)Aa(i, i_0)Ar(i \rightarrow 2l''n'l'\ ^{S'} L'_{J'})}{\sum_{all\ i'_0} Aa(i, i'_0) + \sum_{all\ f'} Ar(i \rightarrow f')}. \quad (23)$$

Here the $1s^2 2p11l$, $1s^2 2p13l$, $1s^2 3l_1 3l_2$, and $1s^2 3l_1 4l_2$ states are selected as autoionization states (i) and the λ values are taken from 6 to 1000Å. From this table, we found that the Qd values become large in the same case where the radiative transitions with large value take place, that is, $\{\Delta J = \Delta L = \Delta l_1$ (or Δl_2)=1$\}$, $\{\Delta J = 0,\ \Delta L = \Delta l_1$ (or Δl_2)=1$\}$, $\{\Delta L = 0,\ \Delta J = \Delta l_1$ (or Δl_2)=1$\}$, and $\{\Delta J = \Delta L = 0,\ \Delta l_1$ (or Δl_2)=1$\}$ as listed in Table III in Sec.3. The Qd values in the case of Fe^{22+} ion are much larger than those in C^{2+} ion[18]. The Qd values in the C^{2+} ion are less than 10^{11}(1/s), on the other hand, those in the Fe^{22+} ion reach a maximum value of 10^{13}(1/s). This means that the dielectronic satellite spectra is more important in the Fe^{22+} ion. In particular, the Qd values from the

$3l-2l'$ transitions around $11\AA$ are larger.

With use of the Qd values, roughly speaking, satellite spectral intensity for the transition can be estimated as the order of 10^{-12}cm^3/s at T_e=300eV and that of 10^{-13}cm^3/s at T_e=1keV, respectively. On the other hand, the excitation rate coefficient of $2s$-$3d$ and $2s$-$3p$ lines in Li-like Fe^{23+} ion which provide us to estimate the line intensity are about 10^{-13} cm^3/s and 10^{-11} cm^3/s at T_e=300eV and 1keV, respectively[20]. Then the excitation rate coefficients of $2s$-$3l$ lines in Be-like Fe^{22+} ion are also about 10^{-13} cm^3/s and 10^{-11} cm^3/s at T_e=300eV and 1keV, respectively[12]. Namely the dielectronic satellite spectra is important at only the low temperature below T_e=300 eV.

5. Dielectronic recombination rate coefficient to the excited states

The DR rate coefficient given in Eq.(2) is important to estimate the population densities of the excited states through the dielectronic recombination processes. We summed up the transitions $i \rightarrow f$ in Eq.(2) for the autoionizing states i $(1s^2n_1l_1n_2l_2\ ^{2S+1}L_J)$. With the use of the numerical value $C(T_e) = 3.3 \times 10^{-24}(I_H/T_e)^{3/2}$ and $g_0 = 2$ in Eq.(2), we obtain the DR rate coefficient to the excited state $1s^22l_1'n'l_2'$ as

$$\alpha_d(1s^22s, 1s^22l_1'n'l_2'\ ^{2S'+1}L'_{J'}) = \frac{3.3\times 10^{-24}}{2}\left(\frac{I_H}{T_e}\right)^{3/2}\sum_{n_1}\sum_{n_2}\sum_{l_2}\sum_{l_1LSJ}$$
$$Q_d(1s^22s, 1s^2n_1l_1n_2l_2\ ^{2S+1}L_J, 1s^22l_1'n'l_2'\ ^{2S'+1}L'_{J'})\exp\left(-\frac{\Delta E_i}{kT_e}\right) \quad (24)$$

where I_H is the ionization potential of a hydrogen atom and n_1 (n_2) is the principal quantum number of the inner (outer) electron.

For the ΔE_n value of $1s^22pnl$ for n >20, the following extrapolation equation is used,

$$\Delta E_n = \Delta E_\infty - \frac{a}{n^2}, \quad (25)$$

with

$$a = 20^2 \times (\Delta E_\infty - \Delta E_{20}) \quad (26)$$

because the energy at $n = 20$ is far from the threshold. Here ΔE_∞ (=48.6 or 64.5 eV) and ΔE_{20} (=32.2 or 47.7 eV) represent the ΔE_i value of the threshold $1s^22p$ and that at the $1s^22p20l$ states, respectively. The detailed explanation about ΔE was done in Sec.3.

In order to obtain the values α_d to the excited state $1s^22l'_1n'l'_2$, two kind of transitions, $1s^22pnl \rightarrow 1s^22l'_1n'l'_2$ and $1s^23l_1nl_2 \rightarrow 1s^22l'_1nl_2$ are taken into account in our calculation. For the $1s^22pnl \rightarrow 1s^22l'_1n'l'_2$ transition, the sum in Eq.(24) up to n=11-500, l=0-8 and for the $1s^23l_1nl_2 \rightarrow 1s^22l'_1n'l'_2$ transition, the sum up to n =3-20, l =0-5 are taken, respectively. The α_d values for each excited state are given in Table V.

6. Total dielectronic recombination rate coefficients

The total DR rate coefficient is obtained by the sum of all the levels,

$$\alpha_d^t = \sum_{n'=2}^{20} \alpha_{n'} + \sum_{n'=21}^{500} \alpha_{n'}, \tag{27}$$

where

$$\alpha_{n'} = \sum_{l'_1 l'_2} \sum_{S'L'J'} \alpha_d(1s^22s, 1s^22l'_1l'_2 \ {}^{2S'+1}L'_{J'}). \tag{28}$$

The second term in the right hand side of Eq.(27) is calculated by extrapolation as discussed in Sec.3 using the values at n =20.

In Fig.7, the total dielectronic recombination rate coefficient is shown with other theoretical results[8, 9, 11]. Our results are smaller than those by McLaughlin & Hahn[8] and Romanic[11] by 20% and larger than those by Roszman's[9] by 20% at 1keV. The processes from the $1s^22pnl$ and those from $1s^23l_1nl_2$ dominate at low temperature($T_e < 200$eV) and high temperature($T_e > 500$eV), respectively. The small hollow is seen around $T_e = 300eV$ just where the processes from the $1s^22pnl$ contribute comparable to those from the $1s^23l_1nl_2$. In the C^{2+} ion, all of the α values from the $1s^23l_1nl_2$ are always smaller than those from the $1s^22pnl$ states[18]. The temperature where α has the maximum is determined by the temperature near $\Delta E/T_e \sim 1$. As mentioned before, the $\Delta E/I_p$ values for the $1s^22pnl$ and those for the $1s^23l_1nl_2$ become smaller and keep constant as Z increase, respectively. Namely the difference of the peak position of α values in T_e for the process from the $1s^22pnl$ and that from the $1s^23l_1nl_2$ increases as Z increases. Therefore, in Fe^{22+} ion which has large Z value, the process from the $1s^23l_1nl_2$ states dominates at high T_e. For the He-like and Li-like ion, since all of the ΔE values increase according to

Z^2, all of the peaks shift according to Z^2. As a result, almost the similar figures are seen between He-like C^{4+} and Fe^{24+} ions[11].

Fig.8 shows $\alpha_{n'}$ given by Eq.(28) for n'=2$\sim$ 6 as a function of T_e. At low T_e, the processes to $n' = 2$ or 3 dominate. On the other hand, as T_e increases, the processes to $n' = 4 \sim 6$ become comparable to that to $n' = 3$. Further the α value to $n' = 2$ decreases rapidly. This comes from the fact that the processes from $1s^2 3l_1 nl_2$ to $n' = 2$ contribute little to dielectronic recombination.

Figs.9(a)-(d) show f_α as a function of n' which is principal quantum number of the final bound state. Here f_α gives the quantity summed up Qd over the autoionization n states, that is,

$$f_\alpha(n') = \sum_{n,l,L,S,J} \sum_{l'',L',S',J'} Qd(i_0, nl^{2S+1}L_J, 2l''n'l' \ {}^{2S'+1}L'_{J'}). \quad (29)$$

With the use of the $f_\alpha(n')$, the n'-dependence for $\alpha_{n'}$ can be understood roughly, though the f_α is independent of T_e. For the $n' < 11$ states, the contribution from transitions $1s^2 2pnl \to 1s^2 2pn'l'$ is significant, since Ar values for these transitions are much larger than that of the $1s^2 2pnl \to 1s^2 2snl$ transition. However, for $n' > 11$, the $1s^2 2pn'l'$ states are autoionizing states and only the $1s^2 2pnl \to 1s^2 2snl$ transition remains. Therefore, big gaps around $n' = 11$ are found in Fig.9(a). For $11 \leq n' \leq 100$, f_α keeps constant. On the other hand, for $n' \geq 200$, f_α decreases according to n^{-3}. This is due to the fact that f_α is proportional to Ar for $11 \leq n' \leq 100$ and Aa for $n' \geq 200$ because of $Aa \gg Ar$ and $Ar \gg Aa$, respectively. For $1s^2 3pnl_2$-$1s^2 2snl_2$ transition, f_α decreases according to n'^{-3} after around n'=10 as is seen from Fig.9(b). Furthermore, the f_α values for $n \geq 13$ equal to 0 in the $1s^2 3snl_2$-$1s^2 2pn_2 l$, and $1s^2 3dnl_2$-$1s^2 2pnl_2$ transitions (see Figs.9(c) and (d)), because $1s^2 2pnl (n \geq 13)$ states are autoionization states. Therefore, f_α for $n > 20$ is ignored in our calculation for $1s^2 3l_1 nl_2$ levels.

Fig.10 shows ratio of $\sum_{n''=2}^{n'} \alpha_{n''}$ to $\sum_{n''=2}^{500} \alpha_{n''}$ as a function of n'. Here the $\alpha_{n''}$ values are given by Eq.(28). The ratios at n' =10 are about 0.7 and 0.85 for T_e=100eV and 1keV, respectively. These values are much larger than that in the case of the C^{2+} ion. In the C^{2+} ion, they are less than 0.1[18].

6. Conclusion

We calculate the radiative transition probability (Ar), autoionization rate (Aa), the intensity factor of the dielectronic satellite spectra (Qd) and the dielectronic recombination rate coefficient (α_d) of Fe^{22+} ion with use of Cowan's code[13, 14]. We treat not only the $1s^2 2l_1 nl_2$ states but also $1s^2 3l_1 nl_2$ states. We confirm the n-dependence for Ar and Aa which are expected theoretically. Namely the Ar values for the $1s^2 2pnl \rightarrow 1s^2 2pn'l'(n' = 2 \sim 4)$ and $1s^2 2pnl \rightarrow 1s^2 2snl$ processes decrease according to n^{-3} and keep constant as n increase, respectively. And the values Aa decrease according to n^{-3}. We used these dependence for the extrapolation for $n > 20$. The Ar values for the $1s^2 2pnl \rightarrow 1s^2 2pn'l'(n' = 2 \sim 4)$ processes are much larger than those for the $1s^2 2pnl \rightarrow 1s^2 2snl$ processes even at large n for Fe^{22+}. In the case of C^{2+}, the differences are not so large. This comes from the fact that the former and the latter increase according to Z^4 and Z, respectively.

Around $n = 20$, the Aa value from the $1s^2 2pnl$ levels is much larger than Ar values, while the Aa value from the $1s^2 3l_1 nl_2$ is much smaller than the Ar value. The Aa values decrease rapidly as l increases for large l. On the other hand, the Ar values keep almost constant for large l. Then we can neglect the dielectronic recombination processes with $l \geq 7$ for large n.

The dielectronic satellite spectra is important only in the low temperature below T_e=300eV. As for the dielectronic recombination, at low $T_e(\leq 200\text{eV})$, the processes from the $1s^2 2pnl$ states dominate. On the other hand, at high $Te(\geq 500\text{eV})$, only the processes from the $1s^2 3l_1 nl_2$ give a significant contribute to the dielectronic recombination. There is a different qualitative feature between α from the $1s^2 2pnl$ states and that from the $1s^2 3l_1 nl_2$ states through Z-scaling. This comes from the fact that the ΔE values for the former ($\Delta n = 0$ transition) and those for the latter ($\Delta n \neq 0$ transition) increase as Z and Z^2 as Z increases, respectively. For He-like ions, only one peak is found since there are only $\Delta n \neq 0$ transitions. Finally the α values for each final bound state are calculated and listed.

Acknowledgment

We wish to thank Dr. U.I.Safronova for her useful discussions and guidance about the Cowan's code.

References

[1] A.Burgess, Astrophys. J., **139** 776(1964), **141** 1588(1965).

[2] M.J. Seaton and P.J. Storey, "Di-electronic recombination" in "atomic processes and applications" edited by P.G. Burke and B.L. Moisewitsch, North-Holland 1976 p.133.

[3] I.Yamada, F.J. Currell, A.Danjo, M.Kimura, A.Matsumoto, N.Nakamura, S.Ohtani, H.A. Sakaue, M.Sakurai, H.Tawara, H.Watanabe, and M.Yoshino, J.Phys.B, **28** L9(1995).

[4] M. Kimura, N. Nakamura, H. Watanabe, I. Yamada, A.Danjo, K.Hosaka, A.Matsumoto, S.Ohtani, H.A. Sakaue, M.Sakurai, H.Tawara and M.Yoshino, J.Phys.B, **28** L643(1995).

[5] N.Nakamura, F.J. Currell. A.Danjo, M.Kimura, A.Mastumoto, S.Ohtani, H.A.Sakaue, M.Sakurai, H.Tawara, H.Watanabe, I.Yamada, and M.Yoshino, J.Phys.B, **28** 2959(1995).

[6] D.L. McKenzie, P.B.Landecker, U.Feldman, and G.A. Doschek, Astrophys. J., **289** 849(1985).

[7] C.C. Klepper, J.T. Hogan, S.J. Tobin, R.C. Isler, D.Guilhem, W.R. Hess, and P.Monier-Garbet, J.Nucl. Mate., **220-222** 521(1994).

[8] D.J. McLaughlin and Y. Hahn, Phys.Rev.A, **29** 712(1984).

[9] L.J. Roszman, Phys.Rev.A, **35** 2122(1987).

[10] D.C. Griffin and M.S. Pindzola, Phys.Rev.A, **35** 2821(1987).

[11] C.J. Romanik, Astrophys. J., **330** 1022(1988).

[12] I.Murakami and T.Kato, Phsica Scripta, to be published(1996).

[13] R.D. Cowan, J.Opt.Soc.Am., **58** 808(1968).

[14] R.D. Cowan, "The theory of atomic structure and spectra", University of California Press, 1981.

[15] Y.Hahn, Adv.Atom and Mol. Phys., **21** 123(1985).

[16] L.A. Vainshtein and U.I. Safronova, Physica Scripta, **31** 519(1985).

[17] T.Shirai, Y.Funatake, K.Mori, J.Sugar, W.L.Wiese, and T.Nakai, J. Phys. Chem. Ref. Data, **19** 174(1990).

[18] T.Kato, U.I.Safronova, and M.Ohira, submitted to NIFS-DATA(1996).

[19] K.Moribayashi and T.Kato, in preparation for publication.

[20] H.L. Zhang, D.H. Sampson, and C.J. Fontes, Atom. Data and Nucl. Data Tables, 31, **44** (1990).

Figure Captions

Fig.1 gAr given in Eq.(17) from the $1s^2 2pnl_2$ to the $1s^2 lnl'$ as a function of n: (a)$l_2 = s$, (b)$l_2 = p$, (c)$l_2 = d$, and (d)$l_2 = f$: The configurations indicated mean final states $1s^2 2lnl'$.

Fig.2 Aa given in Eq.(20) from the $1s^2 2pnl_2$ as a function of n.

Fig.3 gAr given in Eq.(17) from the $1s^2 3l_1 nl_2$ to the $1s^2 2l_1' n'l_2$ as a function of n: (a)$l_1 = s$, $l_2 = p$, (b)$l_1 = s$, $l_2 = d$, (c)$l_1 = p$, $l_2 = p$, (d)$l_1 = p$, $l_2 = d$, (e)$l_1 = d$, $l_2 = p$, and (f)$l_1 = d$, $l_2 = d$.

Fig.4 Aa given in Eq.(20) from the $1s^2 3l_1 nl_2$ as a function of n: (a)$l_1 = s$, $l_2 = p$, (b)$l_1 = s$, $l_2 = d$, (c)$l_1 = p$, $l_2 = p$, (d)$l_1 = p$, $l_2 = d$, (e)$l_1 = d$, $l_2 = p$, and (f)$l_1 = d$, $l_2 = d$.

Fig.5 Ar given in Eq.(22) from the $2pnl_2$ as a function of l_2.

Fig.6 Aa given by Eq.(20) from the $2p20l_2$ as a function of l_2.

Fig.7 α_d^t given by Eq.(27) as a function of T_e. Solid line: present result, dotted line: Romanik[11] dashed-dot line: Roszman[9], and $*$: Mc & Hahn[8].

Fig.8 $\alpha_{n'}$ given by Eq.(28) to the final n' states as a function of T_e.

Fig.9 f_α given in Eq.(29) as a function as n':the processes for (a)$1s^2 2pnl \rightarrow 1s^2 2l_1 n'l'$, (b)$1s^2 3pnl \rightarrow 1s^2 2sn'l'$, (c)$1s^2 3snl \rightarrow 1s^2 2pn'l'$, and (d)$1s^2 3dnl \rightarrow 1s^2 2pn'l'$.

Fig.10 Ratio of $\sum_{n''=2}^{n'} \alpha_{n''}$ to $\sum_{n''=2}^{\infty} \alpha_{n''}$ as a function of n'.

Table I Comparison between our energy level (in units of 1000cm^{-1}) for $1s^2 2l_1 nl_2$ ($n = 2 \sim 5$) and those by others[17]. The first to third columns give the state, present results, and the other results. $\sum gAr$ (in units of 1/s) is also give in fourth column.

	energy	(1000cm^{-1})	
state	present work	Shirai et.al.[17]	$\sum gAr(1/s)$
$1s^2 2s^2\ {}^1S_0$	0.0000		0.0000D+00
$1s^2 2s2p\ {}^3P_0$	347.3849		0.0000D+00
$1s^2 2s2p\ {}^3P_1$	378.2174	379.130	0.1882D+09
$1s^2 2s2p\ {}^3P_2$	469.4410	471.780	0.0000D+00
$1s^2 2s2p\ {}^1P_1$	723.9891	752.840	0.5403D+11
$1s^2 2p^2\ {}^3P_0$	952.8893	956.100	0.1235D+11
$1s^2 2p^2\ {}^3P_1$	1023.7057	1027.200	0.4541D+11
$1s^2 2p^2\ {}^3P_2$	1068.6712	1071.700	0.6588D+11
$1s^2 2p^2\ {}^1D_2$	1195.4688	1204.420	0.5322D+11
$1s^2 2p^2\ {}^1S_0$	1389.0091	1423.000	0.2999D+11
$1s^2 2s3s\ {}^3S_1$	8906.0916		0.1109D+14
$1s^2 2s3s\ {}^1S_0$	8967.8524		0.1341D+13
$1s^2 2s3p\ {}^3P_0$	9071.1666		0.4021D+11
$1s^2 2s3p\ {}^3P_1$	9071.8007		0.1395D+14
$1s^2 2s3p\ {}^1P_1$	9103.9508	9107.000	0.2719D+14
$1s^2 2s3p\ {}^3P_2$	9105.7396		0.3593D+12
$1s^2 2s3d\ {}^3D_1$	9194.9285	9199.000	0.7122D+14
$1s^2 2s3d\ {}^3D_2$	9199.5042	9209.000	0.1156D+15
$1s^2 2s3d\ {}^3D_3$	9206.9365	9212.000	0.1560D+15
$1s^2 2s3d\ {}^1D_2$	9264.5227	9273.000	0.8418D+14
$1s^2 2p3s\ {}^3P_0$	9344.1329	9295.000	0.2404D+13
$1s^2 2p3s\ {}^3P_1$	9360.1533		0.8793D+13
$1s^2 2p3p\ {}^3D_1$	9456.9341	9455.000	0.1422D+14
$1s^2 2p3s\ {}^3P_2$	9467.5091		0.1576D+14
$1s^2 2p3s\ {}^1P_1$	9508.1716	9470.000	0.1135D+14
$1s^2 2p3p\ {}^3D_2$	9520.2011	9524.000	0.2581D+14
$1s^2 2p3p\ {}^3S_1({}^1P_1)$	9521.0900		0.3794D+14
$1s^2 2p3p\ {}^3P_0$	9539.4390		0.6826D+13
$1s^2 2p3d\ {}^3F_2$	9582.1103		0.1346D+14
$1s^2 2p3p\ {}^3P_1$	9612.0438		0.1998D+14
$1s^2 2p3p\ {}^3D_3$	9618.9271	9624.000	0.3435D+14
$1s^2 2p3d\ {}^3F_3$	9623.3964		0.5323D+14
$1s^2 2p3d\ {}^3P_2({}^3D_2)$	9633.4096	9753.000	0.1900D+15
$1s^2 2p3p\ {}^3S_1({}^1P_1)$	9633.7634		0.3794D+14
$1s^2 2p3p\ {}^3P_2$	9636.2749		0.3616D+14
$1s^2 2p3d\ {}^3D_1$	9650.0550	9637.000	0.8162D+14
$1s^2 2p3p\ {}^1D_2$	9695.9224		0.4238D+14
$1s^2 2p3d\ {}^3F_4$	9715.3896		0.2279D+11
$1s^2 2p3d\ {}^1D_2$	9723.0885	9638.000	0.7766D+14
$1s^2 2p3d\ {}^3D_3$	9746.0909	9749.000	0.1723D+15
$1s^2 2p3d\ {}^3P_2({}^3D_2)$	9763.8260	9753.000	0.1900D+15

Table I (continued)

state	energy (1000cm^{-1}) present work	Shirai et.al.[17]	$\sum gAr(1/s)$
$1s^22p3d\ ^3P_1$	9763.9267		0.6008D+14
$1s^22p3p\ ^1S_0$	9764.6273		0.6828D+13
$1s^22p3d\ ^3P_0$	9765.9251		0.1690D+14
$1s^22p3d\ ^1F_3$	9818.8896	9830.000	0.2580D+15
$1s^22p3d\ ^1P_1$	9827.9633	9828.000	0.6827D+14
$1s^22s4s\ ^3S_1$	11956.9647		0.5799D+13
$1s^22s4s\ ^1S_0$	11978.3784	11981.000	0.1460D+13
$1s^22s4p\ ^3P_0$	12022.0180		0.9760D+12
$1s^22s4p\ ^3P_1$	12023.6211	12024.000	0.6389D+13
$1s^22s4p\ ^3P_2$	12036.5661		0.4957D+13
$1s^22s4p\ ^1P_1$	12040.8051	12044.000	0.1786D+14
$1s^22s4d\ ^3D_1$	12073.3000	12073.000	0.2791D+14
$1s^22s4d\ ^3D_2$	12074.9435	12075.000	0.4592D+14
$1s^22s4d\ ^3D_3$	12077.9368	12081.000	0.6291D+14
$1s^22s4d\ ^1D_2$	12095.8155	12098.000	0.4060D+14
$1s^22s4f\ ^3F_2$	12099.3689		0.2018D+14
$1s^22s4f\ ^3F_3$	12100.1046		0.2817D+14
$1s^22s4f\ ^3F_4$	12101.5594		0.3603D+14
$1s^22s4f\ ^1F_3$	12105.7731		0.2749D+14
$1s^22p4s\ ^3P_0$	12365.6176		0.1448D+13
$1s^22p4s\ ^3P_1$	12369.9492		0.5162D+13
$1s^22p4p\ ^3D_1$	12414.5827		0.1099D+14
$1s^22p4p\ ^3P_1$	12440.2134		0.1180D+14
$1s^22p4p\ ^3D_2$	12441.8823	12443.000	0.1930D+14
$1s^22p4p\ ^3P_0$	12443.3447		0.3898D+13
$1s^22p4d\ ^3F_2$	12465.6063		0.1562D+14
$1s^22p4d\ ^3P_2(^3D_2)$	12480.3829		0.8534D+14
$1s^22p4d\ ^3F_3$	12484.5020	12484.000	0.4913D+14
$1s^22p4d\ ^3D_1$	12489.0985		0.3243D+14
$1s^22p4s\ ^3P_2$	12493.8382		0.9762D+13
$1s^22p4f\ ^3G_3$	12494.0227		0.2807D+14
$1s^22p4f\ ^3F_2(^3D_2)$	12497.2232		0.3988D+14
$1s^22p4f\ ^3D_3$	12498.1299		0.5580D+14
$1s^22p4f\ ^3G_4$	12498.2095		0.3503D+14
$1s^22p4s\ ^1P_1$	12499.7779		0.6132D+13
$1s^22p4p\ ^1P_1$	12548.4640		0.1201D+14
$1s^22p4p\ ^3P_2$	12554.4155		0.1971D+14
$1s^22p4p\ ^3D_3$	12555.5399	12560.000	0.2543D+14
$1s^22p4p\ ^3S_1$	12559.4162		0.1203D+14
$1s^22p4p\ ^1D_2$	12578.5215		0.2117D+14
$1s^22p4d\ ^1D_2$	12594.8100	12597.000	0.3124D+14

Table I (continued)

	energy	(1000cm^{-1})	
state	present work	Shirai et.al.[17]	$\sum gAr$(1/s)
$1s^22p4d\ ^3F_4$	12594.9332		0.1832D+14
$1s^22p4p\ ^1S_0$	12601.6971		0.3730D+13
$1s^22p4d\ ^3D_3$	12601.9783	12603.000	0.5983D+14
$1s^22p4d\ ^3P_1$	12608.7309	12615.000	0.2675D+14
$1s^22p4d\ ^3P_2(^3D_2)$	12609.0068	12614.000	0.8534D+14
$1s^22p4d\ ^3P_0$	12609.5607		0.7670D+13
$1s^22p4f\ ^1F_3$	12616.2456		0.2814D+14
$1s^22p4f\ ^3F_4$	12618.7211		0.3575D+14
$1s^22p4f\ ^3F_2(^3D_2)$	12622.1187		0.3988D+14
$1s^22p4f\ ^3D_3$	12622.8548		0.5580D+14
$1s^22p4f\ ^3G_5$	12623.8101		0.4369D+14
$1s^22p4f\ ^1G_4$	12625.6836		0.3445D+14
$1s^22p4d\ ^1F_3$	12626.3489	12631.000	0.9687D+14
$1s^22p4f\ ^3D_1$	12628.2555		0.1206D+14
$1s^22p4d\ ^1P_1$	12630.7654		0.2905D+14
$1s^22p4f\ ^1D_2$	12632.1174		0.1977D+14
$1s^22s5s\ ^3S_1$	13340.1472		0.3262D+13
$1s^22s5s\ ^1S_0$	13350.6150		0.1051D+13
$1s^22s5p\ ^3P_0$	13372.3330		0.7769D+12
$1s^22s5p\ ^3P_1$	13373.2644		0.3910D+13
$1s^22s5p\ ^3P_2$	13379.7439		0.3914D+13
$1s^22s5p\ ^1P_1$	13382.6334	13380.000	0.1040D+14
$1s^22s5d\ ^3D_1$	13398.2552	13369.000	0.1405D+14
$1s^22s5d\ ^3D_2$	13399.0603	13400.000	0.2321D+14
$1s^22s5d\ ^3D_3$	13400.5873	13404.000	0.3192D+14
$1s^22s5d\ ^1D_2$	13408.6652		0.2198D+14
$1s^22s5f\ ^3F_2$	13411.0161		0.1049D+14
$1s^22s5f\ ^3F_3$	13411.4109		0.1465D+14
$1s^22s5f\ ^3F_4$	13412.1359		0.1876D+14
$1s^22s5g\ ^3G_3$	13414.5857		0.8510D+13
$1s^22s5g\ ^3G_4$	13414.6910		0.1094D+14
$1s^22s5f\ ^1F_3$	13414.8637		0.1442D+14
$1s^22s5g\ ^3G_5$	13415.2810		0.1334D+14
$1s^22s5g\ ^1G_4$	13415.3497		0.1088D+14
$1s^22p5s\ ^3P_0$	13740.5573		0.9003D+12
$1s^22p5s\ ^3P_1$	13742.3442		0.3206D+13
$1s^22p5p\ ^3D_1$	13765.8425		0.6810D+13
$1s^22p5p\ ^3P_1$	13778.3225		0.7066D+13
$1s^22p5p\ ^3P_0$	13779.4794		0.2189D+13
$1s^22p5p\ ^3D_2$	13779.5178		0.2300D+14
$1s^22p5d\ ^3F_2$	13791.6814		0.9643D+13
$1s^22p5d\ ^3P_2(^3D_2)$	13799.8628		0.4601D+14

Table I (continued)

	energy	(1000cm^{-1})	
state	present work	Shirai et.al.[17]	$\sum gAr(1/s)$
$1s^22p5d\ ^3F_3$	13801.3344	13804.000	0.2930D+14
$1s^22p5d\ ^3D_1$	13802.7551		0.1650D+14
$1s^22p5f\ ^3G_3$	13805.5873		0.1458D+14
$1s^22p5f\ ^3F_2$	13807.6145		0.2076D+14
$1s^22p5f\ ^3D_3(^3F_3)$	13807.8383		0.2904D+14
$1s^22p5f\ ^3G_4$	13808.0317		0.1819D+14
$1s^22p5g\ ^3H_4$	13808.7443		0.1082D+14
$1s^22p5g\ ^3G_3(^1F_3)$	13809.1446		0.1725D+14
$1s^22p5g\ ^3H_5$	13809.4533		0.1316D+14
$1s^22p5g\ ^3F_4(^1G_4)$	13809.7474		0.2182D+14
$1s^22p5s\ ^3P_2$	13866.1620		0.4483D+13
$1s^22p5s\ ^1P_1$	13869.5662		0.3772D+13
$1s^22p5p\ ^1P_1$	13895.2625		0.7190D+13
$1s^22p5p\ ^3D_2$	13897.6771		0.2300D+14
$1s^22p5p\ ^3D_3$	13899.3086	13904.000	0.1554D+14
$1s^22p5p\ ^3S_1$	13900.5980		0.7470D+13
$1s^22p5p\ ^1D_2$	13909.5561		0.1195D+14
$1s^22p5d\ ^1D_2$	13918.8817	13922.000	0.1645D+14
$1s^22p5d\ ^3F_4$	13919.2935		0.1278D+14
$1s^22p5p\ ^1S_0$	13919.6196		0.2009D+13
$1s^22p5d\ ^3D_3$	13922.0994	13929.000	0.2949D+14
$1s^22p5d\ ^3P_1$	13925.1138		0.1401D+14
$1s^22p5d\ ^3P_2(^3D_2)$	13925.3917		0.4601D+14
$1s^22p5d\ ^3P_0$	13925.4502		0.4071D+13
$1s^22p5f\ ^1F_3$	13929.7345		0.1456D+14
$1s^22p5f\ ^3F_4$	13931.0177		0.1854D+14
$1s^22p5f\ ^3F_2$	13932.6088		0.2076D+14
$1s^22p5f\ ^3D_3(^3F_3)$	13932.8966		0.2904D+14
$1s^22p5f\ ^3G_5$	13933.1734		0.2276D+14
$1s^22p5g\ ^3G_4$	13933.2690		0.1092D+14
$1s^22p5d\ ^1F_3$	13933.3831	13945.000	0.4784D+14
$1s^22p5g\ ^3G_5$	13933.8926		0.1330D+14
$1s^22p5g\ ^3G_3(^1F_3)$	13934.3049		0.1725D+14
$1s^22p5f\ ^1G_4$	13934.6683		0.1787D+14
$1s^22p5g\ ^3F_4(^1G_4)$	13934.8866		0.2182D+14
$1s^22p5g\ ^1H_5$	13935.1630		0.1310D+14
$1s^22p5f\ ^3D_1$	13935.3870		0.6307D+13
$1s^22p5d\ ^1P_1$	13935.5699		0.1524D+14
$1s^22p5g\ ^3H_6$	13935.6891		0.1548D+14
$1s^22p5g\ ^3F_2$	13936.4973		0.6070D+13
$1s^22p5g\ ^3F_3$	13937.1839		0.8520D+13
$1s^22p5f\ ^1D_2$	13937.6619		0.1038D+14

Table II Energy level(in units of $1000\mathrm{cm}^{-1}$), $\sum gAr$ (in units of 1/s), and Aa (in units of 10^{13}/s) for $1s^22pnl_2$(n=11, 13, 20) and $1s^23l_1nl_2$ (n=3, 4). For $1s^23l_1nl_2$, $\sum Aa$ is given in fourth column.

state	energy($1000\mathrm{cm}^{-1}$)	$\sum gAr(1/s)$	Aa(1 /s)
$1s^22p11s$ $^3P_0$	15647.2331	0.1245D+12	0.00000D+00
$1s^22p11s$ $^3P_1$	15647.3615	0.4036D+12	0.00000D+00
$1s^22p11p$ $^3D_1$	15649.6018	0.1451D+13	0.00000D+00
$1s^22p11p$ $^3P_0$	15650.6947	0.3323D+12	0.00000D+00
$1s^22p11p$ $^3P_1(^1P_1)$	15650.6990	0.2925D+13	0.00000D+00
$1s^22p11p$ $^3D_2(^1D_2)$	15650.7981	0.3965D+13	0.00000D+00
$1s^22p11d$ $^3F_2$	15651.9678	0.1151D+13	0.00000D+00
$1s^22p11d$ $^3P_2(^3D_2)$	15652.6700	0.4387D+13	0.00000D+00
$1s^22p11d$ $^3F_3$	15652.7976	0.2812D+13	0.00000D+00
$1s^22p11d$ $^3D_1$	15652.8674	0.1477D+13	0.00000D+00
$1s^22p11f$ $^3G_3$	15653.1884	0.1464D+13	0.00000D+00
$1s^22p11f$ $^3F_2(^3D_2)$	15653.3755	0.2151D+13	0.00000D+00
$1s^22p11f$ $^3D_3(^3F_3)$	15653.3901	0.2873D+13	0.00000D+00
$1s^22p11f$ $^3G_4$	15653.4433	0.1770D+13	0.00000D+00
$1s^22p11g$ $^3H_4$	15653.5150	0.1022D+13	0.00000D+00
$1s^22p11g$ $^3G_3(^1F_3)$	15653.5324	0.1649D+13	0.00000D+00
$1s^22p11g$ $^3F_4(^1G_4)$	15653.5838	0.2090D+13	0.00000D+00
$1s^22p11g$ $^3H_5$	15653.5912	0.1243D+13	0.00000D+00
$1s^22p11s$ $^3P_2$	15772.9685	0.6534D+12	0.18119D+13
$1s^22p11s$ $^1P_1$	15773.2301	0.4501D+12	0.15510D+14
$1s^22p11p$ $^3P_1(^1P_1)$	15775.6569	0.2925D+13	0.85709D+13
$1s^22p11p$ $^3D_2(^1D_2)$	15775.8272	0.3965D+13	0.23866D+13
$1s^22p11p$ $^3D_3$	15776.0679	0.2908D+13	0.99405D+12
$1s^22p11p$ $^3S_1$	15776.1702	0.1740D+13	0.14867D+14
$1s^22p11p$ $^3P_2$	15776.8700	0.1894D+13	0.12840D+13
$1s^22p11p$ $^1S_0$	15777.6913	0.3080D+12	0.28387D+14
$1s^22p11d$ $^1D_2$	15777.8405	0.1701D+13	0.21348D+12
$1s^22p11d$ $^3F_4$	15777.8970	0.1756D+13	0.24760D+12
$1s^22p11d$ $^3D_3$	15778.0985	0.2790D+13	0.37899D+12
$1s^22p11d$ $^3P_1$	15778.3508	0.1350D+13	0.55553D+13
$1s^22p11d$ $^3P_0$	15778.3814	0.4005D+12	0.79394D+13
$1s^22p11d$ $^3P_2(^3D_2)$	15778.3873	0.4387D+13	0.76363D+13
$1s^22p11f$ $^1F_3$	15778.8155	0.1466D+13	0.12016D+13
$1s^22p11f$ $^3F_4$	15778.9369	0.1866D+13	0.17260D+13
$1s^22p11d$ $^1F_3$	15779.0224	0.4084D+13	0.31448D+13
$1s^22p11f$ $^3F_2(^3D_2)$	15779.0512	0.2151D+13	0.39313D+12
$1s^22p11f$ $^3D_3(^3F_3)$	15779.0784	0.2873D+13	0.57809D+12
$1s^22p11f$ $^3G_5$	15779.1066	0.2365D+13	0.47561D+13
$1s^22p11g$ $^3G_4$	15779.1516	0.1070D+13	0.17090D+13

Table II (continued)

state	energy(1000cm^{-1})	$\sum gAr(1/s)$	$Aa(\ 1\ \ /s)$
$1s^22p11d\ ^1P_1$	15779.1948	0.1341D+13	0.59719D+13
$1s^22p11g\ ^3G_5$	15779.2135	0.1304D+13	0.18329D+13
$1s^22p11g\ ^3G_3(^1F_3)$	15779.2308	0.1649D+13	0.26390D+12
$1s^22p11f\ ^3D_1$	15779.2630	0.6335D+12	0.51873D+12
$1s^22p11g\ ^3F_4(^1G_4)$	15779.2823	0.2090D+13	0.21623D+12
$1s^22p11f\ ^1G_4$	15779.2961	0.1732D+13	0.55143D+13
$1s^22p11g\ ^1H_5$	15779.3601	0.1292D+13	0.64105D+13
$1s^22p11g\ ^3H_6$	15779.3943	0.1534D+13	0.64023D+13
$1s^22p11g\ ^3F_2$	15779.4119	0.5926D+12	0.14780D+12
$1s^22p11g\ ^3F_3$	15779.4832	0.8279D+12	0.33883D+12
$1s^22p11f\ ^1D_2$	15779.4843	0.1196D+13	0.35418D+12
$1s^22p13s\ ^3P_0$	15786.1087	0.7407D+11	0.13917D+13
$1s^22p13s\ ^3P_1$	15786.1850	0.2416D+12	0.55504D+13
$1s^22p13p\ ^3D_1$	15787.5415	0.7032D+12	0.11522D+13
$1s^22p13p\ ^3P_1(^1P_1)$	15788.2035	0.1430D+13	0.56517D+13
$1s^22p13p\ ^3P_0$	15788.2080	0.2808D+12	0.83592D+13
$1s^22p13p\ ^3D_2(^1D_2)$	15788.2702	0.2494D+13	0.18626D+13
$1s^22p13d\ ^3F_2$	15788.9715	0.6975D+12	0.13683D+12
$1s^22p13d\ ^3P_2(^3D_2)$	15789.3959	0.2637D+13	0.49550D+13
$1s^22p13d\ ^3F_3$	15789.4849	0.1745D+13	0.78846D+12
$1s^22p13d\ ^3D_1$	15789.5175	0.8844D+12	0.24440D+13
$1s^22p13f\ ^3G_3$	15789.7068	0.8432D+12	0.17220D+13
$1s^22p13f\ ^3F_2(^3D_2)$	15789.8244	0.1181D+13	0.25255D+12
$1s^22p13f\ ^3D_3(^3F_3)$	15789.8308	0.1628D+13	0.35823D+12
$1s^22p13f\ ^3G_4$	15789.8630	0.1014D+13	0.20997D+13
$1s^22p13g\ ^3H_4$	15789.9056	0.5940D+12	0.88698D+12
$1s^22p13g\ ^3G_3(^1F_3)$	15789.9171	0.9514D+12	0.17643D+12
$1s^22p13g\ ^3F_4(^1G_4)$	15789.9481	0.1208D+13	0.13299D+12
$1s^22p13g\ ^3H_5$	15789.9523	0.7202D+12	0.24732D+13
$1s^22p13s\ ^3P_2$	15911.8487	0.3915D+12	0.13071D+13
$1s^22p13s\ ^1P_1$	15912.0035	0.2683D+12	0.55504D+13
$1s^22p13p\ ^3P_1(^1P_1)$	15913.4738	0.1430D+13	0.56517D+13
$1s^22p13p\ ^3D_2(^1D_2)$	15913.5741	0.2494D+13	0.18626D+13
$1s^22p13p\ ^3D_3$	15913.7240	0.1748D+13	0.81151D+12
$1s^22p13p\ ^3S_1$	15913.7830	0.6568D+12	0.95589D+13
$1s^22p13p\ ^3P_2$	15914.2033	0.1262D+13	0.94014D+12
$1s^22p13p\ ^1S_0$	15914.6893	0.2943D+12	0.17662D+14
$1s^22p13d\ ^1D_2$	15914.7946	0.1022D+13	0.11043D+12
$1s^22p13d\ ^3F_4$	15914.8297	0.1059D+13	0.56002D+11

Table II (continued)

state	energy(1000cm^{-1})	$\sum gAr(1/s)$	$Aa(1/s)$
$1s^22p13d$ $^3D_3$	15914.9484	0.1666D+13	0.15768D+12
$1s^22p13d$ $^3P_1$	15915.0997	0.8111D+12	0.35416D+13
$1s^22p13d$ $^3P_0$	15915.1177	0.2404D+12	0.50670D+13
$1s^22p13d$ $^3P_2(^3D_2)$	15915.1226	0.2637D+13	0.49550D+13
$1s^22p13f$ $^1F_3$	15915.3833	0.8240D+12	0.59448D+12
$1s^22p13f$ $^3F_4$	15915.4566	0.1048D+13	0.85875D+12
$1s^22p13d$ $^1F_3$	15915.5015	0.2445D+13	0.15395D+13
$1s^22p13f$ $^3F_2(^3D_2)$	15915.5252	0.1181D+13	0.25255D+12
$1s^22p13f$ $^3D_3(^3F_3)$	15915.5414	0.1628D+13	0.35823D+12
$1s^22p13f$ $^3G_5$	15915.5576	0.1333D+13	0.23641D+13
$1s^22p13g$ $^3G_4$	15915.5871	0.6189D+12	0.88698D+12
$1s^22p13d$ $^1P_1$	15915.6060	0.8068D+12	0.37856D+13
$1s^22p13g$ $^3G_5$	15915.6248	0.7540D+12	0.95406D+12
$1s^22p13g$ $^3G_3(^1F_3)$	15915.6352	0.9514D+12	0.17643D+12
$1s^22p13f$ $^3D_1$	15915.6523	0.3521D+12	0.33654D+12
$1s^22p13g$ $^3F_4(^1G_4)$	15915.6662	0.1208D+13	0.13299D+12
$1s^22p13f$ $^1G_4$	15915.6738	0.9642D+12	0.28097D+13
$1s^22p13g$ $^1H_5$	15915.7136	0.7425D+12	0.33463D+13
$1s^22p13g$ $^3H_6$	15915.7336	0.8862D+12	0.33385D+13
$1s^22p13g$ $^3F_2$	15915.7444	0.3397D+12	0.98431D+11
$1s^22p13f$ $^1D_2$	15915.7865	0.6072D+12	0.22343D+12
$1s^22p13g$ $^3F_3$	15915.7879	0.4738D+12	0.21772D+12
$1s^22p20s$ $^3P_0$	15987.3909	0.2052D+11	0.40611D+12
$1s^22p20s$ $^3P_1$	15987.4112	0.6882D+11	0.15220D+13
$1s^22p20p$ $^3D_1$	15987.7834	0.1966D+12	0.32755D+12
$1s^22p20p$ $^3P_1(^1P_1)$	15987.9636	0.3951D+12	0.15774D+13
$1s^22p20p$ $^3P_0$	15987.9642	0.7051D+11	0.23574D+13
$1s^22p20p$ $^3D_2(^1D_2)$	15987.9826	0.6722D+12	0.54246D+12
$1s^22p20d$ $^3F_2(^3D_2)$	15988.1741	0.1935D+12	0.32269D+11
$1s^22p20d$ $^3P_2(^3D_2)$	15988.2894	0.7330D+12	0.13416D+13
$1s^22p20d$ $^3F_3$	15988.3149	0.9519D+12	0.23012D+12
$1s^22p20d$ $^3D_1$	15988.3224	0.2450D+12	0.66108D+12
$1s^22p20f$ $^3G_3$	15988.3728	0.2200D+12	0.40939D+12
$1s^22p20f$ $^3F_2(^3D_2)$	15988.4057	0.2980D+12	0.67991D+11
$1s^22p20f$ $^3D_3(^3F_3)$	15988.4072	0.4225D+12	0.92246D+11
$1s^22p20f$ $^3G_4$	15988.4161	0.2661D+12	0.50942D+12
$1s^22p20g$ $^3H_4$	15988.4257	0.1566D+12	0.58517D+12
$1s^22p20g$ $^3G_3(^1F_3)$	15988.4290	0.2646D+12	0.53209D+11
$1s^22p20g$ $^3F_4(^1G_4)$	15988.4371	0.3350D+12	0.38366D+11
$1s^22p20g$ $^3H_5$	15988.4383	0.1903D+12	0.60201D+12

Table II (continued)

state	energy(1000cm^{-1})	$\sum gAr$(1/s)	Aa(1/s)
$1s^22p20s$ $^3P_2$	16113.1385	0.1177D+12	0.37611D+12
$1s^22p20s$ $^1P_1$	16113.1797	0.8354D+11	0.26808D+13
$1s^22p20p$ $^3P_1(^1P_1)$	16113.5831	0.3951D+12	0.15774D+13
$1s^22p20p$ $^3D_2$	16113.6098	0.6722D+12	0.54246D+12
$1s^22p20p$ $^3D_3(^1D_2)$	16113.6522	0.4758D+12	0.23715D+12
$1s^22p20p$ $^3S_1$	16113.6673	0.1900D+12	0.25927D+13
$1s^22p20p$ $^3P_2$	16113.7814	0.3355D+12	0.26844D+12
$1s^22p20p$ $^1S_0$	16113.9113	0.7079D+11	0.48141D+13
$1s^22p20d$ $^1D_2$	16113.9442	0.2903D+12	0.27321D+11
$1s^22p20d$ $^3F_4$	16113.9541	0.3106D+12	0.78877D+10
$1s^22p20d$ $^3F_3(^3D_2)$	16113.9857	0.9519D+12	0.23012D+12
$1s^22p20d$ $^3P_1$	16114.0266	0.2283D+12	0.23064D+11
$1s^22p20d$ $^3P_0$	16114.0313	0.6796D+11	0.13640D+13
$1s^22p20d$ $^3P_2(^3D_2)$	16114.0331	0.7330D+12	0.13416D+13
$1s^22p20f$ $^1F_3$	16114.1035	0.2157D+12	0.14038D+12
$1s^22p20f$ $^3F_4$	16114.1236	0.2745D+12	0.20494D+12
$1s^22p20d$ $^1F_3$	16114.1354	0.6794D+12	0.37037D+12
$1s^22p20f$ $^3F_2(^3D_2)$	16114.1422	0.2980D+12	0.67991D+11
$1s^22p20f$ $^3D_3(^3F_3)$	16114.1467	0.4225D+12	0.92246D+11
$1s^22p20f$ $^3G_5$	16114.1507	0.3474D+12	0.56269D+12
$1s^22p20g$ $^3G_4$	16114.1574	0.1793D+12	0.21442D+12
$1s^22p20d$ $^1P_1$	16114.1639	0.2331D+12	0.78202D+12
$1s^22p20g$ $^3G_5$	16114.1675	0.2187D+12	0.23077D+12
$1s^22p20g$ $^3G_3(^1F_3)$	16114.1707	0.2646D+12	0.53209D+11
$1s^22p20f$ $^3D_1$	16114.1766	0.9028D+11	0.88970D+11
$1s^22p20g$ $^3F_4(^1G_4)$	16114.1788	0.3350D+12	0.38366D+11
$1s^22p20f$ $^1G_4$	16114.1831	0.2541D+12	0.68804D+12
$1s^22p20g$ $^1H_5$	16114.1922	0.2163D+12	0.81329D+12
$1s^22p20g$ $^3H_6$	16114.1971	0.2571D+12	0.80966D+12
$1s^22p20g$ $^3F_2$	16114.2005	0.9887D+11	0.30223D+11
$1s^22p20g$ $^3F_3$	16114.2122	0.1381D+12	0.64931D+11
$1s^22p20f$ $^1D_2$	16114.2137	0.1460D+12	0.61361D+11

Table II (continued)

state	energy(1000cm^{-1})	$\sum gAr(1/s)$	$Aa(1/s)$ to $2s$	$\sum Aa(1/s)$
$1s^23s3p\ ^3P_0$	18175.2650	0.1009D+14	0.58203D+14	0.12316D+15
$1s^23s3p\ ^3P_1$	18184.5179	0.3052D+14	0.60554D+14	0.13123D+15
$1s^23s3p\ ^3P_2$	18210.4066	0.5138D+14	0.57618D+14	0.12532D+15
$1s^23s3d\ ^1D_2$	18263.5123	0.1041D+15	0.10646D+15	0.23008D+15
$1s^23s3d\ ^3D_1$	18282.4402	0.7365D+14	0.21147D+14	0.36788D+14
$1s^23s3d\ ^3D_2$	18287.8013	0.1201D+15	0.22802D+14	0.44108D+14
$1s^23s3d\ ^3D_3$	18294.0146	0.1671D+15	0.21145D+14	0.36780D+14
$1s^23s3p\ ^1P_1$	18296.2095	0.3703D+14	0.17226D+15	0.48082D+15
$1s^23p^2\ ^3P_0$	18299.1022	0.1575D+14	0.57373D+13	0.27124D+15
$1s^23p^2\ ^3P_1$	18318.6961	0.4742D+14	0.12302D+03	0.23374D+15
$1s^23p^2\ ^3P_2$	18341.1206	0.8218D+14	0.12826D+14	0.23998D+15
$1s^23p^2\ ^1S_0$	18417.2299	0.1962D+14	0.62735D+14	0.80821D+15
$1s^23p^2\ ^1D_2$	18418.0893	0.1105D+15	0.16799D+15	0.42864D+15
$1s^23p3d\ ^3F_2$	18423.0127	0.1458D+15	0.11038D+12	0.45377D+13
$1s^23p3d\ ^3F_3$	18444.8773	0.2018D+15	0.66003D+12	0.80913D+13
$1s^23p3d\ ^1D_2$	18455.9009	0.1427D+15	0.32496D+12	0.21054D+14
$1s^23p3d\ ^3F_4$	18469.1360	0.2577D+15	0.11491D+12	0.22613D+12
$1s^23p3d\ ^3D_1$	18481.6784	0.8641D+14	0.51749D+12	0.15671D+15
$1s^23p3d\ ^3D_2$	18490.6019	0.1433D+15	0.64428D+12	0.14044D+15
$1s^23p3d\ ^3D_3$	18506.0530	0.2000D+15	0.16989D+13	0.16710D+15
$1s^23p3d\ ^3P_1$	18514.1083	0.8658D+14	0.28298D+13	0.98154D+14
$1s^23p3d\ ^3P_0$	18514.4327	0.2896D+14	0.30666D+13	0.90218D+14
$1s^23p3d\ ^3P_2$	18516.2171	0.1422D+15	0.26863D+13	0.10101D+15
$1s^23d^2\ ^3F_2$	18521.0363	0.2159D+15	0.18437D+12	0.19016D+15
$1s^23d^2\ ^3F_3$	18528.3758	0.2997D+15	0.58155D+05	0.18977D+15
$1s^23d^2\ ^3F_4$	18537.0743	0.3810D+15	0.19288D+13	0.20086D+15
$1s^23d^2\ ^3P_0$	18576.9833	0.4225D+14	0.18231D+12	0.22110D+14
$1s^23d^2\ ^3P_1$	18580.6515	0.1258D+15	0.49098D+03	0.20102D+14
$1s^23d^2\ ^3P_2$	18582.6793	0.2069D+15	0.11760D+12	0.69696D+14
$1s^23d^2\ ^1G_4$	18583.1269	0.3762D+15	0.19099D+15	0.12878D+16
$1s^23p3d\ ^1F_3$	18583.4460	0.2007D+15	0.94980D+14	0.63168D+15
$1s^23d^2\ ^1D_2$	18600.7984	0.1952D+15	0.29137D+12	0.23575D+15
$1s^23p3d\ ^1P_1$	18629.0642	0.7985D+14	0.16217D+12	0.28288D+15
$1s^23d^2\ ^1S_0$	18736.9354	0.3759D+14	0.31480D+14	0.93879D+14
$1s^23s4s\ ^3S_1$	21130.9173	0.1180D+14	0.16984D+13	0.17315D+13
$1s^23s4s\ ^1S_0$	21157.2833	0.4138D+13	0.86975D+14	0.87152D+14
$1s^23s4d\ ^3D_1$	21235.5553	0.3045D+14	0.92551D+13	0.11943D+14
$1s^23s4p\ ^1P_1$	21238.8416	0.1915D+14	0.21838D+14	0.53449D+14
$1s^23s4d\ ^3D_2$	21239.4271	0.5021D+14	0.11531D+14	0.14441D+14

Table II (continued)

state	energy(1000cm^{-1})	$\sum gAr(1/s)$	$Aa(1/s)$ to $2s$	$\sum Aa(1/s)$
$1s^23s4p\ ^3P_0$	21243.4627	0.6135D+13	0.32167D+14	0.53449D+14
$1s^23s4d\ ^3D_3$	21244.7279	0.6876D+14	0.10855D+14	0.13838D+14
$1s^23s4d\ ^1D_2$	21248.9432	0.4897D+14	0.51520D+14	0.67014D+14
$1s^23s4p\ ^3P_1$	21250.6607	0.1893D+14	0.28441D+14	0.47771D+14
$1s^23s4p\ ^3P_2$	21257.8516	0.3103D+14	0.30355D+14	0.50325D+14
$1s^23p4p\ ^1P_1$	21304.6989	0.7269D+14	0.49739D+13	0.32525D+14
$1s^23p4s\ ^3P_0$	21308.1417	0.9360D+13	0.50734D+13	0.25582D+14
$1s^23p4s\ ^3P_1$	21315.8405	0.2811D+14	0.15348D+14	0.51053D+14
$1s^23p4p\ ^3D_2$	21322.7477	0.7118D+14	0.47540D+13	0.38854D+14
$1s^23p4p\ ^1P_1$	21325.0249	0.7269D+14	0.49739D+13	0.32525D+14
$1s^23s4f\ ^3F_2$	21328.5149	0.1575D+14	0.55761D+13	0.61170D+13
$1s^23s4f\ ^3F_3$	21329.9125	0.2127D+14	0.57989D+13	0.63586D+13
$1s^23s4f\ ^3F_4$	21331.7360	0.2639D+14	0.60249D+13	0.65968D+13
$1s^23p4p\ ^3P_0$	21333.3032	0.1135D+14	0.25788D+13	0.16209D+15
$1s^23d4s\ ^1D_2$	21339.7850	0.8224D+14	0.11317D+14	0.77278D+14
$1s^23p4s\ ^3P_2$	21341.3325	0.4947D+14	0.65432D+13	0.29552D+14
$1s^23s4f\ ^1F_3$	21343.2365	0.3389D+14	0.43156D+13	0.42992D+14
$1s^23p4p\ ^3D_3$	21345.3639	0.1071D+15	0.43625D+13	0.11197D+14
$1s^23p4p\ ^3P_1$	21348.0979	0.3819D+14	0.51969D+12	0.89659D+14
$1s^23p4p\ ^3S_1$	21358.7781	0.3916D+14	0.18888D+12	0.37079D+14
$1s^23p4p\ ^3P_2$	21363.5775	0.7403D+14	0.73321D+13	0.10859D+15
$1s^23p4s\ ^1P_1$	21364.3007	0.2950D+14	0.84617D+14	0.25181D+15
$1s^23d4s\ ^3D_1$	21366.2473	0.6226D+14	0.92526D+12	0.48200D+13
$1s^23d4s\ ^3D_2$	21372.6235	0.9240D+14	0.64419D+12	0.34280D+14
$1s^23d4s\ ^3D_3$	21381.2451	0.1267D+15	0.43760D+12	0.15468D+13
$1s^23p4f\ ^3G_3$	21386.9228	0.5955D+14	0.16611D+13	0.85762D+13
$1s^23p4f\ ^3G_4$	21398.2329	0.7889D+14	0.64416D+13	0.17038D+14
$1s^23p4f\ ^3F_3$	21400.8592	0.1316D+15	0.63164D+12	0.70849D+13
$1s^23p4d\ ^3D_1$	21401.4394	0.5166D+14	0.25062D+12	0.14373D+14
$1s^23p4f\ ^3F_2$	21403.3251	0.4552D+14	0.10315D+10	0.14712D+13
$1s^23p4d\ ^3D_2$	21408.1231	0.8170D+14	0.73392D+12	0.14182D+14
$1s^23p4d\ ^3D_3$	21410.6932	0.2359D+15	0.13643D+13	0.15349D+14
$1s^23p4d\ ^1D_2$	21412.9685	0.1610D+15	0.22493D+13	0.14395D+14
$1s^23p4p\ ^1S_0$	21415.7967	0.1365D+14	0.26456D+14	0.46842D+15
$1s^23p4p\ ^1D_2$	21420.4174	0.8730D+14	0.10361D+15	0.23128D+15
$1s^23p4f\ ^3F_3$	21421.3630	0.1316D+15	0.63164D+12	0.70849D+13
$1s^23p4f\ ^3F_4$	21425.5760	0.8827D+14	0.20891D+13	0.31705D+13
$1s^23p4f\ ^3G_5$	21425.5899	0.1086D+15	0.20891D+13	0.79550D+13
$1s^23p4d\ ^3D_3$	21432.9045	0.2359D+15	0.13643D+13	0.15349D+14

Table II (continued)

state	energy(1000cm^{-1})	$\sum gAr(1/s)$	$Aa(1/s)$ to $2s$	$\sum Aa(1/s)$
$1s^23p4d\ ^1D_2$	21435.9849	0.1610D+15	0.22493D+13	0.14395D+14
$1s^23p4d\ ^3F_3$	21440.7867	0.1180D+15	0.23006D+13	0.30016D+13
$1s^23p4d\ ^1P_1$	21442.7602	0.5547D+14	0.19875D+11	0.10121D+14
$1s^23d4d\ ^3D_1$	21443.4922	0.6858D+14	0.53189D+11	0.72395D+12
$1s^23p4f\ ^3D_3$	21444.2548	0.8963D+14	0.28565D+10	0.35128D+13
$1s^23p4f\ ^3D_2$	21444.9671	0.8299D+14	0.13444D+12	0.21205D+13
$1s^23d4d\ ^3G_3$	21452.1622	0.1906D+15	0.87109D+12	0.13242D+14
$1s^23p4d\ ^3F_4$	21454.2805	0.1427D+15	0.26878D+13	0.30284D+13
$1s^23p4f\ ^1G_4$	21454.8069	0.1367D+15	0.78331D+14	0.23401D+15
$1s^23d4p\ ^1D_2$	21457.4129	0.1178D+15	0.69900D+12	0.61168D+13
$1s^23d4d\ ^3G_4$	21457.4337	0.2338D+15	0.84641D+13	0.43265D+14
$1s^23d4d\ ^1P_1$	21460.6963	0.6363D+14	0.49827D+11	0.36318D+13
$1s^23p4d\ ^3P_2$	21461.5009	0.7873D+14	0.48385D+11	0.22530D+14
$1s^23d4d\ ^3D_2$	21463.3507	0.9859D+14	0.66838D+12	0.12775D+14
$1s^23p4d\ ^3P_1$	21465.2142	0.4947D+14	0.10770D+12	0.27119D+14
$1s^23p4d\ ^3P_0$	21466.2223	0.1613D+14	0.33235D+10	0.17315D+14
$1s^23d4d\ ^3G_5$	21466.4644	0.2865D+15	0.12352D+13	0.15283D+14
$1s^23p4f\ ^3D_1$	21468.9240	0.5888D+14	0.17998D+12	0.65454D+13
$1s^23d4p\ ^3F_2$	21468.9648	0.1238D+15	0.45413D+12	0.39912D+13
$1s^23d4d\ ^3D_3$	21469.1768	0.1599D+15	0.21521D+12	0.83595D+13
$1s^23d4p\ ^3F_3$	21473.0062	0.1691D+15	0.95999D+12	0.50594D+13
$1s^23d4p\ ^3D_1$	21477.2908	0.6619D+14	0.84150D+11	0.74804D+14
$1s^23d4d\ ^3F_2$	21479.5310	0.1341D+15	0.27725D+12	0.97856D+14
$1s^23p4f\ ^1D_2$	21481.3849	0.6273D+14	0.70413D+13	0.26114D+14
$1s^23d4p\ ^3D_2$	21484.2893	0.1101D+15	0.15694D+12	0.77264D+14
$1s^23d4d\ ^3F_3$	21485.2719	0.1875D+15	0.18093D+11	0.96861D+14
$1s^23d4d\ ^3F_4$	21490.7478	0.2434D+15	0.15499D+12	0.10253D+15
$1s^23d4p\ ^3D_3$	21491.9659	0.1541D+15	0.12375D+13	0.89885D+14
$1s^23d4d\ ^3S_1$	21493.3534	0.7778D+14	0.69759D+12	0.36107D+13
$1s^23d4p\ ^3P_0$	21493.8888	0.2368D+14	0.14962D+13	0.43935D+14
$1s^23d4p\ ^3P_1$	21494.8835	0.7063D+14	0.14716D+13	0.46180D+14
$1s^23d4p\ ^3P_2$	21499.5008	0.1167D+15	0.15468D+13	0.39332D+14
$1s^23d4d\ ^3P_0$	21506.3436	0.2862D+14	0.32427D+12	0.17444D+14
$1s^23d4f\ ^3H_4$	21508.4313	0.1996D+15	0.90092D+13	0.43856D+14
$1s^23d4d\ ^3P_1$	21509.9802	0.8460D+14	0.24939D+11	0.14365D+14
$1s^23d4d\ ^3P_2$	21512.1569	0.1366D+15	0.35075D+12	0.22016D+14
$1s^23d4f\ ^3H_5$	21515.5351	0.2406D+15	0.11504D+14	0.52684D+14
$1s^23d4f\ ^1G_4$	21515.8876	0.1962D+15	0.24385D+13	0.21003D+14
$1s^23d4f\ ^3H_6$	21522.6505	0.2795D+15	0.11472D+14	0.52434D+14
$1s^23d4f\ ^3F_2$	21527.8767	0.1095D+15	0.63006D+10	0.96534D+13

Table II (continued)

state	energy(1000cm^{-1})	$\sum gAr(1/s)$	$Aa(1/s)$ to $2s$	$\sum Aa(1/s)$
$1s^2 3d4d\ ^1D_2$	21527.9896	0.1138D+15	0.23903D+13	0.12240D+15
$1s^2 3d4f\ ^3F_3$	21532.0578	0.1517D+15	0.14065D+13	0.18477D+14
$1s^2 3d4d\ ^1G_4$	21534.9278	0.1967D+15	0.15386D+14	0.40835D+15
$1s^2 3d4f\ ^3F_4$	21537.8367	0.1917D+15	0.54898D+11	0.10282D+14
$1s^2 3d4p\ ^1F_3$	21539.9946	0.1456D+15	0.60973D+14	0.34458D+15
$1s^2 3d4f\ ^1D_2$	21547.4547	0.1082D+15	0.31022D+11	0.13246D+13
$1s^2 3d4p\ ^1P_1$	21557.7249	0.5934D+14	0.23949D+13	0.17273D+15
$1s^2 3d4f\ ^3G_3$	21559.2303	0.1566D+15	0.28389D+09	0.28636D+14
$1s^2 3d4f\ ^3G_4$	21564.2750	0.1991D+15	0.21928D+11	0.28322D+14
$1s^2 3d4f\ ^3G_5$	21568.8199	0.2417D+15	0.17320D+12	0.29209D+14
$1s^2 3d4f\ ^3D_1$	21571.1528	0.6632D+14	0.41147D+11	0.92013D+12
$1s^2 3d4f\ ^3D_2$	21572.1256	0.1102D+15	0.31022D+11	0.40427D+12
$1s^2 3d4f\ ^3D_3$	21573.8669	0.1533D+15	0.22486D+12	0.24294D+13
$1s^2 3d4f\ ^3P_2$	21585.5318	0.1070D+15	0.23166D+12	0.13685D+13
$1s^2 3d4d\ ^1S_0$	21586.3556	0.2582D+14	0.25030D+14	0.82886D+14
$1s^2 3d4f\ ^3P_1$	21587.3875	0.6386D+14	0.22889D+12	0.13063D+13
$1s^2 3d4f\ ^3P_0$	21588.8011	0.2118D+14	0.22589D+12	0.12606D+13
$1s^2 3d4f\ ^1F_3$	21592.7565	0.1463D+15	0.49951D+13	0.42173D+14
$1s^2 3d4f\ ^1H_5$	21617.9305	0.2465D+15	0.45812D+14	0.22648D+15
$1s^2 3d4f\ ^1P_1$	21626.1895	0.6523D+14	0.42235D+12	0.22996D+13

Table III Comparison between our Ar (in units of 1/s) values from the $1s^22l_1nl_2$ ($n = 2 \sim 5$) to the $1s^22l_12l_2$ and those by others[17]. The first to fourth columns give the lower states, upper states, our results, and other results.

		Ar (1/s)	
lower level	upper level	present work	Shirai et.al.[17]
$1s^22s^2\ ^1S_0$	$1s^22s2p\ ^3P_1$	0.62750D+08	0.48D+08
$1s^22s^2\ ^1S_0$	$1s^22s2p\ ^1P_1$	0.18009D+11	0.195D+11
$1s^22p^2\ ^3P_1$	$1s^22s3p\ ^3P_0$	0.39410D+11	
$1s^22s^2\ ^1S_0$	$1s^22s3p\ ^3P_1$	0.45013D+13	
$1s^22p^2\ ^3P_0$	$1s^22s3p\ ^3P_1$	0.85073D+10	
$1s^22p^2\ ^3P_1$	$1s^22s3p\ ^3P_1$	0.75420D+10	
$1s^22p^2\ ^3P_2$	$1s^22s3p\ ^3P_1$	0.81450D+11	
$1s^22p^2\ ^1D_2$	$1s^22s3p\ ^3P_1$	0.38010D+11	
$1s^22p^2\ ^1S_0$	$1s^22s3p\ ^3P_1$	0.11835D+11	
$1s^22s^2\ ^1S_0$	$1s^22s3p\ ^1P_1$	0.88040D+13	0.114D+14
$1s^22p^2\ ^3P_0$	$1s^22s3p\ ^1P_1$	0.97747D+10	
$1s^22p^2\ ^3P_1$	$1s^22s3p\ ^1P_1$	0.13012D+10	
$1s^22p^2\ ^3P_2$	$1s^22s3p\ ^1P_1$	0.54940D+11	
$1s^22p^2\ ^1D_2$	$1s^22s3p\ ^1P_1$	0.18626D+12	0.17D+12
$1s^22p^2\ ^1S_0$	$1s^22s3p\ ^1P_1$	0.67130D+10	0.14D+12
$1s^22p^2\ ^3P_1$	$1s^22s3p\ ^3P_2$	0.26000D+11	
$1s^22p^2\ ^3P_2$	$1s^22s3p\ ^3P_2$	0.35698D+11	
$1s^22p^2\ ^1D_2$	$1s^22s3p\ ^3P_2$	0.87492D+10	
$1s^22p^2\ ^3P_1$	$1s^22p3s\ ^3P_0$	0.24014D+13	
$1s^22s^2\ ^1S_0$	$1s^22p3s\ ^3P_1$	0.25259D+12	
$1s^22p^2\ ^3P_0$	$1s^22p3s\ ^3P_1$	0.93063D+12	
$1s^22p^2\ ^3P_1$	$1s^22p3s\ ^3P_1$	0.48010D+12	
$1s^22p^2\ ^3P_2$	$1s^22p3s\ ^3P_1$	0.12272D+13	
$1s^22p^2\ ^1D_2$	$1s^22p3s\ ^3P_1$	0.24562D+10	
$1s^22p^2\ ^1S_0$	$1s^22p3s\ ^3P_1$	0.35093D+11	
$1s^22p^2\ ^3P_1$	$1s^22p3s\ ^3P_2$	0.99638D+12	
$1s^22p^2\ ^3P_2$	$1s^22p3s\ ^3P_2$	0.16671D+13	
$1s^22p^2\ ^1D_2$	$1s^22p3s\ ^3P_2$	0.48466D+12	
$1s^22s^2\ ^1S_0$	$1s^22p3s\ ^1P_1$	0.42457D+12	
$1s^22p^2\ ^3P_0$	$1s^22p3s\ ^1P_1$	0.30703D+11	
$1s^22p^2\ ^3P_1$	$1s^22p3s\ ^1P_1$	0.12133D+12	
$1s^22p^2\ ^3P_2$	$1s^22p3s\ ^1P_1$	0.15005D+12	
$1s^22p^2\ ^1D_2$	$1s^22p3s\ ^1P_1$	0.21441D+13	
$1s^22p^2\ ^1S_0$	$1s^22p3s\ ^1P_1$	0.90287D+12	
$1s^22p^2\ ^3P_1$	$1s^22p3d\ ^3F_2$	0.23496D+12	
$1s^22p^2\ ^3P_2$	$1s^22p3d\ ^3F_2$	0.17403D+13	
$1s^22p^2\ ^1D_2$	$1s^22p3d\ ^3F_2$	0.71622D+12	

Table III (continued)

		A_r (1/s)	
lower level	upper level	present work	Shirai et.al.[17]
$1s^22p^2\ ^3P_2$	$1s^22p3d\ ^3F_3$	0.74247D+13	0.77D+13
$1s^22p^2\ ^1D_2$	$1s^22p3d\ ^3F_3$	0.17793D+12	
$1s^22p^2\ ^3P_1$	$1s^22p3d\ ^3P_2$	0.13544D+14	
$1s^22p^2\ ^3P_2$	$1s^22p3d\ ^3P_2$	0.17606D+13	
$1s^22p^2\ ^1D_2$	$1s^22p3d\ ^3P_2$	0.15470D+13	
$1s^22s^2\ ^1S_0$	$1s^22p3d\ ^3D_1$	0.10922D+12	
$1s^22p^2\ ^3P_0$	$1s^22p3d\ ^3D_1$	0.22123D+14	0.24D+14
$1s^22p^2\ ^3P_1$	$1s^22p3d\ ^3D_1$	0.43640D+13	
$1s^22p^2\ ^3P_2$	$1s^22p3d\ ^3D_1$	0.23120D+12	
$1s^22p^2\ ^1D_2$	$1s^22p3d\ ^3D_1$	0.32181D+11	
$1s^22p^2\ ^1S_0$	$1s^22p3d\ ^3D_1$	0.34397D+12	
$1s^22p^2\ ^3P_1$	$1s^22p3d\ ^1D_2$	0.10499D+14	
$1s^22p^2\ ^3P_2$	$1s^22p3d\ ^1D_2$	0.25624D+13	
$1s^22p^2\ ^1D_2$	$1s^22p3d\ ^1D_2$	0.24662D+13	
$1s^22p^2\ ^3P_2$	$1s^22p3d\ ^3D_3$	0.22769D+14	0.23D+14
$1s^22p^2\ ^1D_2$	$1s^22p3d\ ^3D_3$	0.18420D+13	
$1s^22p^2\ ^3P_1$	$1s^22p3d\ ^3P_2$	0.21318D+13	
$1s^22p^2\ ^3P_2$	$1s^22p3d\ ^3P_2$	0.10886D+14	0.12D+14
$1s^22p^2\ ^1D_2$	$1s^22p3d\ ^3P_2$	0.81146D+13	
$1s^22s^2\ ^1S_0$	$1s^22p3d\ ^3P_1$	0.44530D+10	
$1s^22p^2\ ^3P_0$	$1s^22p3d\ ^3P_1$	0.28345D+11	
$1s^22p^2\ ^3P_1$	$1s^22p3d\ ^3P_1$	0.12427D+14	
$1s^22p^2\ ^3P_2$	$1s^22p3d\ ^3P_1$	0.56513D+13	
$1s^22p^2\ ^1D_2$	$1s^22p3d\ ^3P_1$	0.17278D+13	
$1s^22p^2\ ^1S_0$	$1s^22p3d\ ^3P_1$	0.17935D+12	
$1s^22p^2\ ^3P_1$	$1s^22p3d\ ^3P_0$	0.16895D+14	
$1s^22p^2\ ^3P_2$	$1s^22p3d\ ^1F_3$	0.26200D+13	
$1s^22p^2\ ^1D_2$	$1s^22p3d\ ^1F_3$	0.34233D+14	0.35D+14
$1s^22s^2\ ^1S_0$	$1s^22p3d\ ^1P_1$	0.32918D+12	
$1s^22p^2\ ^3P_0$	$1s^22p3d\ ^1P_1$	0.38900D+12	
$1s^22p^2\ ^3P_1$	$1s^22p3d\ ^1P_1$	0.27450D+12	
$1s^22p^2\ ^3P_2$	$1s^22p3d\ ^1P_1$	0.25140D+11	
$1s^22p^2\ ^1D_2$	$1s^22p3d\ ^1P_1$	0.10741D+13	
$1s^22p^2\ ^1S_0$	$1s^22p3d\ ^1P_1$	0.20658D+14	0.21D+14
$1s^22p^2\ ^3P_1$	$1s^22s4p\ ^3P_0$	0.65185D+08	
$1s^22s^2\ ^1S_0$	$1s^22s4p\ ^3P_1$	0.11206D+13	0.12D+13
$1s^22p^2\ ^3P_0$	$1s^22s4p\ ^3P_1$	0.16136D+10	
$1s^22p^2\ ^3P_1$	$1s^22s4p\ ^3P_1$	0.41483D+06	
$1s^22p^2\ ^3P_2$	$1s^22s4p\ ^3P_1$	0.23862D+10	

Table III (continued)

		Ar	(1/s)
lower level	upper level	present work	Shirai et.al.[17]
$1s^22p^2\ ^1D_2$	$1s^22s4p\ ^3P_1$	0.32016D+10	
$1s^22p^2\ ^1S_0$	$1s^22s4p\ ^3P_1$	0.22287D+11	
$1s^22p^2\ ^3P_1$	$1s^22s4p\ ^3P_2$	0.74396D+09	
$1s^22p^2\ ^3P_2$	$1s^22s4p\ ^3P_2$	0.40136D+09	
$1s^22p^2\ ^1D_2$	$1s^22s4p\ ^3P_2$	0.18119D+08	
$1s^22s^2\ ^1S_0$	$1s^22s4p\ ^1P_1$	0.48173D+13	0.497D+13
$1s^22p^2\ ^3P_0$	$1s^22s4p\ ^1P_1$	0.14513D+11	
$1s^22p^2\ ^3P_1$	$1s^22s4p\ ^1P_1$	0.13887D+07	
$1s^22p^2\ ^3P_2$	$1s^22s4p\ ^1P_1$	0.84153D+10	
$1s^22p^2\ ^1D_2$	$1s^22s4p\ ^1P_1$	0.18430D+11	
$1s^22p^2\ ^1S_0$	$1s^22s4p\ ^1P_1$	0.94127D+11	
$1s^22p^2\ ^3P_1$	$1s^22s4f\ ^3F_2$	0.65684D+07	
$1s^22p^2\ ^3P_2$	$1s^22s4f\ ^3F_2$	0.61082D+07	
$1s^22p^2\ ^1D_2$	$1s^22s4f\ ^3F_2$	0.11053D+07	
$1s^22p^2\ ^3P_2$	$1s^22s4f\ ^3F_3$	0.15627D+08	
$1s^22p^2\ ^1D_2$	$1s^22s4f\ ^3F_3$	0.18321D+09	
$1s^22p^2\ ^3P_2$	$1s^22s4f\ ^1F_3$	0.24299D+10	
$1s^22p^2\ ^1D_2$	$1s^22s4f\ ^1F_3$	0.66563D+10	
$1s^22p^2\ ^3P_1$	$1s^22p4s\ ^3P_0$	0.76285D+12	
$1s^22s^2\ ^1S_0$	$1s^22p4s\ ^3P_1$	0.76753D+10	
$1s^22p^2\ ^3P_0$	$1s^22p4s\ ^3P_1$	0.30755D+12	
$1s^22p^2\ ^3P_1$	$1s^22p4s\ ^3P_1$	0.12232D+12	
$1s^22p^2\ ^3P_2$	$1s^22p4s\ ^3P_1$	0.49933D+12	
$1s^22p^2\ ^1D_2$	$1s^22p4s\ ^3P_1$	0.50020D+11	
$1s^22p^2\ ^1S_0$	$1s^22p4s\ ^3P_1$	0.42790D+11	
$1s^22p^2\ ^3P_1$	$1s^22p4d\ ^3F_2$	0.64170D+11	
$1s^22p^2\ ^3P_2$	$1s^22p4d\ ^3F_2$	0.81412D+12	
$1s^22p^2\ ^1D_2$	$1s^22p4d\ ^3F_2$	0.16255D+12	
$1s^22p^2\ ^3P_1$	$1s^22p4d\ ^3P_2$	0.53218D+13	
$1s^22p^2\ ^3P_2$	$1s^22p4d\ ^3P_2$	0.90126D+12	
$1s^22p^2\ ^1D_2$	$1s^22p4d\ ^3P_2$	0.18036D+11	
$1s^22p^2\ ^3P_2$	$1s^22p4d\ ^3F_3$	0.45807D+13	0.46D+13
$1s^22p^2\ ^1D_2$	$1s^22p4d\ ^3F_3$	0.43109D+12	
$1s^22s^2\ ^1S_0$	$1s^22p4d\ ^3D_1$	0.75490D+11	
$1s^22p^2\ ^3P_0$	$1s^22p4d\ ^3D_1$	0.68883D+13	
$1s^22p^2\ ^3P_1$	$1s^22p4d\ ^3D_1$	0.11499D+13	
$1s^22p^2\ ^3P_2$	$1s^22p4d\ ^3D_1$	0.13255D+12	
$1s^22p^2\ ^1D_2$	$1s^22p4d\ ^3D_1$	0.38057D+11	

Table III (continued)

lower level	upper level	Ar (1/s) present work	Shirai et.al.[17]
$1s^22p^2\ ^1S_0$	$1s^22p4d\ ^3D_1$	0.49417D+12	
$1s^22p^2\ ^3P_1$	$1s^22p4s\ ^3P_2$	0.57448D+12	
$1s^22p^2\ ^3P_2$	$1s^22p4s\ ^3P_2$	0.45474D+11	
$1s^22p^2\ ^1D_2$	$1s^22p4s\ ^3P_2$	0.37270D+12	
$1s^22s^2\ ^1S_0$	$1s^22p4s\ ^1P_1$	0.10472D+11	
$1s^22p^2\ ^3P_0$	$1s^22p4s\ ^1P_1$	0.92397D+11	
$1s^22p^2\ ^3P_1$	$1s^22p4s\ ^1P_1$	0.39477D+11	
$1s^22p^2\ ^3P_2$	$1s^22p4s\ ^1P_1$	0.31138D+11	
$1s^22p^2\ ^1D_2$	$1s^22p4s\ ^1P_1$	0.86187D+12	
$1s^22p^2\ ^1S_0$	$1s^22p4s\ ^1P_1$	0.30390D+12	
$1s^22p^2\ ^3P_1$	$1s^22p4d\ ^1D_2$	0.22182D+13	
$1s^22p^2\ ^3P_2$	$1s^22p4d\ ^1D_2$	0.10463D+13	
$1s^22p^2\ ^1D_2$	$1s^22p4d\ ^1D_2$	0.91442D+12	
$1s^22p^2\ ^3P_2$	$1s^22p4d\ ^3D_3$	0.61799D+13	0.61D+13
$1s^22p^2\ ^1D_2$	$1s^22p4d\ ^3D_3$	0.32147D+12	
$1s^22s^2\ ^1S_0$	$1s^22p4d\ ^3P_1$	0.21566D+10	
$1s^22p^2\ ^3P_0$	$1s^22p4d\ ^3P_1$	0.16605D+10	
$1s^22p^2\ ^3P_1$	$1s^22p4d\ ^3P_1$	0.43667D+13	0.45D+13
$1s^22p^2\ ^3P_2$	$1s^22p4d\ ^3P_1$	0.18514D+13	
$1s^22p^2\ ^1D_2$	$1s^22p4d\ ^3P_1$	0.55380D+12	
$1s^22p^2\ ^1S_0$	$1s^22p4d\ ^3P_1$	0.91253D+11	
$1s^22p^2\ ^3P_1$	$1s^22p4d\ ^3P_2$	0.88178D+12	
$1s^22p^2\ ^3P_2$	$1s^22p4d\ ^3P_2$	0.33218D+13	
$1s^22p^2\ ^1D_2$	$1s^22p4d\ ^3P_2$	0.28580D+13	
$1s^22p^2\ ^3P_1$	$1s^22p4d\ ^3P_0$	0.56197D+13	
$1s^22p^2\ ^3P_2$	$1s^22p4d\ ^1F_3$	0.22427D+12	
$1s^22p^2\ ^1D_2$	$1s^22p4d\ ^1F_3$	0.11641D+14	0.12D+14
$1s^22s^2\ ^1S_0$	$1s^22p4d\ ^1P_1$	0.14797D+12	
$1s^22p^2\ ^3P_0$	$1s^22p4d\ ^1P_1$	0.46210D+12	
$1s^22p^2\ ^3P_1$	$1s^22p4d\ ^1P_1$	0.14091D+12	
$1s^22p^2\ ^3P_2$	$1s^22p4d\ ^1P_1$	0.39353D+09	
$1s^22p^2\ ^1D_2$	$1s^22p4d\ ^1P_1$	0.37863D+12	
$1s^22p^2\ ^1S_0$	$1s^22p4d\ ^1P_1$	0.65910D+13	
$1s^22p^2\ ^3P_1$	$1s^22s5p\ ^3P_0$	0.12153D+10	
$1s^22s^2\ ^1S_0$	$1s^22s5p\ ^3P_1$	0.49883D+12	
$1s^22p^2\ ^3P_0$	$1s^22s5p\ ^3P_1$	0.36590D+10	
$1s^22p^2\ ^3P_1$	$1s^22s5p\ ^3P_1$	0.34203D+09	
$1s^22p^2\ ^3P_2$	$1s^22s5p\ ^3P_1$	0.17102D+09	
$1s^22p^2\ ^1D_2$	$1s^22s5p\ ^3P_1$	0.28798D+10	

Table III (continued)

		Ar	(1/s)
lower level	upper level	present work	Shirai et.al.[17]
$1s^22p^2\ ^1S_0$	$1s^22s5p\ ^3P_1$	0.17190D+11	
$1s^22p^2\ ^3P_1$	$1s^22s5p\ ^3P_2$	0.20522D+08	
$1s^22p^2\ ^3P_2$	$1s^22s5p\ ^3P_2$	0.34108D+09	
$1s^22p^2\ ^1D_2$	$1s^22s5p\ ^3P_2$	0.25492D+09	
$1s^22s^2\ ^1S_0$	$1s^22s5p\ ^1P_1$	0.25394D+13	0.25D+13
$1s^22p^2\ ^3P_0$	$1s^22s5p\ ^1P_1$	0.11266D+11	
$1s^22p^2\ ^3P_1$	$1s^22s5p\ ^1P_1$	0.39893D+08	
$1s^22p^2\ ^3P_2$	$1s^22s5p\ ^1P_1$	0.56360D+10	
$1s^22p^2\ ^1D_2$	$1s^22s5p\ ^1P_1$	0.93230D+10	
$1s^22p^2\ ^1S_0$	$1s^22s5p\ ^1P_1$	0.97000D+11	
$1s^22p^2\ ^3P_1$	$1s^22s5f\ ^3F_2$	0.24724D+04	
$1s^22p^2\ ^3P_2$	$1s^22s5f\ ^3F_2$	0.77086D+03	
$1s^22p^2\ ^1D_2$	$1s^22s5f\ ^3F_2$	0.12893D+04	
$1s^22p^2\ ^3P_2$	$1s^22s5f\ ^3F_3$	0.90606D+08	
$1s^22p^2\ ^1D_2$	$1s^22s5f\ ^3F_3$	0.25924D+09	
$1s^22p^2\ ^3P_2$	$1s^22s5f\ ^1F_3$	0.37033D+10	
$1s^22p^2\ ^1D_2$	$1s^22s5f\ ^1F_3$	0.10433D+11	
$1s^22p^2\ ^3P_1$	$1s^22p5s\ ^3P_0$	0.33996D+12	
$1s^22s^2\ ^1S_0$	$1s^22p5s\ ^3P_1$	0.15987D+08	
$1s^22p^2\ ^3P_0$	$1s^22p5s\ ^3P_1$	0.14325D+12	
$1s^22p^2\ ^3P_1$	$1s^22p5s\ ^3P_1$	0.49947D+11	
$1s^22p^2\ ^3P_2$	$1s^22p5s\ ^3P_1$	0.24376D+12	
$1s^22p^2\ ^1D_2$	$1s^22p5s\ ^3P_1$	0.37397D+11	
$1s^22p^2\ ^1S_0$	$1s^22p5s\ ^3P_1$	0.23001D+11	
$1s^22p^2\ ^3P_1$	$1s^22p5d\ ^3F_2$	0.44344D+11	
$1s^22p^2\ ^3P_2$	$1s^22p5d\ ^3F_2$	0.36790D+12	
$1s^22p^2\ ^1D_2$	$1s^22p5d\ ^3F_2$	0.68190D+11	
$1s^22p^2\ ^3P_1$	$1s^22p5d\ ^3P_2$	0.27490D+13	
$1s^22p^2\ ^3P_2$	$1s^22p5d\ ^3P_2$	0.27398D+12	
$1s^22p^2\ ^1D_2$	$1s^22p5d\ ^3P_2$	0.47450D+11	
$1s^22p^2\ ^3P_2$	$1s^22p5d\ ^3F_3$	0.24327D+13	0.23D+13
$1s^22p^2\ ^1D_2$	$1s^22p5d\ ^3F_3$	0.33859D+12	
$1s^22s^2\ ^1S_0$	$1s^22p5d\ ^3D_1$	0.52653D+11	
$1s^22p^2\ ^3P_0$	$1s^22p5d\ ^3D_1$	0.31276D+13	
$1s^22p^2\ ^3P_1$	$1s^22p5d\ ^3D_1$	0.47490D+12	
$1s^22p^2\ ^3P_2$	$1s^22p5d\ ^3D_1$	0.70980D+11	
$1s^22p^2\ ^1D_2$	$1s^22p5d\ ^3D_1$	0.17725D+11	
$1s^22p^2\ ^1S_0$	$1s^22p5d\ ^3D_1$	0.30813D+12	

Table III (continued)

		Ar	(1/s)
lower level	upper level	present work	Shirai et.al.[17]
$1s^22p^2\ ^3P_2$	$1s^22p5g\ ^3G_3$	0.25691D+10	
$1s^22p^2\ ^1D_2$	$1s^22p5g\ ^3G_3$	0.44254D+09	
$1s^22p^2\ ^3P_1$	$1s^22p5s\ ^3P_2$	0.43028D+11	
$1s^22p^2\ ^3P_2$	$1s^22p5s\ ^3P_2$	0.18674D+12	
$1s^22p^2\ ^1D_2$	$1s^22p5s\ ^3P_2$	0.10122D+12	
$1s^22s^2\ ^1S_0$	$1s^22p5s\ ^1P_1$	0.28633D+09	
$1s^22p^2\ ^3P_0$	$1s^22p5s\ ^1P_1$	0.21441D+11	
$1s^22p^2\ ^3P_1$	$1s^22p5s\ ^1P_1$	0.28649D+11	
$1s^22p^2\ ^3P_2$	$1s^22p5s\ ^1P_1$	0.18668D+11	
$1s^22p^2\ ^1D_2$	$1s^22p5s\ ^1P_1$	0.44113D+12	
$1s^22p^2\ ^1S_0$	$1s^22p5s\ ^1P_1$	0.15931D+12	
$1s^22p^2\ ^3P_1$	$1s^22p5d\ ^1D_2$	0.92998D+12	
$1s^22p^2\ ^3P_2$	$1s^22p5d\ ^1D_2$	0.50306D+12	
$1s^22p^2\ ^1D_2$	$1s^22p5d\ ^1D_2$	0.40896D+12	
$1s^22p^2\ ^3P_2$	$1s^22p5d\ ^3D_3$	0.26561D+13	0.25D+13
$1s^22p^2\ ^1D_2$	$1s^22p5d\ ^3D_3$	0.11569D+12	
$1s^22s^2\ ^1S_0$	$1s^22p5d\ ^3P_1$	0.13889D+10	
$1s^22p^2\ ^3P_0$	$1s^22p5d\ ^3P_1$	0.28861D+10	
$1s^22p^2\ ^3P_1$	$1s^22p5d\ ^3P_1$	0.20584D+13	
$1s^22p^2\ ^3P_2$	$1s^22p5d\ ^3P_1$	0.85987D+12	
$1s^22p^2\ ^1D_2$	$1s^22p5d\ ^3P_1$	0.25361D+12	
$1s^22p^2\ ^1S_0$	$1s^22p5d\ ^3P_1$	0.43467D+11	
$1s^22p^2\ ^3P_1$	$1s^22p5d\ ^3P_2$	0.42936D+12	
$1s^22p^2\ ^3P_2$	$1s^22p5d\ ^3P_2$	0.14963D+13	
$1s^22p^2\ ^1D_2$	$1s^22p5d\ ^3P_2$	0.13470D+13	
$1s^22p^2\ ^3P_1$	$1s^22p5d\ ^3P_0$	0.26176D+13	
$1s^22p^2\ ^3P_2$	$1s^22p5d\ ^1F_3$	0.39657D+11	
$1s^22p^2\ ^1D_2$	$1s^22p5d\ ^1F_3$	0.53754D+13	0.49D+13
$1s^22p^2\ ^3P_2$	$1s^22p5g\ ^3G_3$	0.13432D+10	
$1s^22p^2\ ^1D_2$	$1s^22p5g\ ^3G_3$	0.29051D+11	
$1s^22s^2\ ^1S_0$	$1s^22p5d\ ^1P_1$	0.91713D+11	
$1s^22p^2\ ^3P_0$	$1s^22p5d\ ^1P_1$	0.29566D+12	
$1s^22p^2\ ^3P_1$	$1s^22p5d\ ^1P_1$	0.79137D+11	
$1s^22p^2\ ^3P_2$	$1s^22p5d\ ^1P_1$	0.16381D+09	
$1s^22p^2\ ^1D_2$	$1s^22p5d\ ^1P_1$	0.19361D+12	
$1s^22p^2\ ^1S_0$	$1s^22p5d\ ^1P_1$	0.29984D+13	
$1s^22p^2\ ^3P_1$	$1s^22p5g\ ^3F_2$	0.28108D+09	
$1s^22p^2\ ^3P_2$	$1s^22p5g\ ^3F_2$	0.25262D+09	
$1s^22p^2\ ^3P_2$	$1s^22p5g\ ^3F_3$	0.15181D+10	
$1s^22p^2\ ^1D_2$	$1s^22p5g\ ^3F_3$	0.66453D+10	
$1s^22p^2\ ^1D_2$	$1s^22p5g\ ^3F_2$	0.13651D+08	

Table III (continued)

		Ar	(1/s)
lower level	upper level	present work	Shirai et.al.[17]
$1s^22s2p\ ^3P_0$	$1s^22p^2\ ^3P_1$	0.65150D+10	0.662D+10
$1s^22s2p\ ^3P_0$	$1s^22s3s\ ^3S_1$	0.43203D+12	
$1s^22s2p\ ^3P_0$	$1s^22s3d\ ^3D_1$	0.13321D+14	0.13D+14
$1s^22s2p\ ^3P_0$	$1s^22p3p\ ^3D_1$	0.11430D+13	
$1s^22s2p\ ^3P_0$	$1s^22p3p\ ^3S_1$	0.35763D+13	
$1s^22s2p\ ^3P_0$	$1s^22p3p\ ^3P_1$	0.39743D+12	
$1s^22s2p\ ^3P_0$	$1s^22p3p\ ^3S_1$	0.31173D+11	
$1s^22s2p\ ^3P_0$	$1s^22s4s\ ^3S_1$	0.14467D+12	
$1s^22s2p\ ^3P_0$	$1s^22s4d\ ^3D_1$	0.40397D+13	0.40D+13
$1s^22s2p\ ^3P_0$	$1s^22p4p\ ^3D_1$	0.81303D+12	
$1s^22s2p\ ^3P_0$	$1s^22p4p\ ^3P_1$	0.18903D+13	
$1s^22s2p\ ^3P_0$	$1s^22p4p\ ^1P_1$	0.13789D+11	
$1s^22s2p\ ^3P_0$	$1s^22p4p\ ^3S_1$	0.10305D+05	
$1s^22s2p\ ^3P_0$	$1s^22p4f\ ^3D_1$	0.55650D+08	
$1s^22s2p\ ^3P_0$	$1s^22s5s\ ^3S_1$	0.61277D+11	
$1s^22s2p\ ^3P_0$	$1s^22s5d\ ^3D_1$	0.18019D+13	0.18D+13
$1s^22s2p\ ^3P_0$	$1s^22p5p\ ^3D_1$	0.45323D+12	
$1s^22s2p\ ^3P_0$	$1s^22p5p\ ^3P_1$	0.10033D+13	
$1s^22s2p\ ^3P_0$	$1s^22p5p\ ^1P_1$	0.82843D+09	
$1s^22s2p\ ^3P_0$	$1s^22p5p\ ^3S_1$	0.47687D+09	
$1s^22s2p\ ^3P_0$	$1s^22p5f\ ^3D_1$	0.57383D+09	
$1s^22s2p\ ^3P_1$	$1s^22p^2\ ^3P_0$	0.12315D+11	0.124D+11
$1s^22s2p\ ^3P_1$	$1s^22p^2\ ^3P_1$	0.41270D+10	0.419D+10
$1s^22s2p\ ^3P_1$	$1s^22p^2\ ^3P_2$	0.53354D+10	0.546D+10
$1s^22s2p\ ^3P_1$	$1s^22p^2\ ^1D_2$	0.49374D+09	0.44D+9
$1s^22s2p\ ^3P_1$	$1s^22p^2\ ^1S_0$	0.18458D+09	
$1s^22s2p\ ^3P_1$	$1s^22s3s\ ^3S_1$	0.12434D+13	
$1s^22s2p\ ^3P_1$	$1s^22s3s\ ^1S_0$	0.26550D+11	
$1s^22s2p\ ^3P_1$	$1s^22s3d\ ^3D_1$	0.95917D+13	0.93D+13
$1s^22s2p\ ^3P_1$	$1s^22s3d\ ^3D_2$	0.17434D+14	0.17D+14
$1s^22s2p\ ^3P_1$	$1s^22s3d\ ^1D_2$	0.14662D+12	
$1s^22s2p\ ^3P_1$	$1s^22p3p\ ^3D_2$	0.46192D+13	
$1s^22s2p\ ^3P_1$	$1s^22p3p\ ^3S_1$	0.11360D+13	
$1s^22s2p\ ^3P_1$	$1s^22p3p\ ^3P_0$	0.65580D+13	
$1s^22s2p\ ^3P_1$	$1s^22p3p\ ^3P_1$	0.19002D+13	
$1s^22s2p\ ^3P_1$	$1s^22p3p\ ^3S_1$	0.12437D+12	
$1s^22s2p\ ^3P_1$	$1s^22p3p\ ^3P_2$	0.25912D+12	
$1s^22s2p\ ^3P_1$	$1s^22p3p\ ^1D_2$	0.25248D+12	
$1s^22s2p\ ^3P_1$	$1s^22p3p\ ^3D_1$	0.22618D+13	

Table III (continued)

		Ar	(1/s)
lower level	upper level	present work	Shirai et.al.[17]
$1s^22s2p\ ^3P_1$	$1s^22p3p\ ^1S_0$	0.24966D+12	
$1s^22s2p\ ^3P_1$	$1s^22s4s\ ^3S_1$	0.41493D+12	
$1s^22s2p\ ^3P_1$	$1s^22s4s\ ^1S_0$	0.18496D+11	
$1s^22s2p\ ^3P_1$	$1s^22s4d\ ^3D_1$	0.29131D+13	
$1s^22s2p\ ^3P_1$	$1s^22s4d\ ^3D_2$	0.53824D+13	0.53D+13
$1s^22s2p\ ^3P_1$	$1s^22s4d\ ^1D_2$	0.36208D+11	
$1s^22s2p\ ^3P_1$	$1s^22p4p\ ^3D_1$	0.13835D+13	
$1s^22s2p\ ^3P_1$	$1s^22p4p\ ^3P_1$	0.76180D+12	
$1s^22s2p\ ^3P_1$	$1s^22p4p\ ^3D_2$	0.24070D+13	
$1s^22s2p\ ^3P_1$	$1s^22p4p\ ^3P_0$	0.26936D+13	
$1s^22s2p\ ^3P_1$	$1s^22p4f\ ^3F_2$	0.19260D+10	
$1s^22s2p\ ^3P_1$	$1s^22p4p\ ^1P_1$	0.45630D+12	
$1s^22s2p\ ^3P_1$	$1s^22p4p\ ^3P_2$	0.19800D+11	
$1s^22s2p\ ^3P_1$	$1s^22p4p\ ^3S_1$	0.18424D+12	
$1s^22s2p\ ^3P_1$	$1s^22p4p\ ^1D_2$	0.26512D+12	
$1s^22s2p\ ^3P_1$	$1s^22p4p\ ^1S_0$	0.31006D+12	
$1s^22s2p\ ^3P_1$	$1s^22p4f\ ^3F_2$	0.21966D+08	
$1s^22s2p\ ^3P_1$	$1s^22p4f\ ^3D_1$	0.75213D+07	
$1s^22s2p\ ^3P_1$	$1s^22p4f\ ^1D_2$	0.87096D+08	
$1s^22s2p\ ^3P_1$	$1s^22s5s\ ^3S_1$	0.17552D+12	
$1s^22s2p\ ^3P_1$	$1s^22s5s\ ^1S_0$	0.12118D+11	
$1s^22s2p\ ^3P_1$	$1s^22s5d\ ^3D_1$	0.13017D+13	
$1s^22s2p\ ^3P_1$	$1s^22s5d\ ^3D_2$	0.24172D+13	0.25D+13
$1s^22s2p\ ^3P_1$	$1s^22s5d\ ^1D_2$	0.14242D+11	
$1s^22s2p\ ^3P_1$	$1s^22p5p\ ^3D_1$	0.78273D+12	
$1s^22s2p\ ^3P_1$	$1s^22p5p\ ^3P_1$	0.43123D+12	
$1s^22s2p\ ^3P_1$	$1s^22p5p\ ^3P_0$	0.12761D+13	
$1s^22s2p\ ^3P_1$	$1s^22p5p\ ^3D_2$	0.12330D+13	
$1s^22s2p\ ^3P_1$	$1s^22p5f\ ^3F_2$	0.19173D+10	
$1s^22s2p\ ^3P_1$	$1s^22p5p\ ^1P_1$	0.17815D+12	
$1s^22s2p\ ^3P_1$	$1s^22p5p\ ^3D_2$	0.41970D+11	
$1s^22s2p\ ^3P_1$	$1s^22p5p\ ^3S_1$	0.12604D+12	
$1s^22s2p\ ^3P_1$	$1s^22p5p\ ^1D_2$	0.16362D+12	
$1s^22s2p\ ^3P_1$	$1s^22p5p\ ^1S_0$	0.22921D+12	
$1s^22s2p\ ^3P_1$	$1s^22p5f\ ^3F_2$	0.22424D+08	
$1s^22s2p\ ^3P_1$	$1s^22p5f\ ^3D_1$	0.25570D+09	
$1s^22s2p\ ^3P_1$	$1s^22p5f\ ^1D_2$	0.61180D+09	
$1s^22s2p\ ^3P_2$	$1s^22p^2\ ^3P_1$	0.44810D+10	0.451D+10
$1s^22s2p\ ^3P_2$	$1s^22p^2\ ^3P_2$	0.73242D+10	0.756D+10

Table III (continued)

		Ar	(1/s)
lower level	upper level	present work	Shirai et.al.[17]
$1s^22s2p\ ^3P_2$	$1s^22p^2\ ^1D_2$	0.51046D+10	0.494D+10
$1s^22s2p\ ^3P_2$	$1s^22s3s\ ^3S_1$	0.19960D+13	
$1s^22s2p\ ^3P_2$	$1s^22s3d\ ^3D_1$	0.62090D+12	
$1s^22s2p\ ^3P_2$	$1s^22s3d\ ^3D_2$	0.55562D+13	0.54D+13
$1s^22s2p\ ^3P_2$	$1s^22s3d\ ^3D_3$	0.22283D+14	0.22D+14
$1s^22s2p\ ^3P_2$	$1s^22s3d\ ^1D_2$	0.26904D+11	
$1s^22s2p\ ^3P_2$	$1s^22p3p\ ^3D_1$	0.17301D+09	
$1s^22s2p\ ^3P_2$	$1s^22p3p\ ^3D_2$	0.10883D+12	
$1s^22s2p\ ^3P_2$	$1s^22p3p\ ^3S_1$	0.63077D+11	
$1s^22s2p\ ^3P_2$	$1s^22p3p\ ^3P_1$	0.70627D+12	
$1s^22s2p\ ^3P_2$	$1s^22p3p\ ^3D_3$	0.49026D+13	0.52D+13
$1s^22s2p\ ^3P_2$	$1s^22p3p\ ^3S_1$	0.56037D+13	
$1s^22s2p\ ^3P_2$	$1s^22p3p\ ^3P_2$	0.47776D+13	0.49D+13
$1s^22s2p\ ^3P_2$	$1s^22p3p\ ^1D_2$	0.14174D+13	
$1s^22s2p\ ^3P_2$	$1s^22s4s\ ^3S_1$	0.67060D+12	
$1s^22s2p\ ^3P_2$	$1s^22s4d\ ^3D_1$	0.19322D+12	
$1s^22s2p\ ^3P_2$	$1s^22s4d\ ^3D_2$	0.17210D+13	
$1s^22s2p\ ^3P_2$	$1s^22s4d\ ^3D_3$	0.69559D+13	0.71D+13
$1s^22s2p\ ^3P_2$	$1s^22s4d\ ^1D_2$	0.17841D+11	
$1s^22s2p\ ^3P_2$	$1s^22p4p\ ^3D_1$	0.92477D+06	
$1s^22s2p\ ^3P_2$	$1s^22p4p\ ^3P_1$	0.66080D+09	
$1s^22s2p\ ^3P_2$	$1s^22p4p\ ^3D_2$	0.17987D+10	
$1s^22s2p\ ^3P_2$	$1s^22p4f\ ^3G_3$	0.16843D+08	
$1s^22s2p\ ^3P_2$	$1s^22p4f\ ^3F_2$	0.43734D+09	
$1s^22s2p\ ^3P_2$	$1s^22p4f\ ^3D_3$	0.11601D+10	
$1s^22s2p\ ^3P_2$	$1s^22p4p\ ^1P_1$	0.85360D+12	
$1s^22s2p\ ^3P_2$	$1s^22p4p\ ^3P_2$	0.21182D+13	
$1s^22s2p\ ^3P_2$	$1s^22p4p\ ^3D_3$	0.26241D+13	
$1s^22s2p\ ^3P_2$	$1s^22p4p\ ^3S_1$	0.21190D+13	
$1s^22s2p\ ^3P_2$	$1s^22p4p\ ^1D_2$	0.78892D+12	
$1s^22s2p\ ^3P_2$	$1s^22p4f\ ^1F_3$	0.21033D+06	
$1s^22s2p\ ^3P_2$	$1s^22p4f\ ^3F_2$	0.35228D+08	
$1s^22s2p\ ^3P_2$	$1s^22p4f\ ^3D_3$	0.14248D+09	
$1s^22s2p\ ^3P_2$	$1s^22p4f\ ^3D_1$	0.16450D+07	
$1s^22s2p\ ^3P_2$	$1s^22p4f\ ^1D_2$	0.21796D+09	
$1s^22s2p\ ^3P_2$	$1s^22s5s\ ^3S_1$	0.28416D+12	
$1s^22s2p\ ^3P_2$	$1s^22s5d\ ^3D_1$	0.86960D+11	
$1s^22s2p\ ^3P_2$	$1s^22s5d\ ^3D_2$	0.77226D+12	
$1s^22s2p\ ^3P_2$	$1s^22s5d\ ^3D_3$	0.31311D+13	0.30D+13
$1s^22s2p\ ^3P_2$	$1s^22s5d\ ^1D_2$	0.10426D+11	

Table III (continued)

		Ar	(1/s)
lower level	upper level	present work	Shirai et.al.[17]
$1s^22s2p\ ^3P_2$	$1s^22s5g\ ^3G_3$	0.17193D+00	
$1s^22s2p\ ^3P_2$	$1s^22p5p\ ^3D_1$	0.66447D+08	
$1s^22s2p\ ^3P_2$	$1s^22p5p\ ^3P_1$	0.10119D+10	
$1s^22s2p\ ^3P_2$	$1s^22p5p\ ^3D_2$	0.85984D+08	
$1s^22s2p\ ^3P_2$	$1s^22p5f\ ^3G_3$	0.15224D+08	
$1s^22s2p\ ^3P_2$	$1s^22p5f\ ^3F_2$	0.12218D+09	
$1s^22s2p\ ^3P_2$	$1s^22p5f\ ^3D_3$	0.91756D+09	
$1s^22s2p\ ^3P_2$	$1s^22p5p\ ^1P_1$	0.54833D+12	
$1s^22s2p\ ^3P_2$	$1s^22p5p\ ^3D_2$	0.10660D+13	
$1s^22s2p\ ^3P_2$	$1s^22p5p\ ^3D_3$	0.14294D+13	
$1s^22s2p\ ^3P_2$	$1s^22p5p\ ^3S_1$	0.10581D+13	
$1s^22s2p\ ^3P_2$	$1s^22p5p\ ^1D_2$	0.42284D+12	
$1s^22s2p\ ^3P_2$	$1s^22p5f\ ^1F_3$	0.40004D+04	
$1s^22s2p\ ^3P_2$	$1s^22p5f\ ^3F_2$	0.66254D+08	
$1s^22s2p\ ^3P_2$	$1s^22p5f\ ^3D_3$	0.11437D+06	
$1s^22s2p\ ^3P_2$	$1s^22p5f\ ^3D_1$	0.23106D+07	
$1s^22s2p\ ^3P_2$	$1s^22p5f\ ^1D_2$	0.48682D+08	
$1s^22s2p\ ^1P_1$	$1s^22p^2\ ^3P_0$	0.33120D+08	0.21D8
$1s^22s2p\ ^1P_1$	$1s^22p^2\ ^3P_1$	0.12097D+08	0.70D+7
$1s^22s2p\ ^1P_1$	$1s^22p^2\ ^3P_2$	0.51678D+09	0.35D+9
$1s^22s2p\ ^1P_1$	$1s^22p^2\ ^1D_2$	0.50452D+10	0.454D+10
$1s^22s2p\ ^1P_1$	$1s^22p^2\ ^1S_0$	0.29805D+11	0.328D+11
$1s^22s2p\ ^1P_1$	$1s^22s3\ ^3S_1$	0.25503D+11	
$1s^22s2p\ ^1P_1$	$1s^22s3s\ ^1S_0$	0.13143D+13	
$1s^22s2p\ ^1P_1$	$1s^22s3d\ ^3D_1$	0.20772D+12	
$1s^22s2p\ ^1P_1$	$1s^22s3d\ ^3D_2$	0.12016D+12	
$1s^22s2p\ ^1P_1$	$1s^22s3d\ ^1D_2$	0.16663D+14	
$1s^22s2p\ ^1P_1$	$1s^22p3p\ ^3D_1$	0.13310D+13	
$1s^22s2p\ ^1P_1$	$1s^22p3p\ ^3D_2$	0.43088D+12	
$1s^22s2p\ ^1P_1$	$1s^22p3p\ ^3S_1$	0.14316D+13	
$1s^22s2p\ ^1P_1$	$1s^22p3p\ ^3P_0$	0.26355D+12	
$1s^22s2p\ ^1P_1$	$1s^22p3p\ ^3P_1$	0.36493D+13	
$1s^22s2p\ ^1P_1$	$1s^22p3p\ ^3S_1$	0.66923D+12	
$1s^22s2p\ ^1P_1$	$1s^22p3p\ ^3P_2$	0.21890D+13	
$1s^22s2p\ ^1P_1$	$1s^22p3p\ ^1D_2$	0.68004D+13	0.68D+13
$1s^22s2p\ ^1P_1$	$1s^22p3p\ ^1S_0$	0.65685D+13	
$1s^22s2p\ ^1P_1$	$1s^22s4s\ ^3S_1$	0.92620D+10	
$1s^22s2p\ ^1P_1$	$1s^22s4s\ ^1S_0$	0.76997D+12	0.16D+13
$1s^22s2p\ ^1P_1$	$1s^22s4d\ ^3D_1$	0.74093D+11	
$1s^22s2p\ ^1P_1$	$1s^22s4d\ ^3D_2$	0.13811D+11	

Table III (continued)

		Ar	(1/s)
lower level	upper level	present work	Shirai et.al.[17]
$1s^22s2p\ ^1P_1$	$1s^22s4d\ ^1D_2$	0.60714D+13	0.62D+13
$1s^22s2p\ ^1P_1$	$1s^22p4p\ ^3D_1$	0.46317D+12	
$1s^22s2p\ ^1P_1$	$1s^22p4p\ ^3P_1$	0.29244D+12	
$1s^22s2p\ ^1P_1$	$1s^22p4p\ ^3D_2$	0.45850D+12	
$1s^22s2p\ ^1P_1$	$1s^22p4p\ ^3P_0$	0.28077D+12	
$1s^22s2p\ ^1P_1$	$1s^22p4f\ ^3F_2$	0.47602D+09	
$1s^22s2p\ ^1P_1$	$1s^22p4p\ ^1P_1$	0.16788D+13	
$1s^22s2p\ ^1P_1$	$1s^22p4p\ ^3P_2$	0.82858D+12	
$1s^22s2p\ ^1P_1$	$1s^22p4p\ ^3S_1$	0.70557D+12	
$1s^22s2p\ ^1P_1$	$1s^22p4p\ ^1D_2$	0.21972D+13	
$1s^22s2p\ ^1P_1$	$1s^22p4p\ ^1S_0$	0.25333D+13	
$1s^22s2p\ ^1P_1$	$1s^22p4f\ ^3F_2$	0.82368D+10	
$1s^22s2p\ ^1P_1$	$1s^22p4f\ ^3D_1$	0.43453D+08	
$1s^22s2p\ ^1P_1$	$1s^22p4f\ ^1D_2$	0.15022D+11	
$1s^22s2p\ ^1P_1$	$1s^22s5s\ ^3S_1$	0.39717D+10	
$1s^22s2p\ ^1P_1$	$1s^22s5s\ ^1S_0$	0.48107D+12	
$1s^22s2p\ ^1P_1$	$1s^22s5d\ ^3D_1$	0.34270D+11	
$1s^22s2p\ ^1P_1$	$1s^22s5d\ ^3D_2$	0.26088D+10	
$1s^22s2p\ ^1P_1$	$1s^22s5d\ ^1D_2$	0.29410D+13	0.28D+13
$1s^22s2p\ ^1P_1$	$1s^22p5p\ ^3D_1$	0.24119D+12	
$1s^22s2p\ ^1P_1$	$1s^22p5p\ ^3P_1$	0.13066D+12	
$1s^22s2p\ ^1P_1$	$1s^22p5p\ ^3P_0$	0.16437D+12	
$1s^22s2p\ ^1P_1$	$1s^22p5p\ ^3D_2$	0.28312D+12	
$1s^22s2p\ ^1P_1$	$1s^22p5f\ ^3F_2$	0.59628D+09	
$1s^22s2p\ ^1P_1$	$1s^22p5p\ ^1P_1$	0.86923D+12	
$1s^22s2p\ ^1P_1$	$1s^22p5p\ ^3D_2$	0.40378D+12	
$1s^22s2p\ ^1P_1$	$1s^22p5p\ ^3S_1$	0.49663D+12	
$1s^22s2p\ ^1P_1$	$1s^22p5p\ ^1D_2$	0.10079D+13	
$1s^22s2p\ ^1P_1$	$1s^22p5p\ ^1S_0$	0.10487D+13	
$1s^22s2p\ ^1P_1$	$1s^22p5f\ ^3F_2$	0.49854D+10	
$1s^22s2p\ ^1P_1$	$1s^22p5f\ ^3D_1$	0.39707D+08	
$1s^22s2p\ ^1P_1$	$1s^22p5f\ ^1D_2$	0.11817D+11	

Table IV $\lambda(\AA)$, $gAr(1/s)$, $\sum Ar$, $Aa(1/s)$, and Qd from the upper level to the lower level.

lower level	upper level	$\lambda(\AA)$	$gAr(1/s)$	$\sum Ar$	$Aa(1/s)$	Qd
$1s^22s2p\ ^3P_2$	$1s^22p11p\ ^3D_2$	6.53321	0.53620D+12	0.27382D+12	0.23866D+13	0.48101D+12
$1s^22s2p\ ^3P_2$	$1s^22p11p\ ^3D_3$	6.53311	0.10379D+13	0.27445D+12	0.99405D+12	0.81334D+12
$1s^22s2p\ ^1P_1$	$1s^22p11p\ ^3P_2$	6.64319	0.39400D+12	0.27210D+12	0.12840D+13	0.32511D+12
$1s^22p3p\ ^3D_3$	$1s^22p11d\ ^3F_4$	16.23643	0.82234D+12	0.19861D+12	0.24760D+12	0.45631D+12
$1s^22p^2\ ^3P_2$	$1s^22p11d\ ^3D_3$	6.79835	0.13944D+13	0.39938D+12	0.37899D+12	0.67893D+12
$1s^22p^2\ ^3P_1$	$1s^22p11d\ ^3P_1$	6.77753	0.50007D+12	0.44984D+12	0.55553D+13	0.46261D+12
$1s^22p^2\ ^3P_2$	$1s^22p11d\ ^3P_2$	6.79822	0.57323D+12	0.44936D+12	0.76363D+13	0.54137D+12
$1s^22p^2\ ^1D_2$	$1s^22p11d\ ^3P_2$	6.85731	0.55557D+12	0.44936D+12	0.76363D+13	0.52469D+12
$1s^22p3p\ ^1D_2$	$1s^22p11d\ ^1F_3$	16.43888	0.45401D+12	0.57831D+12	0.31448D+13	0.38349D+12
$1s^22p^2\ ^1S_0$	$1s^22p11d\ ^1P_1$	6.94917	0.60853D+12	0.44017D+12	0.59719D+13	0.56676D+12
$1s^22p3d\ ^1D_2$	$1s^22p11f\ ^1F_3$	16.51326	0.43091D+12	0.21409D+12	0.12016D+13	0.36575D+12
$1s^22p3d\ ^3D_3$	$1s^22p11f\ ^3F_4$	16.57587	0.54286D+12	0.21122D+12	0.17260D+13	0.48367D+12
$1s^22p4d\ ^3D_3$	$1s^22p11f\ ^3F_4$	31.47646	0.33161D+12	0.21122D+12	0.17260D+13	0.29545D+12
$1s^22p3d\ ^3P_2$	$1s^22p11f\ ^3D_3$	16.62439	0.34845D+12	0.20852D+12	0.57809D+12	0.25608D+12
$1s^22p3d\ ^3F_4$	$1s^22p11f\ ^3G_5$	16.49139	0.97964D+12	0.22258D+12	0.47561D+13	0.93584D+12
$1s^22p4d\ ^3F_4$	$1s^22p11f\ ^3G_5$	31.40501	0.54667D+12	0.22258D+12	0.47561D+13	0.52223D+12
$1s^22p5d\ ^3F_4$	$1s^22p11f\ ^3G_5$	53.76820	0.31581D+12	0.22258D+12	0.47561D+13	0.30169D+12
$1s^22p3d\ ^1F_3$	$1s^22p11f\ ^1G_4$	16.77695	0.49172D+12	0.19075D+12	0.55143D+13	0.47528D+12
$1s^22p4d\ ^1F_3$	$1s^22p11f\ ^1G_4$	31.71539	0.34934D+12	0.19075D+12	0.55143D+13	0.33766D+12
$1s^22p4f\ ^3F_4$	$1s^22p11g\ ^3G_5$	31.64046	0.30657D+12	0.12286D+12	0.18329D+13	0.28731D+12
$1s^22p5f\ ^3F_4$	$1s^22p11g\ ^3G_5$	54.10618	0.25716D+12	0.12286D+12	0.18329D+13	0.24101D+12
$1s^22p4f\ ^1G_4$	$1s^22p11g\ ^1H_5$	31.70848	0.32203D+12	0.12106D+12	0.64105D+13	0.31606D+12
$1s^22p5f\ ^1G_4$	$1s^22p11g\ ^1H_5$	54.20768	0.27613D+12	0.12106D+12	0.64105D+13	0.27101D+12
$1s^22p4f\ ^3G_5$	$1s^22p11g\ ^3H_6$	31.68935	0.40649D+12	0.12232D+12	0.64023D+13	0.39887D+12
$1s^22p5f\ ^3G_5$	$1s^22p11g\ ^3H_6$	54.16296	0.35144D+12	0.12232D+12	0.64023D+13	0.34485D+12
$1s^22p6f\ ^3G_5$	$1s^22p11g\ ^3H_6$	88.10639	0.25807D+12	0.12232D+12	0.64023D+13	0.25323D+12
$1s^22p6g\ ^3H_6$	$1s^22p11h\ ^3I_7$	88.21890	0.25987D+12	0.66703D+11	0.60226D+13	0.25702D+12
$1s^22s2p\ ^3P_1$	$1s^22p13p\ ^3D_2$	6.48926	0.36985D+12	0.32783D+12	0.18626D+13	0.31450D+12
$1s^22s2p\ ^3P_2$	$1s^22p13p\ ^3D_2$	6.47494	0.32148D+12	0.32783D+12	0.18626D+13	0.27336D+12
$1s^22s2p\ ^3P_2$	$1s^22p13p\ ^3D_3$	6.47488	0.62823D+12	0.16714D+12	0.81151D+12	0.52094D+12
$1s^22p^2\ ^3P_1$	$1s^22p13d\ ^3P_2$	6.77246	0.65980D+12	0.53030D+12	0.49550D+13	0.59601D+12
$1s^22p3p\ ^3S_1$	$1s^22p13d\ ^3P_2$	15.95324	0.21184D+12	0.53030D+12	0.49550D+13	0.19136D+12
$1s^22p3p\ ^3D_2$	$1s^22p13d\ ^3F_3$	15.95072	0.31147D+12	0.25009D+12	0.78846D+12	0.23647D+12
$1s^22p^2\ ^3P_0$	$1s^22p13d\ ^3D_1$	6.74008	0.42727D+12	0.29409D+12	0.24440D+13	0.38138D+12
$1s^22p^2\ ^3P_2$	$1s^22p13d\ ^3D_3$	6.73569	0.82744D+12	0.23975D+12	0.15768D+12	0.32828D+12
$1s^22p^2\ ^3P_1$	$1s^22p13d\ ^3P_1$	6.71529	0.30079D+12	0.27169D+12	0.35416D+13	0.27936D+12
$1s^22p^2\ ^3P_2$	$1s^22p13d\ ^3P_2$	6.73561	0.34233D+12	0.53030D+12	0.49550D+13	0.30923D+12
$1s^22p^2\ ^1D_2$	$1s^22p13d\ ^3P_2$	6.79361	0.33442D+12	0.53030D+12	0.49550D+13	0.30209D+12
$1s^22p3p\ ^1D_2$	$1s^22p13d\ ^1F_3$	16.07816	0.27616D+12	0.34803D+12	0.15395D+13	0.22524D+12
$1s^22p^2\ ^1S_0$	$1s^22p13d\ ^1P_1$	6.88391	0.36528D+12	0.26638D+12	0.37856D+13	0.34127D+12
$1s^22p3d\ ^3F_2$	$1s^22p13f\ ^3G_3$	16.10918	0.33400D+12	0.12880D+12	0.17220D+13	0.31076D+12

Table IV (continue)

lower level	upper level	$\lambda(\AA)$	$gAr(1/s)$	$\sum Ar$	$Aa(1/s)$	Qd
$1s^22p3s\ ^1P_1$	$1s^23s^2\ ^1S_0$	11.64241	0.27587D+13	0.58250D+13	0.13576D+15	0.26397D+13
$1s^22s3s\ ^3S_1$	$1s^23s3p\ ^3P_0$	10.78845	0.76268D+13	0.10088D+14	0.58203D+14	0.33314D+13
$1s^22s3s\ ^3S_1$	$1s^23s3p\ ^3P_1$	10.77769	0.22533D+14	0.10173D+14	0.60554D+14	0.96497D+13
$1s^22s3s\ ^3S_1$	$1s^23s3p\ ^3P_2$	10.74770	0.38748D+14	0.10277D+14	0.57618D+14	0.16464D+14
$1s^22p3p\ ^3D_3$	$1s^23s3p\ ^3P_2$	11.63944	0.62247D+13	0.10277D+14	0.57618D+14	0.26449D+13
$1s^22s3s\ ^1S_0$	$1s^23s3p\ ^1P_1$	10.72000	0.20011D+14	0.12343D+14	0.17226D+15	0.69897D+13
$1s^22p3p\ ^3S_1$	$1s^23s3p\ ^1P_1$	11.54408	0.94524D+12	0.12343D+14	0.17226D+15	0.33016D+12
$1s^22s3p\ ^3P_1$	$1s^23s3d\ ^1D_2$	10.82257	0.20443D+14	0.20819D+14	0.10646D+15	0.86739D+13
$1s^22s3p\ ^1P_1$	$1s^23s3d\ ^1D_2$	10.86036	0.33101D+14	0.20819D+14	0.10646D+15	0.14045D+14
$1s^22p3s\ ^3P_1$	$1s^23s3d\ ^1D_2$	11.17119	0.15455D+14	0.20819D+14	0.10646D+15	0.65575D+13
$1s^22p3s\ ^1P_1$	$1s^23s3d\ ^1D_2$	11.35902	0.26705D+14	0.20819D+14	0.10646D+15	0.11331D+14
$1s^22p3s\ ^3P_0$	$1s^23s3d\ ^3D_1$	11.12775	0.37358D+14	0.24550D+14	0.21147D+14	0.12880D+14
$1s^22p3s\ ^3P_1$	$1s^23s3d\ ^3D_1$	11.14762	0.22777D+14	0.24550D+14	0.21147D+14	0.78529D+13
$1s^22p3s\ ^1P_1$	$1s^23s3d\ ^3D_1$	11.33465	0.46923D+13	0.24550D+14	0.21147D+14	0.16178D+13
$1s^22p3s\ ^3P_1$	$1s^23s3d\ ^3D_2$	11.14096	0.60706D+14	0.24018D+14	0.22802D+14	0.20319D+14
$1s^22p3s\ ^3P_2$	$1s^23s3d\ ^3D_2$	11.27583	0.25929D+14	0.24018D+14	0.22802D+14	0.86786D+13
$1s^22p3s\ ^1P_1$	$1s^23s3d\ ^3D_2$	11.32777	0.21313D+14	0.24018D+14	0.22802D+14	0.71336D+13
$1s^22p3s\ ^3P_2$	$1s^23s3d\ ^3D_3$	11.26793	0.15277D+15	0.23875D+14	0.21145D+14	0.53256D+14
$1s^22p3d\ ^3F_4$	$1s^23s3d\ ^3D_3$	11.59170	0.76039D+13	0.23875D+14	0.21145D+14	0.26507D+13
$1s^22s3p\ ^3P_2$	$1s^23p^2\ ^3P_2$	10.77166	0.52951D+14	0.16436D+14	0.12826D+14	0.26486D+13
$1s^22s3p\ ^3P_1$	$1s^23p^2\ ^1D_2$	10.64450	0.48592D+13	0.22096D+14	0.16799D+15	0.18111D+13
$1s^22s3p\ ^1P_1$	$1s^23p^2\ ^1D_2$	10.68105	0.16534D+14	0.22096D+14	0.16799D+15	0.61623D+13
$1s^22p3s\ ^3P_1$	$1s^23p^2\ ^1D_2$	10.98156	0.95042D+13	0.22096D+14	0.16799D+15	0.35423D+13
$1s^22p3s\ ^1P_1$	$1s^23p^2\ ^1D_2$	11.16301	0.40016D+14	0.22096D+14	0.16799D+15	0.14914D+14
$1s^22p3d\ ^3F_2$	$1s^23p^2\ ^1D_2$	11.25592	0.74537D+13	0.22096D+14	0.16799D+15	0.27780D+13
$1s^22p3d\ ^3P_2$	$1s^23p^2\ ^1D_2$	11.32129	0.86539D+13	0.22096D+14	0.16799D+15	0.32254D+13
$1s^22p3d\ ^1D_2$	$1s^23p^2\ ^1D_2$	11.43741	0.14248D+14	0.22096D+14	0.16799D+15	0.53103D+13
$1s^22p3d\ ^1P_1$	$1s^23p^2\ ^1D_2$	11.57627	0.43870D+13	0.22096D+14	0.16799D+15	0.16351D+13
$1s^22p3p\ ^3D_2$	$1s^23p3d\ ^3F_3$	11.20489	0.86020D+14	0.28834D+14	0.66003D+12	0.15376D+13
$1s^22s3d\ ^1D_2$	$1s^23p3d\ ^1F_3$	10.73085	0.30605D+14	0.28676D+14	0.94980D+14	0.44019D+13
$1s^22p3p\ ^3D_2$	$1s^23p3d\ ^1F_3$	11.03358	0.19829D+14	0.28676D+14	0.94980D+14	0.28520D+13
$1s^22p3p\ ^3P_2$	$1s^23p3d\ ^1F_3$	11.17672	0.23984D+14	0.28676D+14	0.94980D+14	0.34496D+13
$1s^22p3p\ ^1D_2$	$1s^23p3d\ ^1F_3$	11.25173	0.12425D+15	0.28676D+14	0.94980D+14	0.17871D+14
$1s^22p3d\ ^1P_1$	$1s^23d^2\ ^1S_0$	11.16419	0.31609D+14	0.37593D+14	0.31480D+14	0.75685D+13
$1s^22p3d\ ^3D_3$	$1s^23d^2\ ^3F_4$	11.31322	0.23631D+15	0.42332D+14	0.19288D+13	0.18741D+13
$1s^22p3d\ ^3F_3$	$1s^23d^2\ ^1G_4$	11.10128	0.29946D+14	0.41801D+14	0.19099D+15	0.43014D+13
$1s^22p3d\ ^1F_3$	$1s^23d^2\ ^1G_4$	11.34755	0.33778D+15	0.41801D+14	0.19099D+15	0.48518D+14
$1s^22s4s\ ^3S_1$	$1s^23p4s\ ^3P_1$	10.68504	0.18854D+14	0.93702D+13	0.15348D+14	0.47891D+13
$1s^22s4s\ ^3S_1$	$1s^23p4s\ ^3P_2$	10.65602	0.35183D+14	0.98948D+13	0.65432D+13	0.58360D+13
$1s^22s4s\ ^1S_0$	$1s^23p4s\ ^1P_1$	10.65425	0.16148D+14	0.98335D+13	0.84617D+14	0.52224D+13
$1s^22s4p\ ^3P_1$	$1s^23d4s\ ^1D_2$	10.67874	0.17982D+14	0.16448D+14	0.11317D+14	0.21713D+13
$1s^22p4s\ ^1P_1$	$1s^23d4s\ ^1D_2$	11.25082	0.39870D+14	0.16448D+14	0.11317D+14	0.48142D+13
$1s^22p4p\ ^3D_2$	$1s^23d4p\ ^3F_3$	11.07282	0.79744D+14	0.24159D+14	0.95999D+12	0.26200D+13
$1s^22p3p\ ^1D_2$	$1s^23d4p\ ^1F_3$	8.44304	0.13638D+14	0.20795D+14	0.60973D+14	0.22759D+13

Table IV (continue)

lower level	upper level	$\lambda(\AA)$	$gAr(1/s)$	$\sum Ar$	$Aa(1/s)$	Qd
$1s^22s4d\ ^1D_2$	$1s^23d4p\ ^1F_3$	10.58853	0.14773D+14	0.20795D+14	0.60973D+14	0.24653D+13
$1s^22p4p\ ^3D_2$	$1s^23d4p\ ^1F_3$	10.99129	0.16451D+14	0.20795D+14	0.60973D+14	0.27453D+13
$1s^22p4p\ ^3P_2$	$1s^23d4p\ ^1F_3$	11.12894	0.14669D+14	0.20795D+14	0.60973D+14	0.24479D+13
$1s^22p4p\ ^3D_3$	$1s^23d4p\ ^3F_4$	11.19866	0.16395D+15	0.23821D+14	0.90436D+12	0.51172D+13
$1s^22p4f\ ^3G_3$	$1s^23s4f\ ^3F_2$	11.31927	0.27839D+13	0.31499D+13	0.55761D+13	0.16751D+13
$1s^22p4f\ ^3F_2$	$1s^23s4f\ ^3F_2$	11.48581	0.34387D+13	0.31499D+13	0.55761D+13	0.20691D+13
$1s^22p4f\ ^3F_4$	$1s^23s4f\ ^3F_3$	11.47949	0.42123D+13	0.30387D+13	0.57989D+13	0.25993D+13
$1s^22p4f\ ^3D_3$	$1s^23s4f\ ^3F_3$	11.48494	0.28362D+13	0.30387D+13	0.57989D+13	0.17502D+13
$1s^22p4f\ ^3D_3$	$1s^23s4f\ ^3F_4$	11.32041	0.35584D+13	0.29326D+13	0.60249D+13	0.22498D+13
$1s^22p4f\ ^3G_4$	$1s^23s4f\ ^3F_4$	11.32051	0.43377D+13	0.29326D+13	0.60249D+13	0.27425D+13
$1s^22p4f\ ^3F_4$	$1s^23s4f\ ^3F_4$	11.47708	0.44519D+13	0.29326D+13	0.60249D+13	0.28147D+13
$1s^22p4f\ ^3G_5$	$1s^23s4f\ ^3F_4$	11.48379	0.81945D+13	0.29326D+13	0.60249D+13	0.51809D+13
$1s^22s4f\ ^3F_2$	$1s^23p4f\ ^3G_3$	10.71147	0.25960D+14	0.85067D+13	0.16611D+13	0.25243D+13
$1s^22s4f\ ^1F_3$	$1s^23p4f\ ^1D_2$	10.61138	0.27012D+14	0.12546D+14	0.70413D+13	0.49198D+13
$1s^22p4d\ ^1D_2$	$1s^23p4f\ ^1D_2$	11.19218	0.93989D+13	0.12546D+14	0.70413D+13	0.17119D+13
$1s^22s4f\ ^3F_3$	$1s^23p4f\ ^3G_4$	10.69935	0.20518D+14	0.87660D+13	0.64416D+13	0.51221D+13
$1s^22s4f\ ^3F_4$	$1s^23p4f\ ^3G_4$	10.70101	0.35221D+14	0.87660D+13	0.64416D+13	0.87926D+13
$1s^22s4f\ ^1F_3$	$1s^23p4f\ ^3G_4$	10.70584	0.86883D+13	0.87660D+13	0.64416D+13	0.21689D+13
$1s^22p4d\ ^3F_3$	$1s^23p4f\ ^3G_4$	11.15826	0.82661D+13	0.87660D+13	0.64416D+13	0.20636D+13
$1s^22s4f\ ^3F_3$	$1s^23p4f\ ^3F_4$	10.66814	0.35642D+14	0.98078D+13	0.86367D+12	0.23719D+13
$1s^22s4f\ ^3F_4$	$1s^23p4f\ ^3F_4$	10.66979	0.25912D+14	0.98078D+13	0.86367D+12	0.17244D+13
$1s^22s4f\ ^3F_4$	$1s^23p4f\ ^3G_5$	10.66978	0.75116D+14	0.98726D+13	0.20891D+13	0.88022D+13
$1s^22p4d\ ^3F_4$	$1s^23p4f\ ^3G_5$	11.26266	0.24641D+14	0.98726D+13	0.20891D+13	0.28875D+13
$1s^22p3d\ ^3F_3$	$1s^23p4f\ ^1G_4$	8.41776	0.94891D+13	0.15189D+14	0.78331D+14	0.29828D+13
$1s^22p3d\ ^1F_3$	$1s^23p4f\ ^1G_4$	8.55860	0.13720D+14	0.15189D+14	0.78331D+14	0.43127D+13
$1s^22s4f\ ^1F_3$	$1s^23p4f\ ^1G_4$	10.64139	0.39841D+14	0.15189D+14	0.78331D+14	0.12524D+14
$1s^22p4d\ ^3D_3$	$1s^23p4f\ ^1G_4$	11.23461	0.10884D+14	0.15189D+14	0.78331D+14	0.34213D+13
$1s^22p4d\ ^1F_3$	$1s^23p4f\ ^1G_4$	11.26545	0.54224D+14	0.15189D+14	0.78331D+14	0.17045D+14
$1s^22p4f\ ^1D_2$	$1s^23d4f\ ^1F_3$	11.15992	0.28398D+14	0.20906D+14	0.49951D+13	0.22488D+13
$1s^22p4f\ ^3G_3$	$1s^23d4f\ ^3H_4$	11.09335	0.16279D+15	0.22175D+14	0.90092D+13	0.22211D+14
$1s^22p4f\ ^1G_4$	$1s^23d4f\ ^3H_4$	11.25778	0.20816D+14	0.22175D+14	0.90092D+13	0.28401D+13
$1s^22p4f\ ^3G_4$	$1s^23d4f\ ^3H_5$	11.08976	0.11057D+15	0.21873D+14	0.11504D+14	0.17060D+14
$1s^22p4f\ ^3F_4$	$1s^23d4f\ ^3H_5$	11.23998	0.66203D+14	0.21873D+14	0.11504D+14	0.10215D+14
$1s^22p4f\ ^3G_5$	$1s^23d4f\ ^3H_5$	11.24641	0.12322D+14	0.21873D+14	0.11504D+14	0.19012D+13
$1s^22p4f\ ^1G_4$	$1s^23d4f\ ^3H_5$	11.24878	0.51449D+14	0.21873D+14	0.11504D+14	0.79383D+13
$1s^22p4f\ ^3D_3$	$1s^23d4f\ ^1G_4$	11.08923	0.33060D+14	0.21798D+14	0.24385D+13	0.18835D+13
$1s^22p4f\ ^3G_4$	$1s^23d4f\ ^1G_4$	11.08933	0.39707D+14	0.21798D+14	0.24385D+13	0.22622D+13
$1s^22p4f\ ^1F_3$	$1s^23d4f\ ^1G_4$	11.23641	0.79681D+14	0.21798D+14	0.24385D+13	0.45397D+13
$1s^22p4f\ ^3G_5$	$1s^23d4f\ ^3H_6$	11.23742	0.27946D+15	0.21503D+14	0.11472D+14	0.43360D+14
$1s^22p4f\ ^3D_3$	$1s^23d4f\ ^3F_3$	11.06938	0.47979D+14	0.21678D+14	0.14065D+13	0.16805D+13
$1s^22p4f\ ^1F_3$	$1s^23d4f\ ^1F_3$	11.14019	0.29545D+14	0.20906D+14	0.49951D+13	0.23396D+13
$1s^22p4f\ ^3D_3$	$1s^23d4f\ ^1F_3$	11.14839	0.36437D+14	0.20906D+14	0.49951D+13	0.28854D+13
$1s^22p4f\ ^3G_4$	$1s^23d4f\ ^1H_5$	10.96525	0.64997D+14	0.22407D+14	0.45812D+14	0.11964D+14
$1s^22p4f\ ^1G_4$	$1s^23d4f\ ^1H_5$	11.12069	0.17681D+15	0.22407D+14	0.45812D+14	0.32545D+14

Table V α values (in units of cm^3/s) to the final bound states as a function of T_e(eV).

T_e	$1s^22s^2\ ^1S_0$	$1s^22s2p\ ^3P_0$	$1s^22s2p\ ^1P_1$	$1s^22s2p\ ^3P_1$	$1s^22s2p\ ^3P_2$	$1s^22p^2\ ^1S_0$
1.00	0.3560D-14	0.5563D-14	0.2345D-12	0.7293D-13	0.5199D-12	0.1247D-12
2.00	0.2912D-13	0.7130D-13	0.1505D-11	0.5510D-12	0.3216D-11	0.9205D-12
3.00	0.4762D-13	0.1395D-12	0.2217D-11	0.8932D-12	0.4663D-11	0.1425D-11
4.00	0.5598D-13	0.1862D-12	0.2452D-11	0.1062D-11	0.5104D-11	0.1615D-11
5.00	0.5916D-13	0.2200D-12	0.2488D-11	0.1149D-11	0.5138D-11	0.1661D-11
6.00	0.5989D-13	0.2465D-12	0.2448D-11	0.1199D-11	0.5021D-11	0.1646D-11
7.00	0.5945D-13	0.2684D-12	0.2381D-11	0.1231D-11	0.4852D-11	0.1608D-11
8.00	0.5844D-13	0.2867D-12	0.2305D-11	0.1252D-11	0.4672D-11	0.1559D-11
9.00	0.5715D-13	0.3018D-12	0.2230D-11	0.1265D-11	0.4495D-11	0.1509D-11
10.00	0.5572D-13	0.3139D-12	0.2156D-11	0.1272D-11	0.4327D-11	0.1458D-11
20.00	0.4186D-13	0.3353D-12	0.1594D-11	0.1166D-11	0.3109D-11	0.1059D-11
30.00	0.3189D-13	0.2908D-12	0.1227D-11	0.9670D-12	0.2364D-11	0.8048D-12
40.00	0.2505D-13	0.2435D-12	0.9724D-12	0.7939D-12	0.1863D-11	0.6334D-12
50.00	0.2024D-13	0.2044D-12	0.7916D-12	0.6590D-12	0.1511D-11	0.5132D-12
60.00	0.1676D-13	0.1734D-12	0.6591D-12	0.5554D-12	0.1255D-11	0.4258D-12
70.00	0.1416D-13	0.1490D-12	0.5590D-12	0.4750D-12	0.1063D-11	0.3603D-12
80.00	0.1216D-13	0.1295D-12	0.4815D-12	0.4116D-12	0.9144D-12	0.3098D-12
90.00	0.1058D-13	0.1138D-12	0.4201D-12	0.3608D-12	0.7971D-12	0.2699D-12
100.00	0.9319D-14	0.1010D-12	0.3706D-12	0.3194D-12	0.7027D-12	0.2378D-12
200.00	0.3812D-14	0.4257D-13	0.1527D-12	0.1335D-12	0.2883D-12	0.9743D-13
300.00	0.2189D-14	0.2460D-13	0.8772D-13	0.7692D-13	0.1652D-12	0.5581D-13
400.00	0.1463D-14	0.1647D-13	0.5857D-13	0.5143D-13	0.1102D-12	0.3720D-13
500.00	0.1066D-14	0.1200D-13	0.4262D-13	0.3745D-13	0.8008D-13	0.2704D-13
600.00	0.8216D-15	0.9241D-14	0.3280D-13	0.2882D-13	0.6157D-13	0.2079D-13
700.00	0.6582D-15	0.7397D-14	0.2624D-13	0.2306D-13	0.4923D-13	0.1663D-13
800.00	0.5427D-15	0.6094D-14	0.2161D-13	0.1900D-13	0.4053D-13	0.1369D-13
900.00	0.4575D-15	0.5134D-14	0.1820D-13	0.1600D-13	0.3411D-13	0.1152D-13
1000.00	0.3925D-15	0.4401D-14	0.1560D-13	0.1371D-13	0.2923D-13	0.9874D-14
2000.00	0.1420D-15	0.1585D-14	0.5618D-14	0.4935D-14	0.1050D-13	0.3549D-14
3000.00	0.7791D-16	0.8680D-15	0.3077D-14	0.2702D-14	0.5747D-14	0.1943D-14
4000.00	0.5082D-16	0.5655D-15	0.2005D-14	0.1760D-14	0.3743D-14	0.1265D-14
5000.00	0.3646D-16	0.4054D-15	0.1437D-14	0.1262D-14	0.2683D-14	0.9069D-15
6000.00	0.2778D-16	0.3088D-15	0.1095D-14	0.9610D-15	0.2043D-14	0.6906D-15
7000.00	0.2208D-16	0.2453D-15	0.8695D-15	0.7633D-15	0.1623D-14	0.5485D-15
8000.00	0.1808D-16	0.2009D-15	0.7122D-15	0.6251D-15	0.1329D-14	0.4492D-15
9000.00	0.1517D-16	0.1684D-15	0.5971D-15	0.5242D-15	0.1114D-14	0.3766D-15
10000.00	0.1296D-16	0.1439D-15	0.5101D-15	0.4477D-15	0.9515D-15	0.3217D-15

Table V (continued)

T_e	$1s^22p^2\ ^3P_0$	$1s^22p^2\ ^3P_1$	$1s^22p^2\ ^3P_2$	$1s^22p^2\ ^1D_2$	$1s^22s3s\ ^1S_0$	$1s^22s3s\ ^3S_1$
1.00	0.4066D-13	0.2258D-12	0.3966D-12	0.6625D-12	0.6905D-15	0.1392D-14
2.00	0.4513D-12	0.1609D-11	0.3042D-11	0.4796D-11	0.5458D-14	0.9939D-14
3.00	0.8430D-12	0.2468D-11	0.4882D-11	0.7360D-11	0.8821D-14	0.1526D-13
4.00	0.1073D-11	0.2801D-11	0.5690D-11	0.8295D-11	0.1030D-13	0.1728D-13
5.00	0.1195D-11	0.2909D-11	0.5981D-11	0.8498D-11	0.1084D-13	0.1784D-13
6.00	0.1257D-11	0.2929D-11	0.6031D-11	0.8400D-11	0.1094D-13	0.1782D-13
7.00	0.1283D-11	0.2913D-11	0.5966D-11	0.8182D-11	0.1083D-13	0.1755D-13
8.00	0.1289D-11	0.2882D-11	0.5844D-11	0.7921D-11	0.1062D-13	0.1719D-13
9.00	0.1281D-11	0.2845D-11	0.5694D-11	0.7649D-11	0.1036D-13	0.1680D-13
10.00	0.1266D-11	0.2804D-11	0.5530D-11	0.7382D-11	0.1009D-13	0.1639D-13
20.00	0.9917D-12	0.2319D-11	0.3996D-11	0.5318D-11	0.7514D-14	0.1270D-13
30.00	0.7544D-12	0.1861D-11	0.2961D-11	0.4025D-11	0.5797D-14	0.1046D-13
40.00	0.5890D-12	0.1506D-11	0.2285D-11	0.3161D-11	0.5311D-14	0.1252D-13
50.00	0.4734D-12	0.1240D-11	0.1825D-11	0.2558D-11	0.6539D-14	0.2171D-13
60.00	0.3901D-12	0.1040D-11	0.1498D-11	0.2121D-11	0.9411D-14	0.3759D-13
70.00	0.3282D-12	0.8860D-12	0.1257D-11	0.1793D-11	0.1340D-13	0.5760D-13
80.00	0.2808D-12	0.7659D-12	0.1073D-11	0.1541D-11	0.1792D-13	0.7907D-13
90.00	0.2437D-12	0.6700D-12	0.9301D-12	0.1342D-11	0.2251D-13	0.1001D-12
100.00	0.2140D-12	0.5923D-12	0.8161D-12	0.1182D-11	0.2688D-13	0.1195D-12
200.00	0.8618D-13	0.2460D-12	0.3272D-12	0.4836D-12	0.4940D-13	0.2078D-12
300.00	0.4904D-13	0.1415D-12	0.1860D-12	0.2768D-12	0.5095D-13	0.2061D-12
400.00	0.3258D-13	0.9450D-13	0.1235D-12	0.1845D-12	0.4707D-13	0.1857D-12
500.00	0.2363D-13	0.6877D-13	0.8952D-13	0.1341D-12	0.4218D-13	0.1638D-12
600.00	0.1814D-13	0.5291D-13	0.6871D-13	0.1030D-12	0.3752D-13	0.1440D-12
700.00	0.1449D-13	0.4232D-13	0.5487D-13	0.8238D-13	0.3341D-13	0.1272D-12
800.00	0.1192D-13	0.3485D-13	0.4513D-13	0.6780D-13	0.2987D-13	0.1130D-12
900.00	0.1002D-13	0.2935D-13	0.3796D-13	0.5707D-13	0.2684D-13	0.1010D-12
1000.00	0.8585D-14	0.2515D-13	0.3251D-13	0.4890D-13	0.2425D-13	0.9093D-13
2000.00	0.3077D-14	0.9045D-14	0.1165D-13	0.1756D-13	0.1116D-13	0.4108D-13
3000.00	0.1683D-14	0.4952D-14	0.6370D-14	0.9612D-14	0.6652D-14	0.2434D-13
4000.00	0.1096D-14	0.3226D-14	0.4147D-14	0.6260D-14	0.4525D-14	0.1651D-13
5000.00	0.7850D-15	0.2312D-14	0.2971D-14	0.4486D-14	0.3329D-14	0.1212D-13
6000.00	0.5977D-15	0.1761D-14	0.2262D-14	0.3417D-14	0.2580D-14	0.9384D-14
7000.00	0.4746D-15	0.1398D-14	0.1797D-14	0.2713D-14	0.2075D-14	0.7541D-14
8000.00	0.3887D-15	0.1145D-14	0.1471D-14	0.2222D-14	0.1715D-14	0.6230D-14
9000.00	0.3259D-15	0.9602D-15	0.1233D-14	0.1863D-14	0.1449D-14	0.5260D-14
10000.00	0.2783D-15	0.8202D-15	0.1053D-14	0.1591D-14	0.1245D-14	0.4517D-14

Table V (continued)

T_e	$1s^22s3p\,^3P_0$	$1s^22s3p\,^1P_1$	$1s^22s3p\,^3P_1$	$1s^22s3p\,^3P_2$	$1s^22s3d\,^3D_1$	$1s^22s3d\,^1D_2$
1.00	0.6749D-16	0.3816D-14	0.2446D-14	0.4027D-15	0.5752D-15	0.2487D-14
2.00	0.5352D-15	0.2605D-13	0.1584D-13	0.2687D-14	0.5522D-14	0.1968D-13
3.00	0.8551D-15	0.3985D-13	0.2347D-13	0.4014D-14	0.9729D-14	0.3179D-13
4.00	0.9931D-15	0.4538D-13	0.2607D-13	0.4485D-14	0.1198D-13	0.3713D-13
5.00	0.1046D-14	0.4727D-13	0.2656D-13	0.4607D-14	0.1305D-13	0.3906D-13
6.00	0.1063D-14	0.4768D-13	0.2625D-13	0.4598D-14	0.1351D-13	0.3942D-13
7.00	0.1063D-14	0.4745D-13	0.2563D-13	0.4544D-14	0.1363D-13	0.3902D-13
8.00	0.1055D-14	0.4694D-13	0.2492D-13	0.4473D-14	0.1356D-13	0.3827D-13
9.00	0.1044D-14	0.4630D-13	0.2420D-13	0.4398D-14	0.1337D-13	0.3735D-13
10.00	0.1030D-14	0.4559D-13	0.2349D-13	0.4322D-14	0.1312D-13	0.3636D-13
20.00	0.8535D-15	0.3740D-13	0.1778D-13	0.3557D-14	0.9948D-14	0.2701D-13
30.00	0.6846D-15	0.3015D-13	0.1396D-13	0.2896D-14	0.7499D-14	0.2048D-13
40.00	0.5563D-15	0.2651D-13	0.1239D-13	0.2638D-14	0.5901D-14	0.1637D-13
50.00	0.4668D-15	0.2830D-13	0.1389D-13	0.3080D-14	0.4955D-14	0.1434D-13
60.00	0.4086D-15	0.3541D-13	0.1832D-13	0.4266D-14	0.4490D-14	0.1406D-13
70.00	0.3759D-15	0.4629D-13	0.2478D-13	0.6010D-14	0.4355D-14	0.1509D-13
80.00	0.3656D-15	0.5908D-13	0.3223D-13	0.8065D-14	0.4425D-14	0.1693D-13
90.00	0.3764D-15	0.7228D-13	0.3985D-13	0.1023D-13	0.4611D-14	0.1918D-13
100.00	0.4074D-15	0.8491D-13	0.4710D-13	0.1235D-13	0.4850D-14	0.2157D-13
200.00	0.1326D-14	0.1440D-12	0.8121D-13	0.2510D-13	0.6449D-14	0.3571D-13
300.00	0.2090D-14	0.1389D-12	0.7907D-13	0.2721D-13	0.6333D-14	0.3621D-13
400.00	0.2375D-14	0.1219D-12	0.6988D-13	0.2577D-13	0.5726D-14	0.3299D-13
500.00	0.2392D-14	0.1051D-12	0.6059D-13	0.2340D-13	0.5064D-14	0.2925D-13
600.00	0.2290D-14	0.9087D-13	0.5258D-13	0.2098D-13	0.4464D-14	0.2580D-13
700.00	0.2143D-14	0.7914D-13	0.4593D-13	0.1877D-13	0.3949D-14	0.2282D-13
800.00	0.1987D-14	0.6952D-13	0.4044D-13	0.1684D-13	0.3512D-14	0.2030D-13
900.00	0.1835D-14	0.6160D-13	0.3590D-13	0.1517D-13	0.3143D-14	0.1817D-13
1000.00	0.1693D-14	0.5501D-13	0.3211D-13	0.1372D-13	0.2831D-14	0.1636D-13
2000.00	0.8508D-15	0.2392D-13	0.1407D-13	0.6349D-14	0.1283D-14	0.7399D-14
3000.00	0.5210D-15	0.1398D-13	0.8245D-14	0.3788D-14	0.7606D-15	0.4385D-14
4000.00	0.3590D-15	0.9412D-14	0.5559D-14	0.2578D-14	0.5159D-15	0.2973D-14
5000.00	0.2661D-15	0.6882D-14	0.4068D-14	0.1897D-14	0.3790D-15	0.2183D-14
6000.00	0.2073D-15	0.5312D-14	0.3141D-14	0.1470D-14	0.2934D-15	0.1690D-14
7000.00	0.1673D-15	0.4259D-14	0.2520D-14	0.1182D-14	0.2358D-15	0.1358D-14
8000.00	0.1387D-15	0.3513D-14	0.2079D-14	0.9775D-15	0.1948D-15	0.1122D-14
9000.00	0.1174D-15	0.2962D-14	0.1754D-14	0.8257D-15	0.1645D-15	0.9472D-15
10000.00	0.1010D-15	0.2542D-14	0.1505D-14	0.7094D-15	0.1413D-15	0.8134D-15

Table V (continued)

T_e	$1s^22s3d\ ^3D_2$	$1s^22s3d\ ^3D_3$	$1s^22p3s\ ^3P_0$	$1s^22p3s\ ^1P_1$	$1s^22p3s\ ^3P_1$	$1s^22p3s\ ^3P_2$
1.00	0.1367D-14	0.2069D-14	0.1733D-14	0.8329D-13	0.9075D-14	0.1571D-12
2.00	0.1074D-13	0.1401D-13	0.2201D-13	0.5277D-12	0.8831D-13	0.9720D-12
3.00	0.1739D-13	0.2098D-13	0.4293D-13	0.7718D-12	0.1593D-12	0.1410D-11
4.00	0.2037D-13	0.2333D-13	0.5721D-13	0.8483D-12	0.2029D-12	0.1543D-11
5.00	0.2148D-13	0.2370D-13	0.6748D-13	0.8560D-12	0.2313D-12	0.1554D-11
6.00	0.2173D-13	0.2328D-13	0.7554D-13	0.8378D-12	0.2520D-12	0.1518D-11
7.00	0.2155D-13	0.2257D-13	0.8218D-13	0.8106D-12	0.2680D-12	0.1468D-11
8.00	0.2117D-13	0.2176D-13	0.8771D-13	0.7811D-12	0.2807D-12	0.1413D-11
9.00	0.2068D-13	0.2094D-13	0.9225D-13	0.7519D-12	0.2909D-12	0.1360D-11
10.00	0.2014D-13	0.2013D-13	0.9593D-13	0.7241D-12	0.2987D-12	0.1309D-11
20.00	0.1493D-13	0.1396D-13	0.1022D-12	0.5211D-12	0.3008D-12	0.9413D-12
30.00	0.1126D-13	0.1029D-13	0.8874D-13	0.3969D-12	0.2566D-12	0.7165D-12
40.00	0.8940D-14	0.8077D-14	0.7550D-13	0.3164D-12	0.2167D-12	0.5706D-12
50.00	0.7699D-14	0.6917D-14	0.6702D-13	0.2672D-12	0.1919D-12	0.4806D-12
60.00	0.7307D-14	0.6549D-14	0.6346D-13	0.2409D-12	0.1820D-12	0.4313D-12
70.00	0.7511D-14	0.6729D-14	0.6360D-13	0.2302D-12	0.1832D-12	0.4095D-12
80.00	0.8079D-14	0.7247D-14	0.6603D-13	0.2293D-12	0.1911D-12	0.4049D-12
90.00	0.8835D-14	0.7946D-14	0.6961D-13	0.2339D-12	0.2025D-12	0.4100D-12
100.00	0.9658D-14	0.8722D-14	0.7358D-13	0.2411D-12	0.2151D-12	0.4198D-12
200.00	0.1478D-13	0.1440D-13	0.9329D-13	0.2898D-12	0.2797D-12	0.4814D-12
300.00	0.1509D-13	0.1570D-13	0.8720D-13	0.2759D-12	0.2645D-12	0.4450D-12
400.00	0.1393D-13	0.1512D-13	0.7631D-13	0.2460D-12	0.2332D-12	0.3889D-12
500.00	0.1250D-13	0.1393D-13	0.6602D-13	0.2159D-12	0.2027D-12	0.3367D-12
600.00	0.1113D-13	0.1264D-13	0.5730D-13	0.1895D-12	0.1766D-12	0.2925D-12
700.00	0.9914D-14	0.1141D-13	0.5010D-13	0.1671D-12	0.1548D-12	0.2559D-12
800.00	0.8868D-14	0.1031D-13	0.4417D-13	0.1483D-12	0.1368D-12	0.2258D-12
900.00	0.7974D-14	0.9342D-14	0.3926D-13	0.1326D-12	0.1218D-12	0.2008D-12
1000.00	0.7207D-14	0.8497D-14	0.3516D-13	0.1193D-12	0.1092D-12	0.1800D-12
2000.00	0.3322D-14	0.4024D-14	0.1552D-13	0.5380D-13	0.4850D-13	0.7970D-13
3000.00	0.1982D-14	0.2421D-14	0.9126D-14	0.3187D-13	0.2857D-13	0.4691D-13
4000.00	0.1348D-14	0.1654D-14	0.6163D-14	0.2160D-13	0.1932D-13	0.3170D-13
5000.00	0.9924D-15	0.1221D-14	0.4516D-14	0.1586D-13	0.1416D-13	0.2323D-13
6000.00	0.7693D-15	0.9477D-15	0.3490D-14	0.1228D-13	0.1095D-13	0.1796D-13
7000.00	0.6187D-15	0.7632D-15	0.2801D-14	0.9867D-14	0.8791D-14	0.1442D-13
8000.00	0.5116D-15	0.6315D-15	0.2312D-14	0.8152D-14	0.7259D-14	0.1190D-13
9000.00	0.4321D-15	0.5338D-15	0.1951D-14	0.6882D-14	0.6125D-14	0.1004D-13
10000.00	0.3713D-15	0.4589D-15	0.1675D-14	0.5910D-14	0.5258D-14	0.8621D-14

Table V (continued)

T_e	$1s^22p3p\,^1S_0$	$1s^22p3p\,^3P_0$	$1s^22p3p\,^3S_1$	$1s^22p3p\,^3P_1$	$1s^22p3p\,^3D_1$	$1s^22p3p\,^3P_2$
1.00	0.2114D-13	0.5884D-14	0.9870D-13	0.5826D-13	0.1159D-13	0.9713D-13
2.00	0.1518D-12	0.6928D-13	0.6998D-12	0.3982D-12	0.1600D-12	0.6653D-12
3.00	0.2325D-12	0.1321D-12	0.1071D-11	0.5989D-12	0.3175D-12	0.1005D-11
4.00	0.2617D-12	0.1698D-12	0.1212D-11	0.6679D-12	0.4159D-12	0.1125D-11
5.00	0.2680D-12	0.1905D-12	0.1254D-11	0.6800D-12	0.4710D-12	0.1148D-11
6.00	0.2649D-12	0.2012D-12	0.1256D-11	0.6696D-12	0.5000D-12	0.1131D-11
7.00	0.2580D-12	0.2061D-12	0.1243D-11	0.6506D-12	0.5133D-12	0.1098D-11
8.00	0.2498D-12	0.2075D-12	0.1223D-11	0.6289D-12	0.5170D-12	0.1059D-11
9.00	0.2414D-12	0.2067D-12	0.1201D-11	0.6068D-12	0.5146D-12	0.1019D-11
10.00	0.2331D-12	0.2045D-12	0.1177D-11	0.5853D-12	0.5083D-12	0.9788D-12
20.00	0.1690D-12	0.1609D-12	0.9461D-12	0.4212D-12	0.3910D-12	0.6703D-12
30.00	0.1285D-12	0.1224D-12	0.7515D-12	0.3186D-12	0.2926D-12	0.4885D-12
40.00	0.1013D-12	0.9550D-13	0.6055D-12	0.2503D-12	0.2263D-12	0.3745D-12
50.00	0.8220D-13	0.7678D-13	0.4990D-12	0.2032D-12	0.1813D-12	0.2992D-12
60.00	0.6833D-13	0.6337D-13	0.4207D-12	0.1698D-12	0.1501D-12	0.2475D-12
70.00	0.5795D-13	0.5348D-13	0.3623D-12	0.1455D-12	0.1278D-12	0.2108D-12
80.00	0.4997D-13	0.4598D-13	0.3177D-12	0.1274D-12	0.1113D-12	0.1842D-12
90.00	0.4369D-13	0.4016D-13	0.2831D-12	0.1135D-12	0.9888D-13	0.1643D-12
100.00	0.3865D-13	0.3553D-13	0.2555D-12	0.1026D-12	0.8924D-13	0.1491D-12
200.00	0.1664D-13	0.1595D-13	0.1337D-12	0.5585D-13	0.4981D-13	0.8848D-13
300.00	0.1003D-13	0.1028D-13	0.9147D-13	0.3957D-13	0.3719D-13	0.6738D-13
400.00	0.6982D-14	0.7615D-14	0.6880D-13	0.3049D-13	0.3008D-13	0.5443D-13
500.00	0.5262D-14	0.6041D-14	0.5448D-13	0.2455D-13	0.2518D-13	0.4526D-13
600.00	0.4168D-14	0.4984D-14	0.4462D-13	0.2035D-13	0.2152D-13	0.3840D-13
700.00	0.3415D-14	0.4221D-14	0.3745D-13	0.1724D-13	0.1868D-13	0.3309D-13
800.00	0.2870D-14	0.3643D-14	0.3204D-13	0.1486D-13	0.1641D-13	0.2889D-13
900.00	0.2458D-14	0.3189D-14	0.2782D-13	0.1297D-13	0.1456D-13	0.2550D-13
1000.00	0.2137D-14	0.2825D-14	0.2446D-13	0.1146D-13	0.1303D-13	0.2271D-13
2000.00	0.8300D-15	0.1202D-14	0.9955D-14	0.4766D-14	0.5774D-14	0.9832D-14
3000.00	0.4684D-15	0.7007D-15	0.5700D-14	0.2749D-14	0.3408D-14	0.5750D-14
4000.00	0.3100D-15	0.4717D-15	0.3800D-14	0.1839D-14	0.2307D-14	0.3874D-14
5000.00	0.2245D-15	0.3451D-15	0.2762D-14	0.1340D-14	0.1693D-14	0.2835D-14
6000.00	0.1721D-15	0.2664D-15	0.2124D-14	0.1032D-14	0.1310D-14	0.2189D-14
7000.00	0.1374D-15	0.2137D-15	0.1698D-14	0.8262D-15	0.1052D-14	0.1756D-14
8000.00	0.1129D-15	0.1763D-15	0.1398D-14	0.6807D-15	0.8692D-15	0.1449D-14
9000.00	0.9497D-16	0.1487D-15	0.1177D-14	0.5734D-15	0.7337D-15	0.1222D-14
10000.00	0.8130D-16	0.1276D-15	0.1008D-14	0.4916D-15	0.6300D-15	0.1048D-14

Table V (continued)

T_e	$1s^22p3p\ ^1D_2$	$1s^22p3p\ ^3D_2$	$1s^22p3p\ ^3D_3$	$1s^22p3d\ ^3P_0$	$1s^22p3d\ ^1P_1$	$1s^22p3d\ ^3P_1$
1.00	0.1152D-12	0.3322D-13	0.1632D-12	0.1573D-13	0.3401D-13	0.3998D-13
2.00	0.8146D-12	0.3483D-12	0.1089D-11	0.1177D-12	0.2574D-12	0.2970D-12
3.00	0.1239D-11	0.6409D-12	0.1620D-11	0.1818D-12	0.3992D-12	0.4578D-12
4.00	0.1389D-11	0.8101D-12	0.1794D-11	0.2052D-12	0.4516D-12	0.5161D-12
5.00	0.1417D-11	0.8996D-12	0.1816D-11	0.2102D-12	0.4634D-12	0.5285D-12
6.00	0.1398D-11	0.9441D-12	0.1777D-11	0.2077D-12	0.4585D-12	0.5219D-12
7.00	0.1358D-11	0.9631D-12	0.1716D-11	0.2021D-12	0.4469D-12	0.5078D-12
8.00	0.1313D-11	0.9666D-12	0.1647D-11	0.1955D-12	0.4329D-12	0.4912D-12
9.00	0.1266D-11	0.9607D-12	0.1578D-11	0.1886D-12	0.4183D-12	0.4739D-12
10.00	0.1221D-11	0.9487D-12	0.1511D-11	0.1819D-12	0.4039D-12	0.4570D-12
20.00	0.8775D-12	0.7415D-12	0.1012D-11	0.1305D-12	0.2920D-12	0.3278D-12
30.00	0.6646D-12	0.5634D-12	0.7288D-12	0.9859D-13	0.2213D-12	0.2476D-12
40.00	0.5233D-12	0.4400D-12	0.5549D-12	0.7736D-13	0.1742D-12	0.1942D-12
50.00	0.4269D-12	0.3549D-12	0.4408D-12	0.6259D-13	0.1423D-12	0.1572D-12
60.00	0.3605D-12	0.2953D-12	0.3621D-12	0.5193D-13	0.1207D-12	0.1305D-12
70.00	0.3146D-12	0.2525D-12	0.3058D-12	0.4397D-13	0.1063D-12	0.1107D-12
80.00	0.2825D-12	0.2210D-12	0.2641D-12	0.3787D-13	0.9677D-13	0.9557D-13
90.00	0.2598D-12	0.1974D-12	0.2325D-12	0.3308D-13	0.9055D-13	0.8373D-13
100.00	0.2433D-12	0.1791D-12	0.2079D-12	0.2924D-13	0.8651D-13	0.7429D-13
200.00	0.1810D-12	0.1060D-12	0.1108D-12	0.1257D-13	0.7575D-13	0.3355D-13
300.00	0.1483D-12	0.8122D-13	0.8454D-13	0.7597D-14	0.6664D-13	0.2131D-13
400.00	0.1224D-12	0.6608D-13	0.7052D-13	0.5307D-14	0.5702D-13	0.1550D-13
500.00	0.1023D-12	0.5527D-13	0.6056D-13	0.4010D-14	0.4872D-13	0.1208D-13
600.00	0.8677D-13	0.4709D-13	0.5278D-13	0.3182D-14	0.4193D-13	0.9822D-14
700.00	0.7462D-13	0.4071D-13	0.4649D-13	0.2612D-14	0.3643D-13	0.8217D-14
800.00	0.6497D-13	0.3563D-13	0.4131D-13	0.2197D-14	0.3197D-13	0.7020D-14
900.00	0.5717D-13	0.3151D-13	0.3698D-13	0.1884D-14	0.2831D-13	0.6095D-14
1000.00	0.5079D-13	0.2812D-13	0.3334D-13	0.1639D-14	0.2527D-13	0.5360D-14
2000.00	0.2161D-13	0.1226D-13	0.1529D-13	0.6389D-15	0.1099D-13	0.2199D-14
3000.00	0.1254D-13	0.7184D-14	0.9122D-14	0.3609D-15	0.6427D-14	0.1265D-14
4000.00	0.8417D-14	0.4846D-14	0.6210D-14	0.2390D-15	0.4328D-14	0.8462D-15
5000.00	0.6142D-14	0.3548D-14	0.4572D-14	0.1731D-15	0.3166D-14	0.6164D-15
6000.00	0.4734D-14	0.2741D-14	0.3545D-14	0.1327D-15	0.2444D-14	0.4746D-15
7000.00	0.3793D-14	0.2199D-14	0.2852D-14	0.1060D-15	0.1960D-14	0.3799D-15
8000.00	0.3126D-14	0.1815D-14	0.2359D-14	0.8712D-16	0.1617D-14	0.3130D-15
9000.00	0.2635D-14	0.1531D-14	0.1993D-14	0.7327D-16	0.1363D-14	0.2636D-15
10000.00	0.2260D-14	0.1314D-14	0.1712D-14	0.6273D-16	0.1170D-14	0.2260D-15

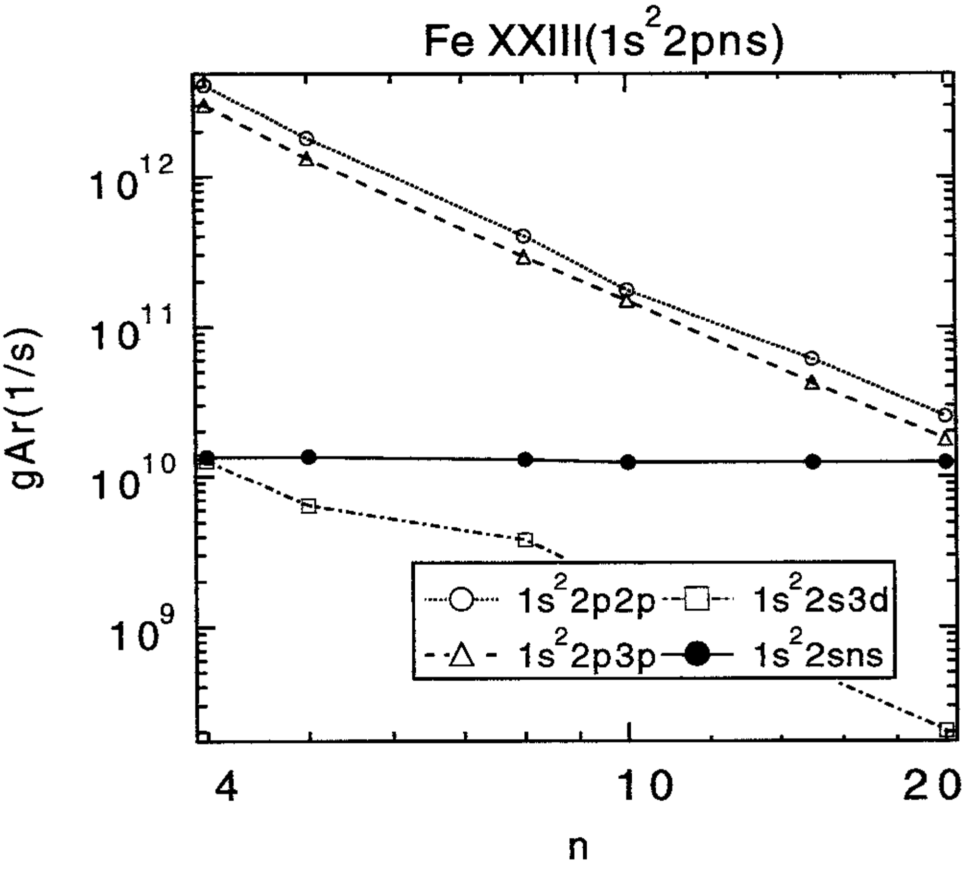
Fe XXIII(1s2 2pns)
1s2 2p2p
1s2 2s3d
1s2 2p3p
1s2 2sns
gAr(1/s)
10^{12}
10^{11}
10^{10}
10^{9}
4
10
20
n

Fig.1(a)

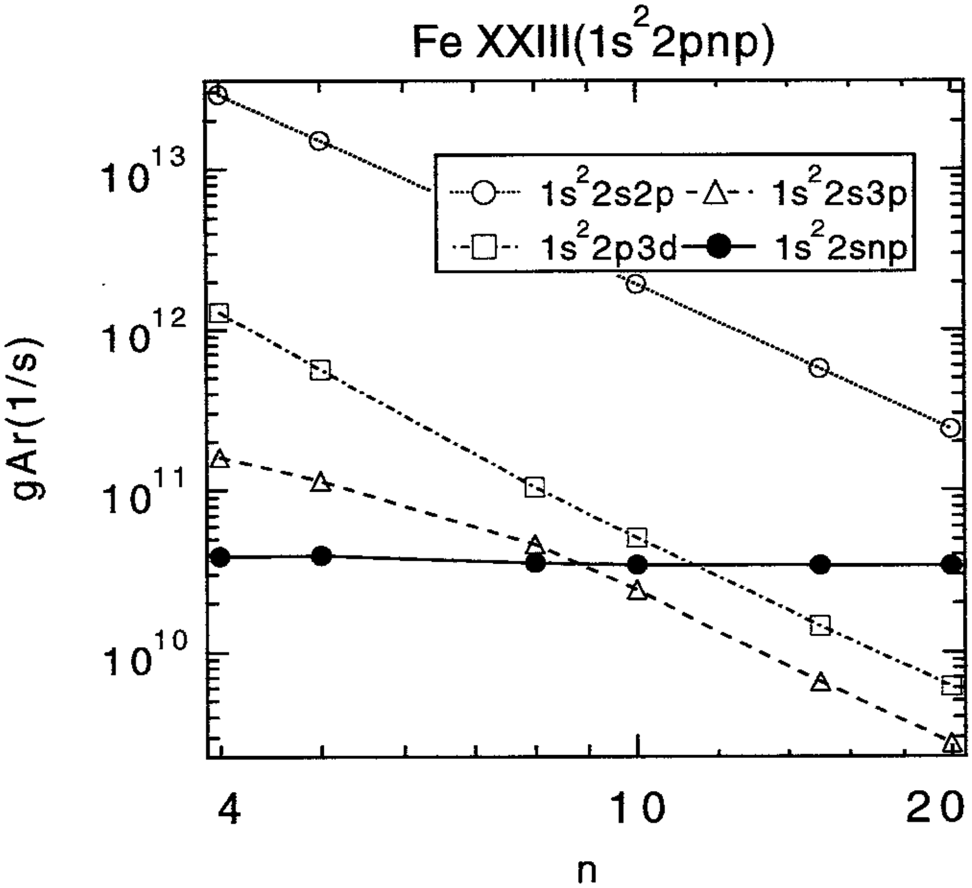
Fe XXIII(1s2 2pnp)
1s2 2s2p
1s2 2s3p
1s2 2p3d
1s2 2snp
gAr(1/s)
10^{13}
10^{12}
10^{11}
10^{10}
4
10
20
n

Fig.1(b)

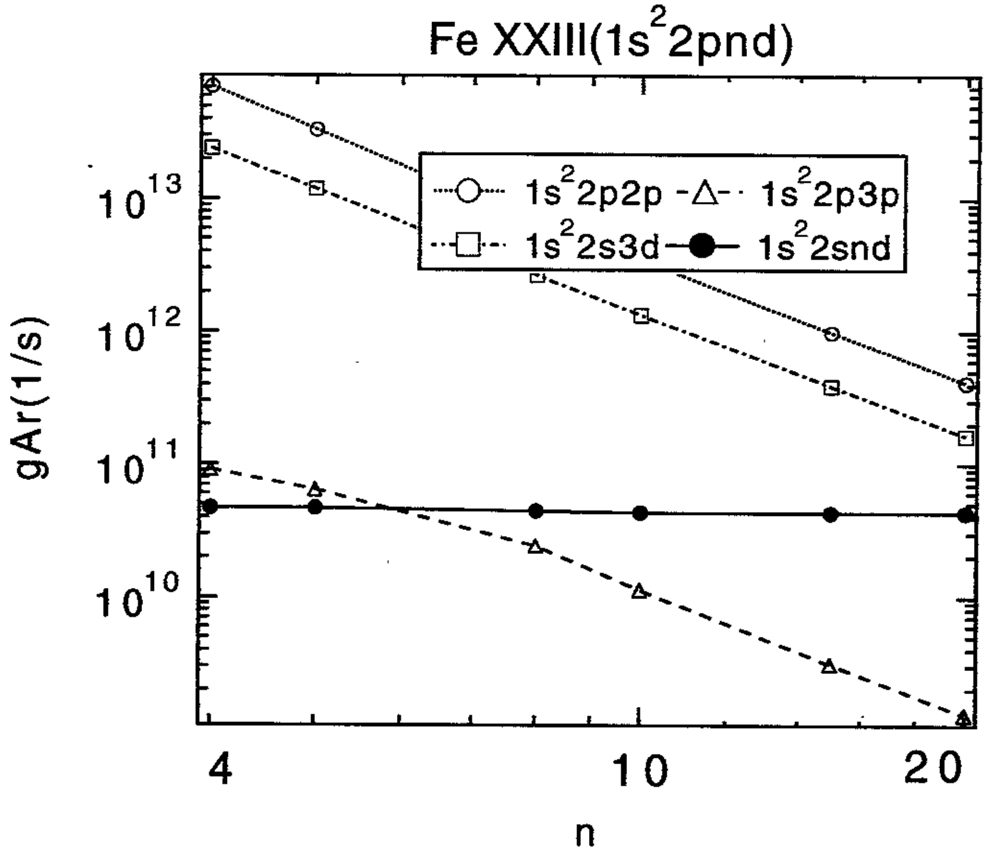
Fe XXIII(1s^{2}2pnd)
1s^{2}2p2p
1s^{2}2p3p
1s^{2}2s3d
1s^{2}2snd
gAr(1/s)
10^{13}
10^{12}
10^{11}
10^{10}
4
10
20
n

Fig.1(c)

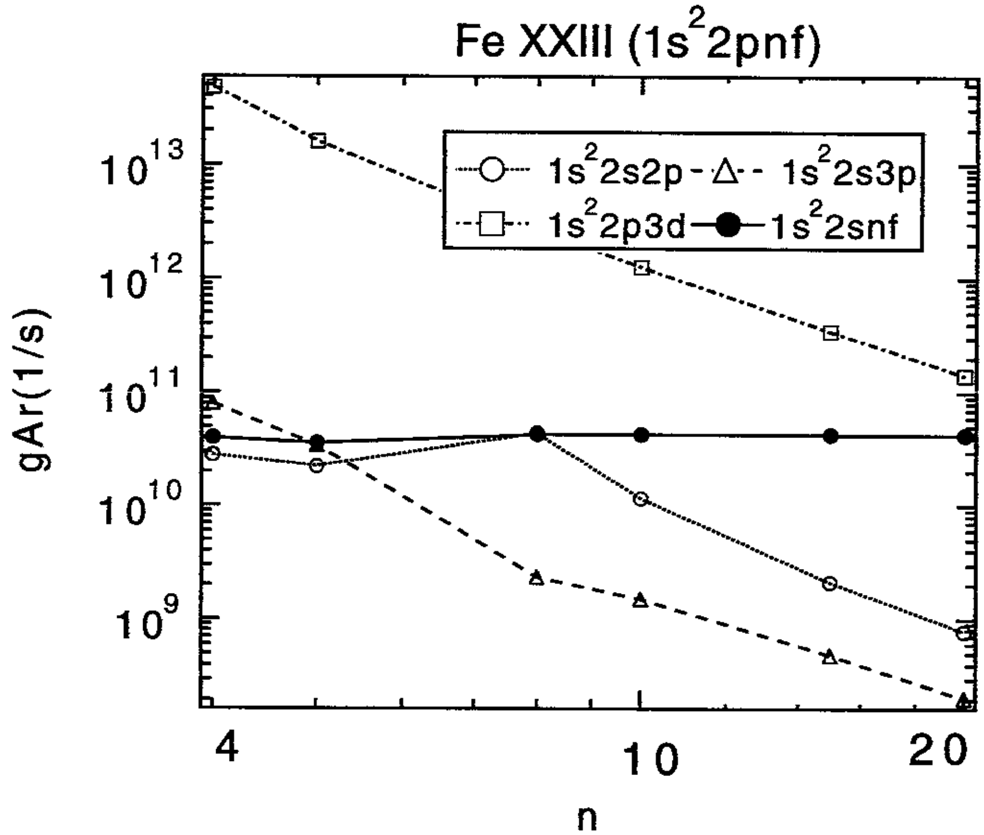
Fe XXIII (1s^{2}2pnf)
1s^{2}2s2p
1s^{2}2s3p
1s^{2}2p3d
1s^{2}2snf
gAr(1/s)
10^{13}
10^{12}
10^{11}
10^{10}
10^{9}
4
10
20
n

Fig.1(d)

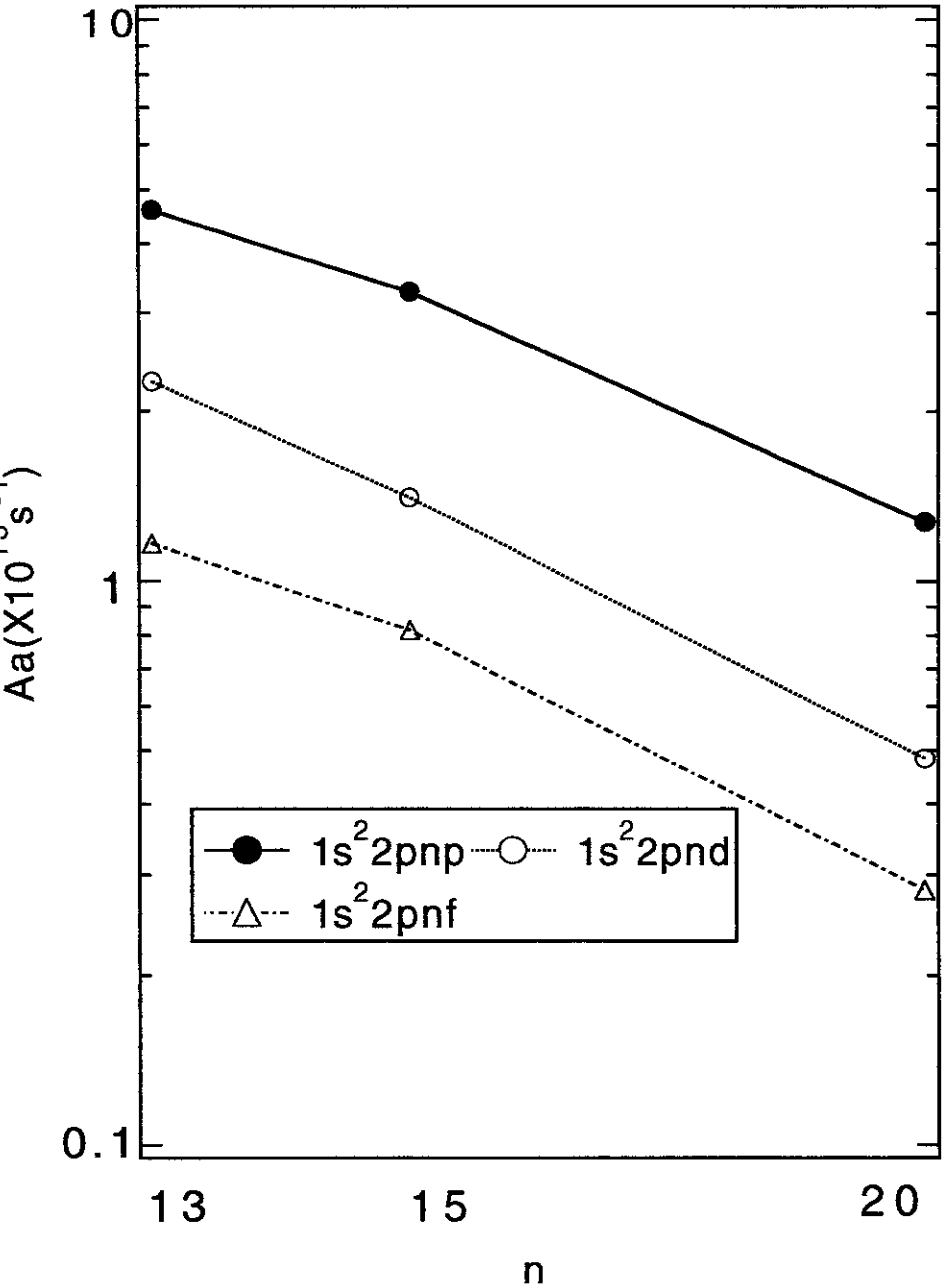

Fig.2

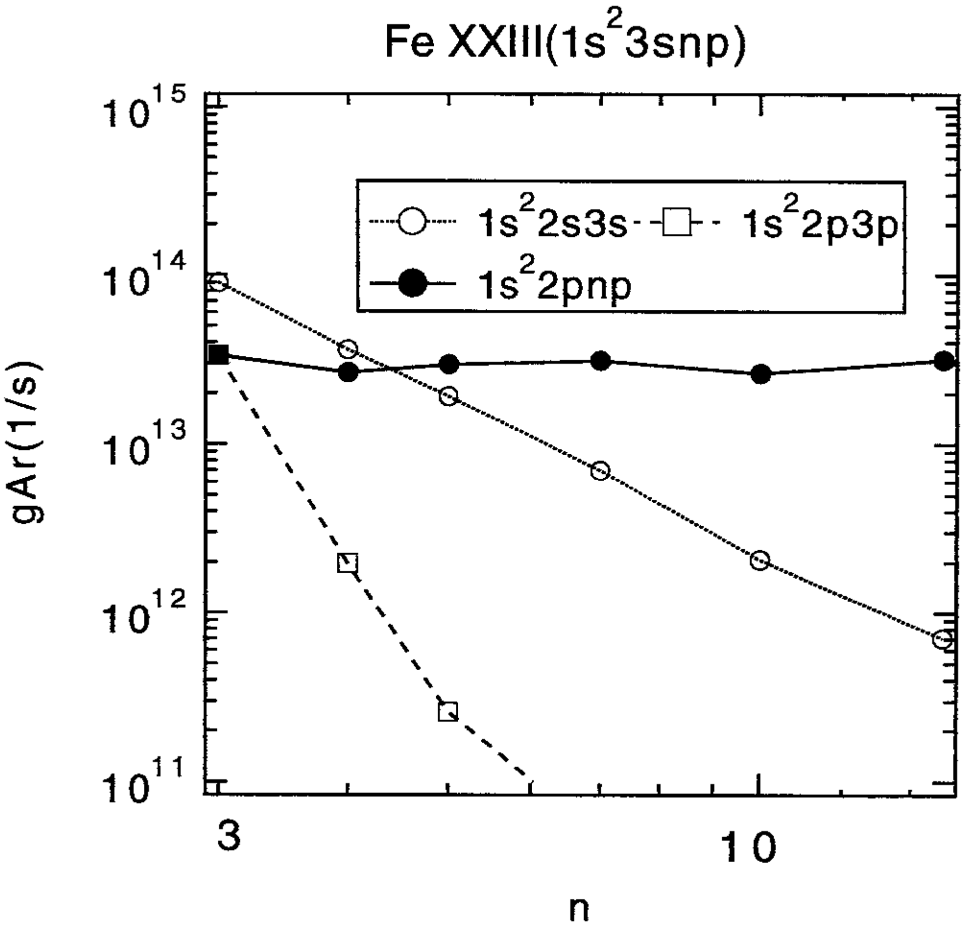
Fe XXIII(1s^{2}3snp)
10^{15}
10^{14}
10^{13}
10^{12}
10^{11}
gAr(1/s)
1s^{2}2s3s
1s^{2}2p3p
1s^{2}2pnp
3
10
n

Fig.3(a)

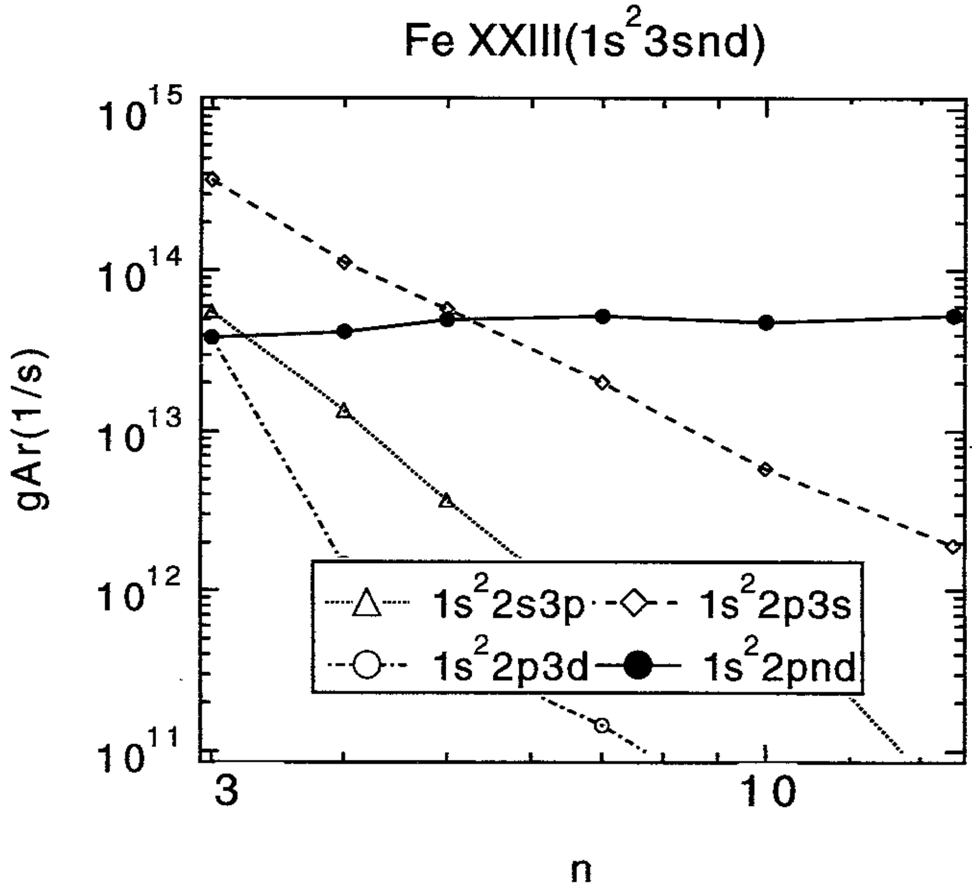
Fe XXIII(1s^{2}3snd)
10^{15}
10^{14}
10^{13}
10^{12}
10^{11}
gAr(1/s)
1s^{2}2s3p
1s^{2}2p3s
1s^{2}2p3d
1s^{2}2pnd
3
10
n

Fig.3(b)

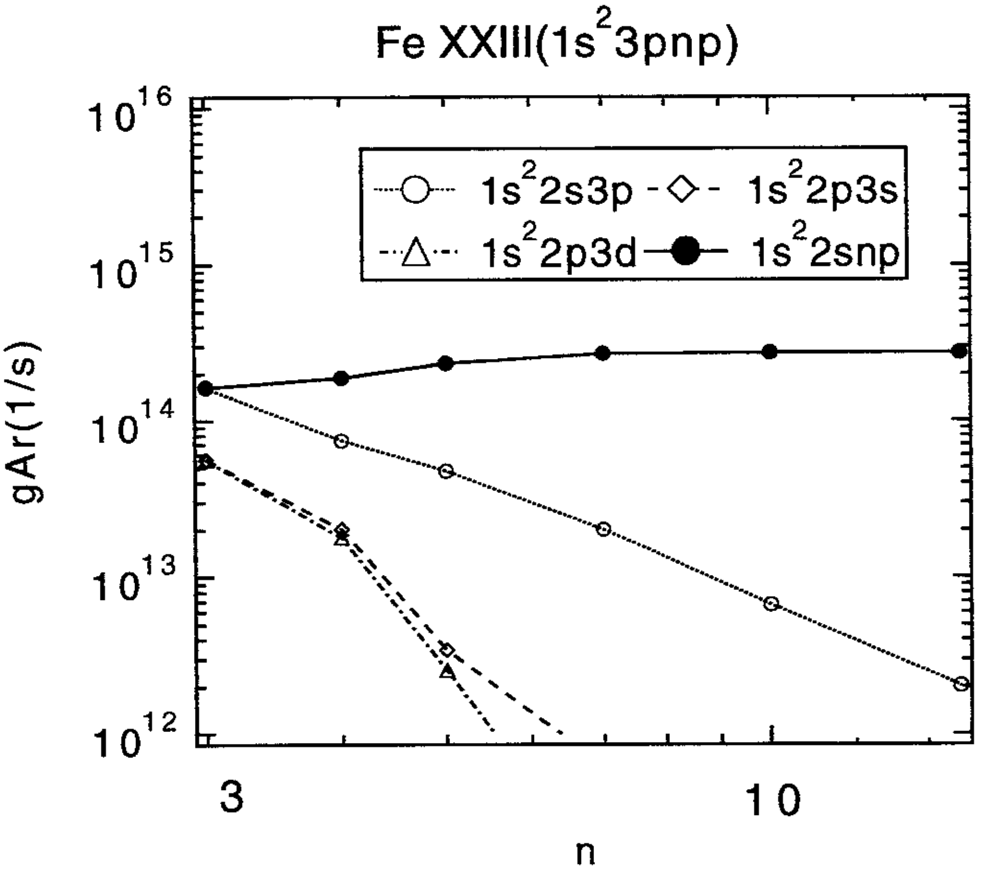

Fe XXIII(1s^{2}3pnp)
1s^{2}2s3p
1s^{2}2p3s
1s^{2}2p3d
1s^{2}2snp
gAr(1/s)
10^{16}
10^{15}
10^{14}
10^{13}
10^{12}
3
10
n

Fig.3(c)

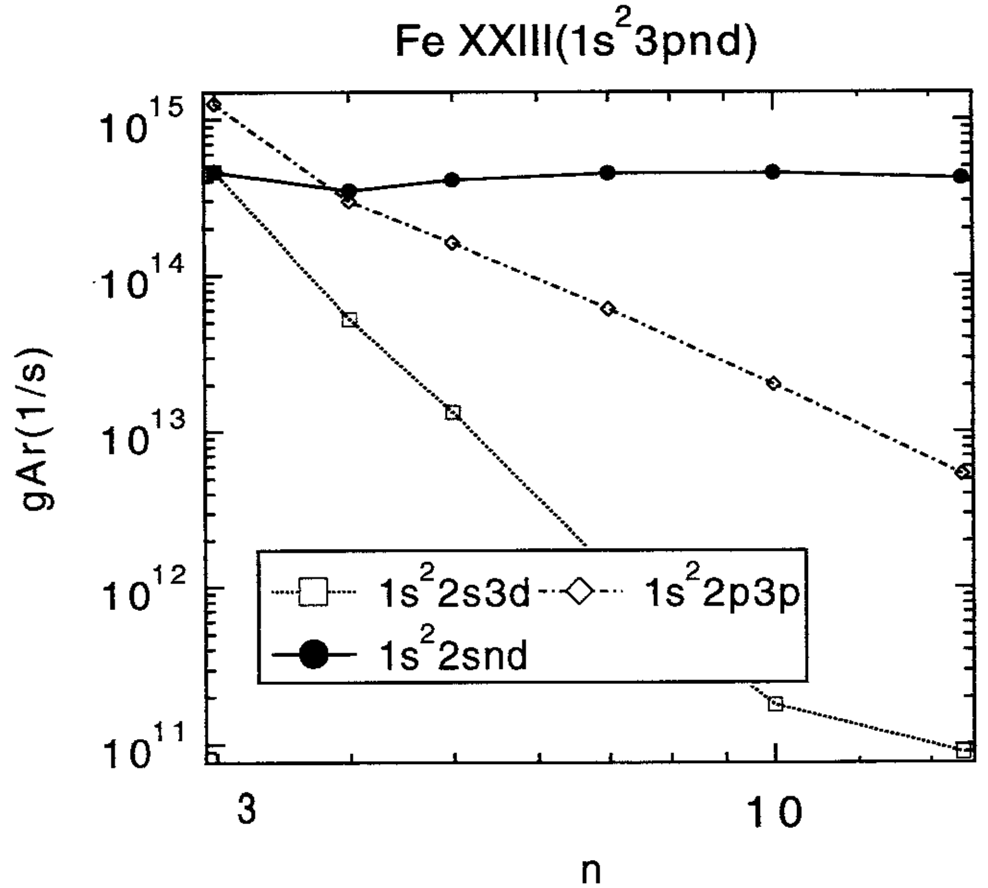

Fe XXIII(1s^{2}3pnd)
1s^{2}2s3d
1s^{2}2p3p
1s^{2}2snd
gAr(1/s)
10^{15}
10^{14}
10^{13}
10^{12}
10^{11}
3
10
n

Fig,3(d)

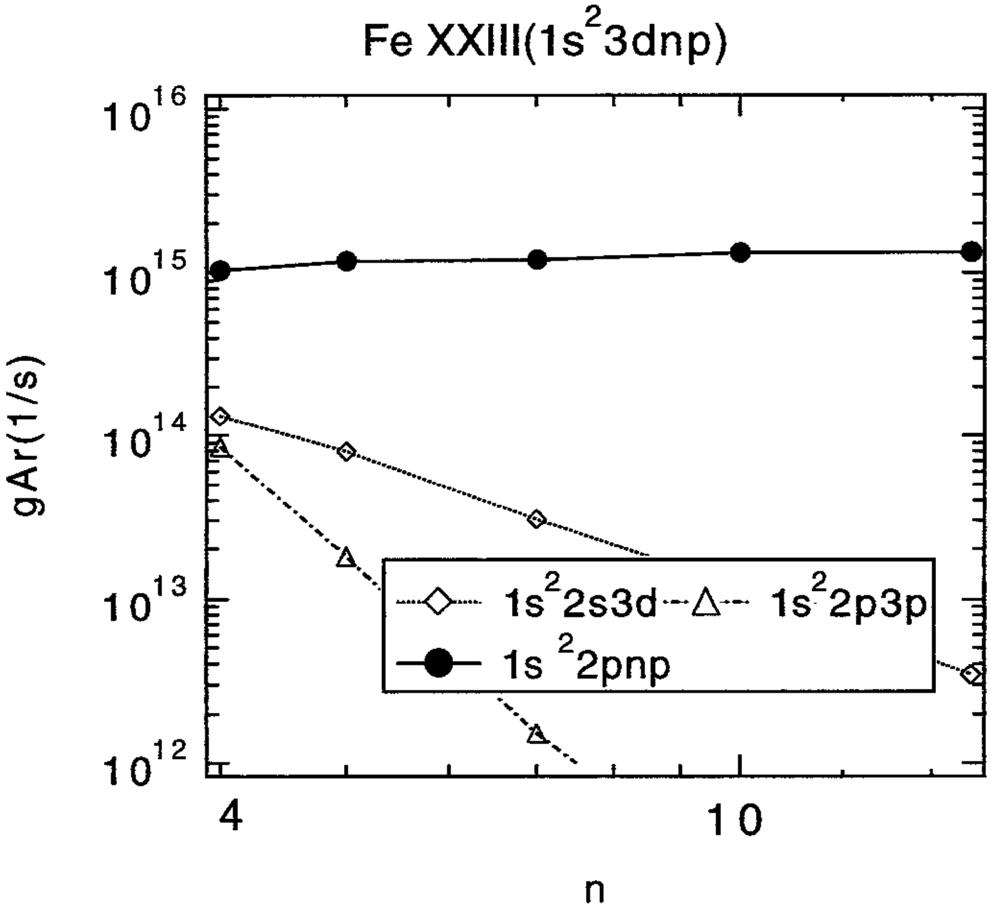
Fe XXIII(1s^{2}3dnp)
10^{16}
10^{15}
10^{14}
10^{13}
10^{12}
gAr(1/s)
1s^{2}2s3d
1s^{2}2p3p
1s ^{2}2pnp
4
10
n

Fig.3(e)

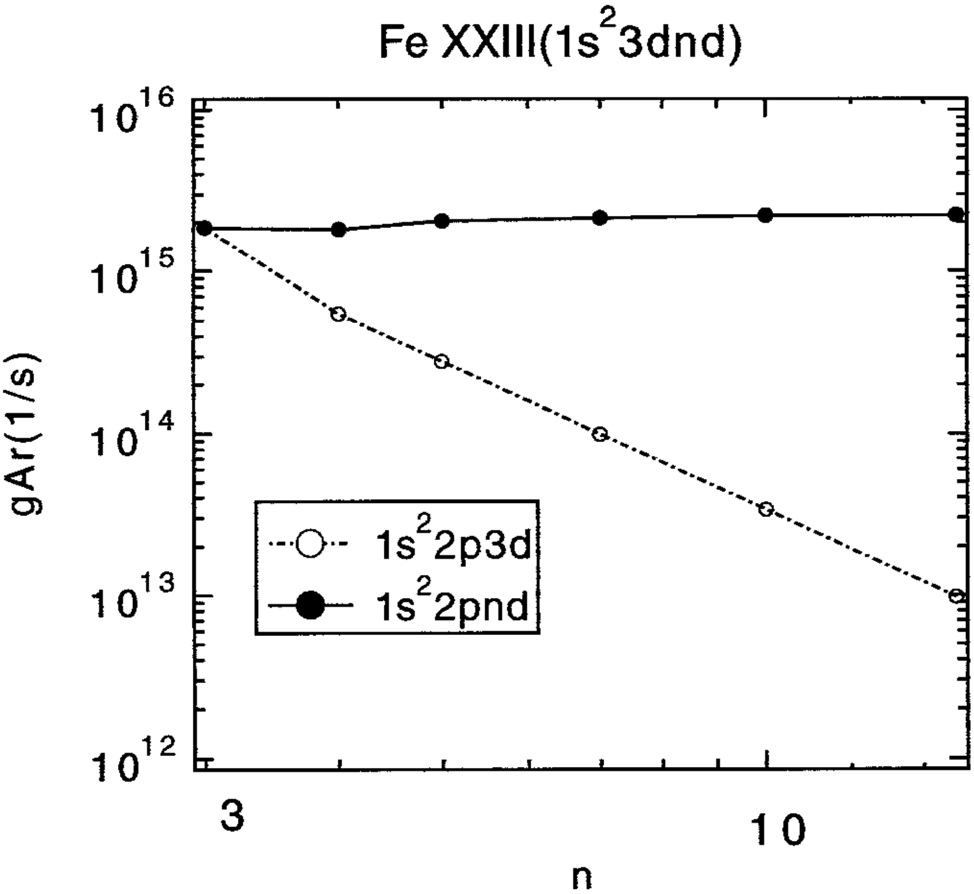
Fe XXIII(1s^{2}3dnd)
10^{16}
10^{15}
10^{14}
10^{13}
10^{12}
gAr(1/s)
1s^{2}2p3d
1s^{2}2pnd
3
10
n

Fig.3(f)

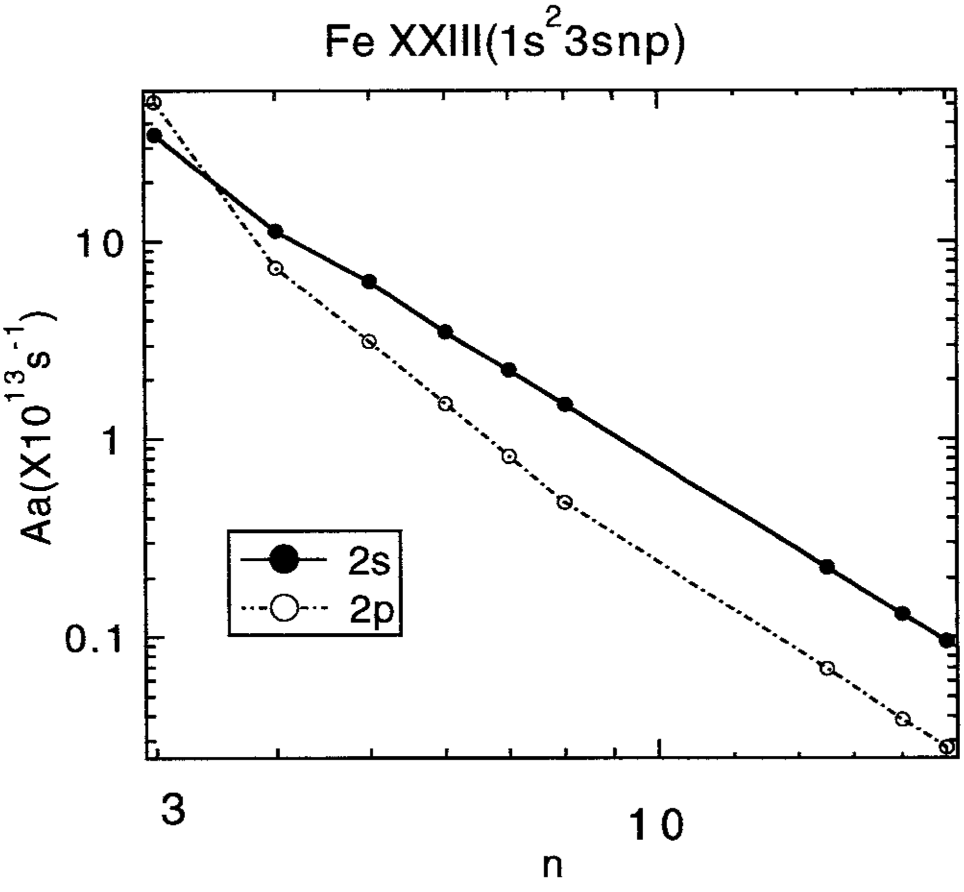

Fe XXIII(1s^{2}3snp)
10
1
0.1
Aa(X10^{13}s^{-1})
2s
2p
3
10
n

Fig.4(a)

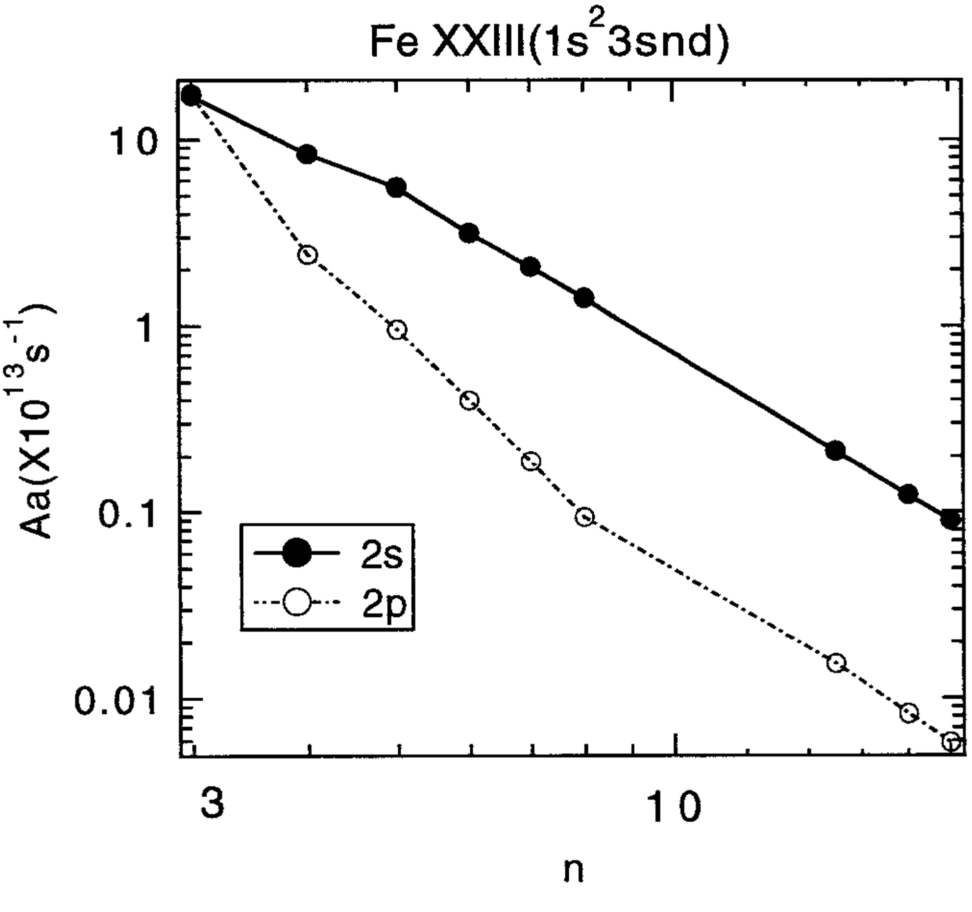

Fe XXIII(1s^{2}3snd)
10
1
0.1
0.01
Aa(X10^{13}s^{-1})
2s
2p
3
10
n

Fig.4(b)

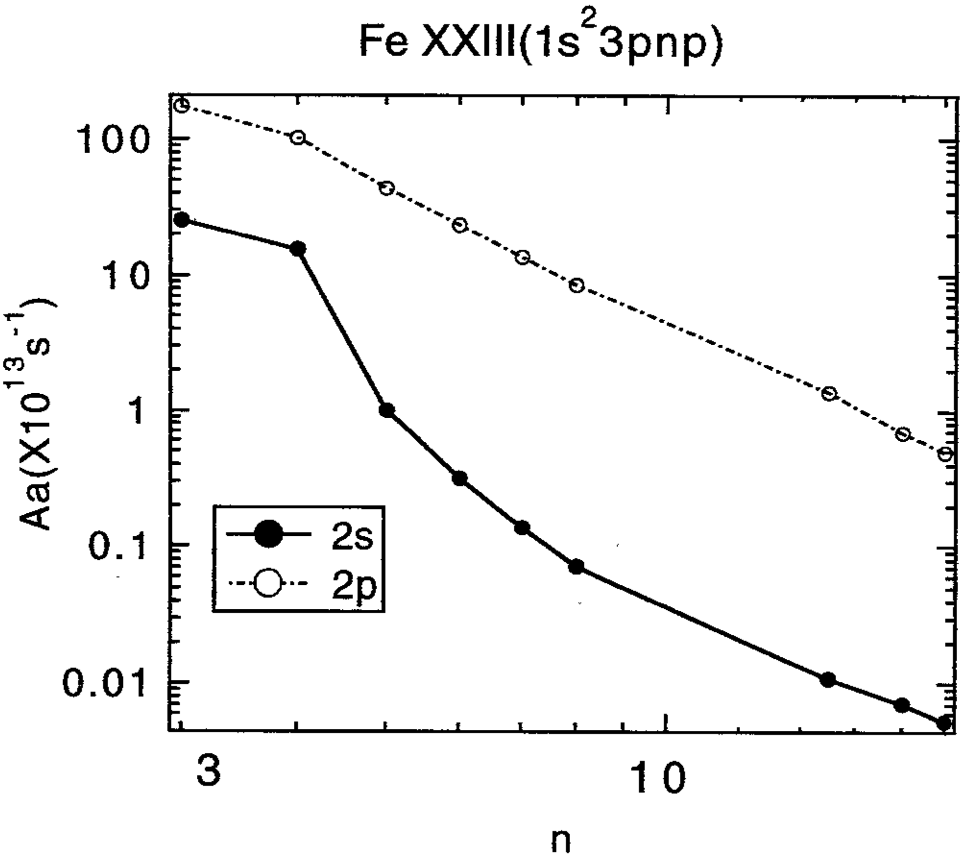

Fe XXIII(1s2 3pnp)
100
10
1
0.1
0.01
Aa(X10 13 s -1)
3
10
n
2s
2p

Fig.4(c)

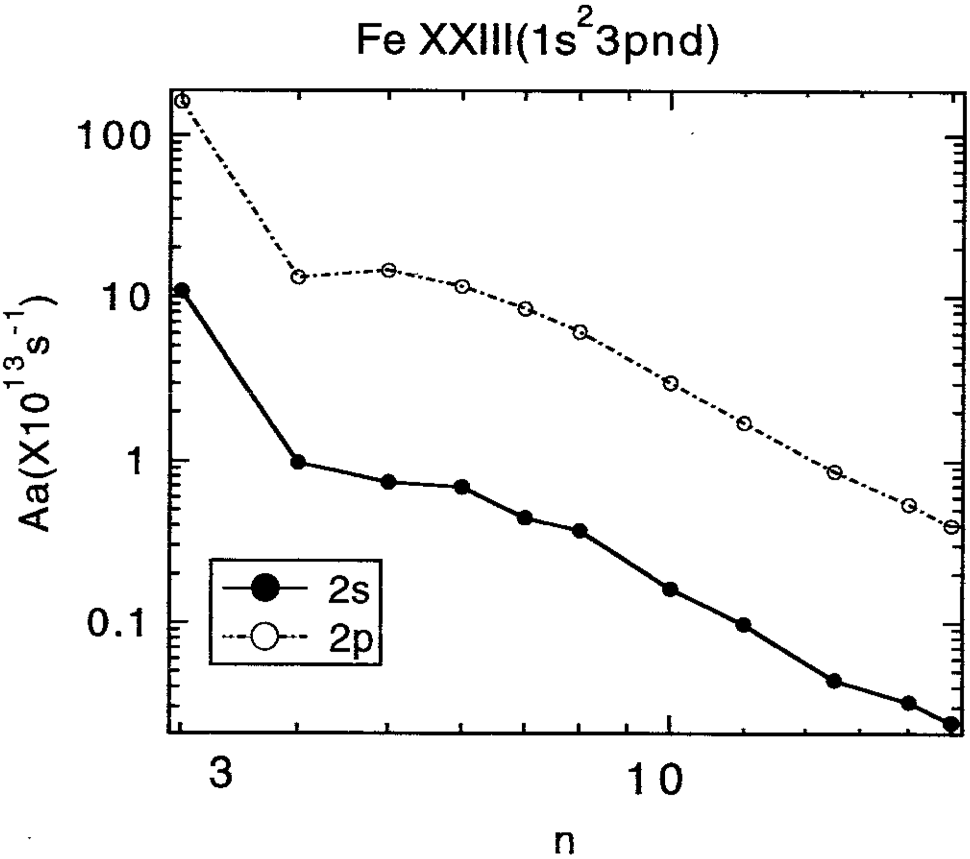

Fe XXIII(1s2 3pnd)
100
10
1
0.1
Aa(X10 13 s -1)
3
10
n
2s
2p

Fig.4(d)

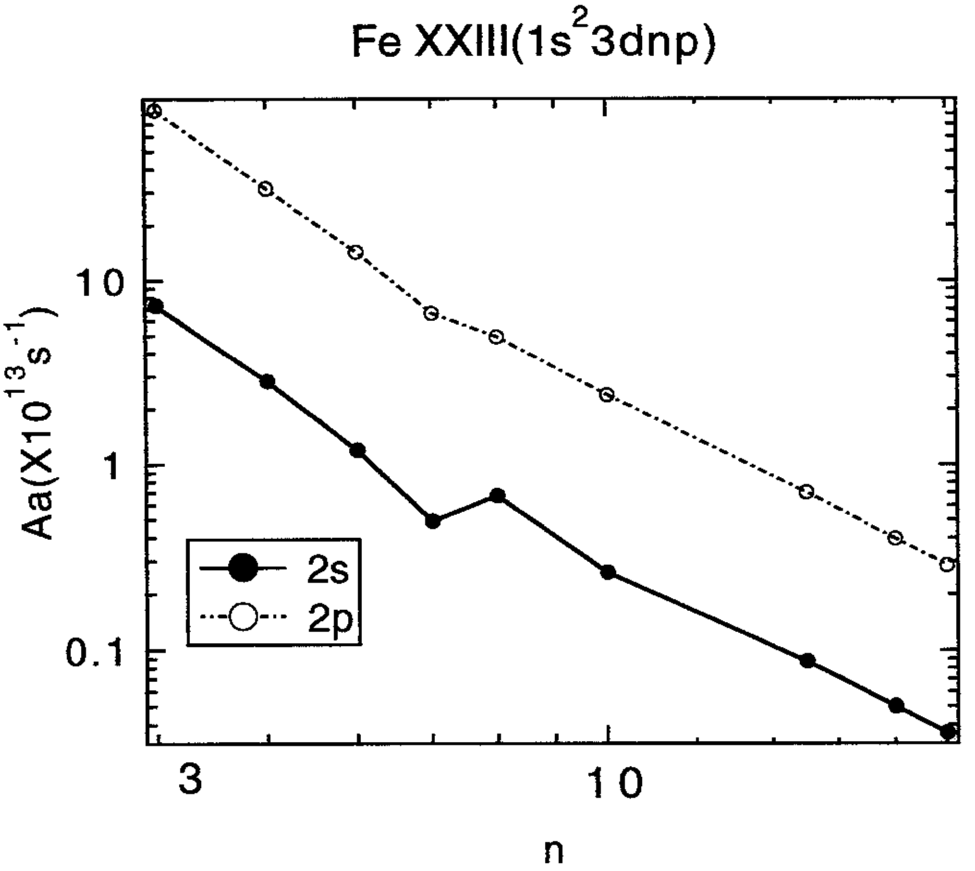
Fe XXIII(1s^{2}3dnp)
10
1
0.1
Aa(X10^{13}s^{-1})
2s
2p
3
10
n

Fig.4(e)

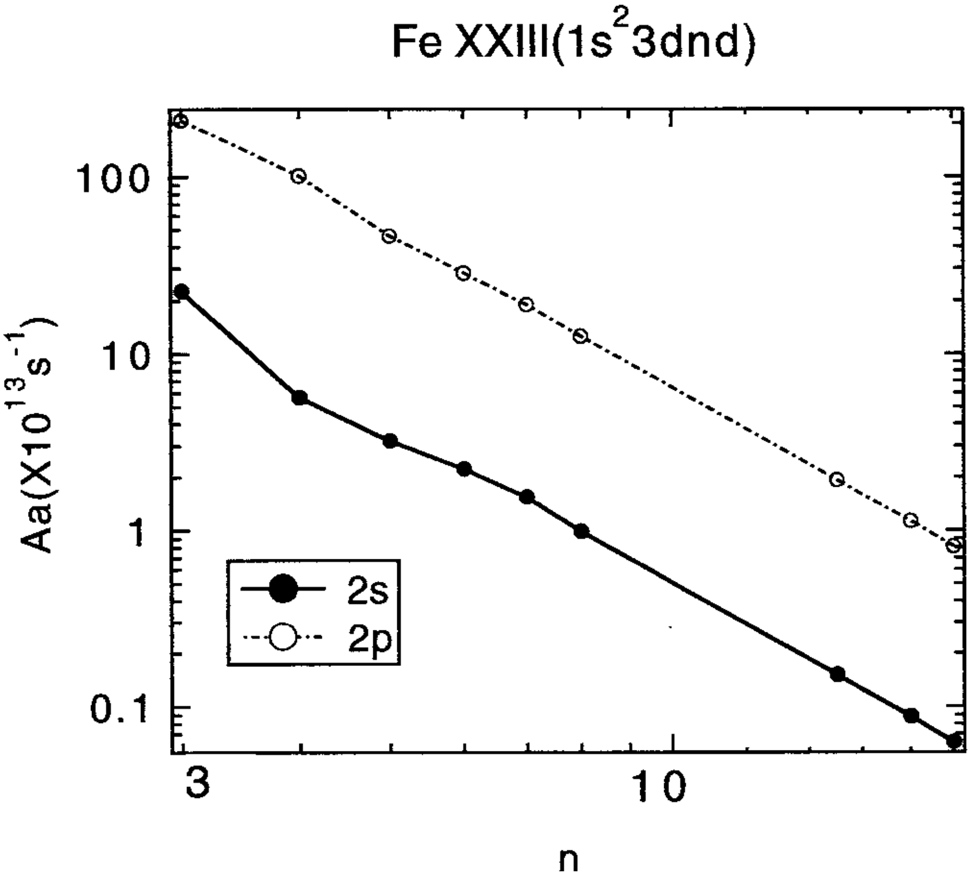
Fe XXIII(1s^{2}3dnd)
100
10
1
0.1
Aa(X10^{13}s^{-1})
2s
2p
3
10
n

Fig.4(f)

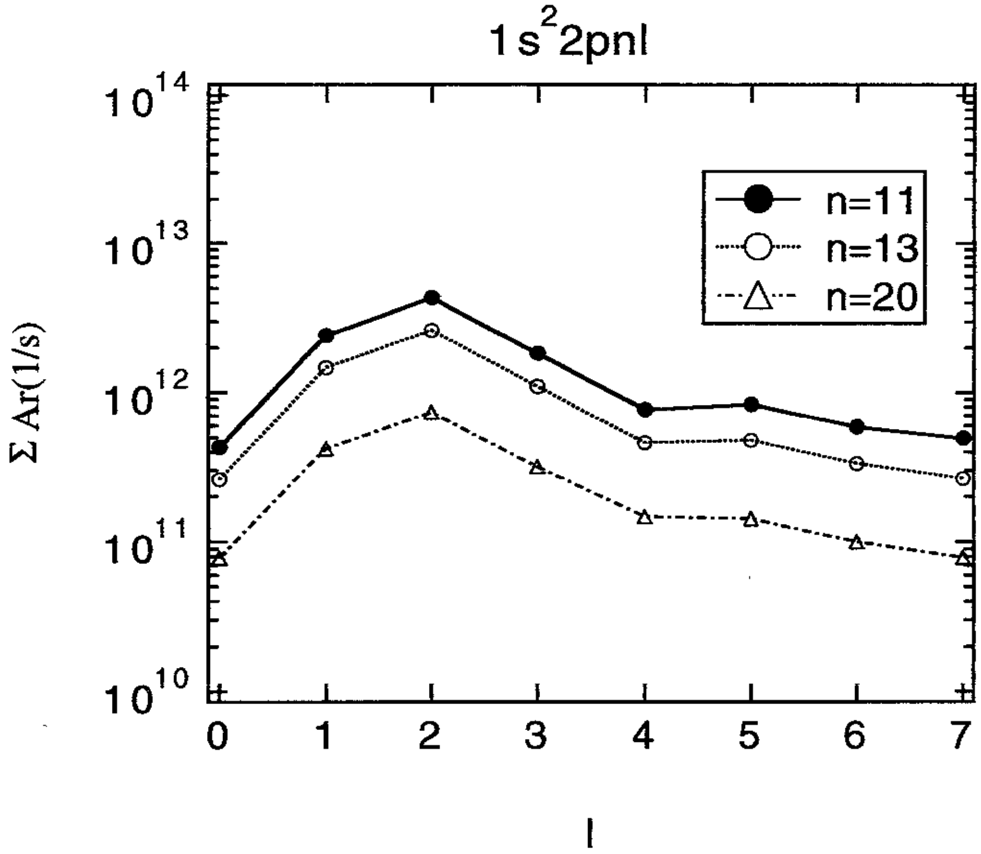
1s²2pnl
10¹⁴
10¹³
10¹²
10¹¹
10¹⁰
Σ Ar(1/s)
n=11
n=13
n=20
0
1
2
3
4
5
6
7
l

Fig.5

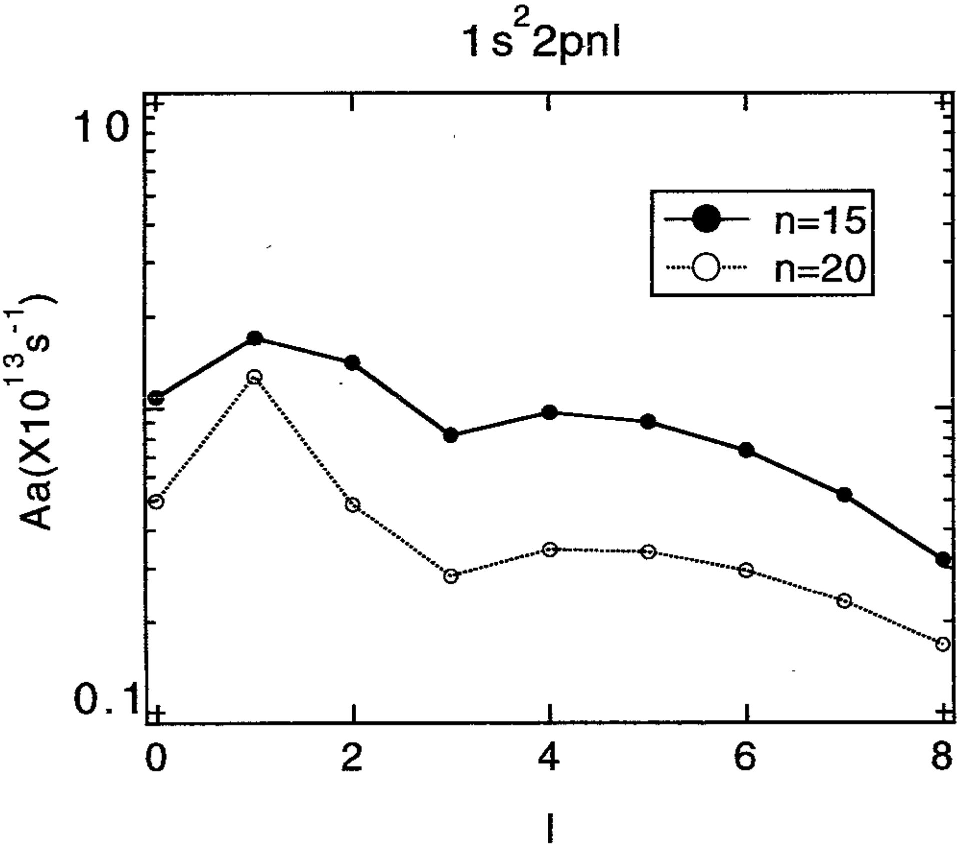
1s²2pnl
10
0.1
Aa(X10¹³s⁻¹)
n=15
n=20
0
2
4
6
8
l

Fig.6

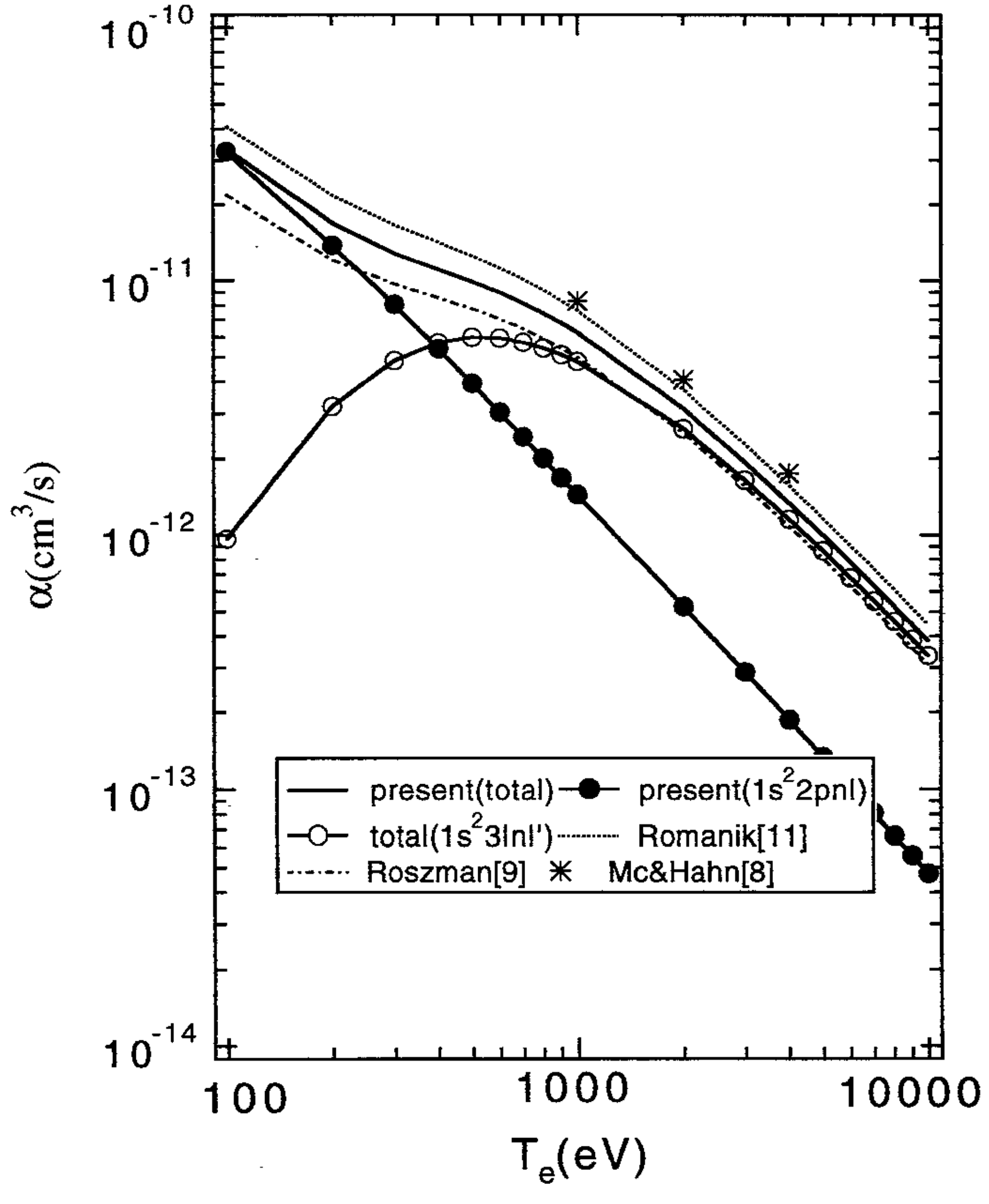

10^-10
10^-11
10^-12
10^-13
10^-14
α(cm^3/s)
100
1000
10000
T_e(eV)
present(total)
present(1s^2 2pnl)
total(1s^2 3lnl')
Romanik[11]
Roszman[9]
Mc&Hahn[8]

Fig.7

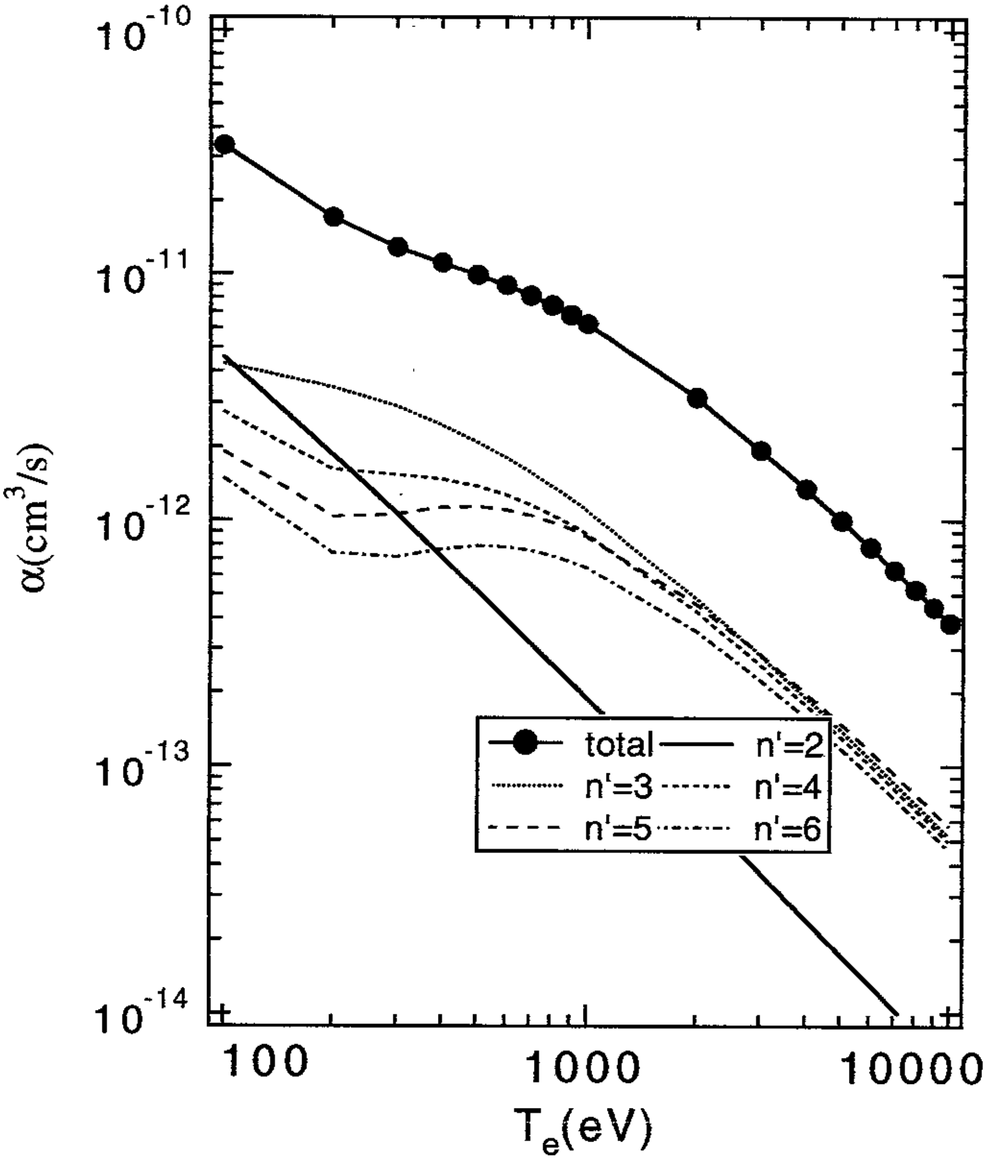

10^{-10}
10^{-11}
10^{-12}
10^{-13}
10^{-14}
$\alpha(cm^3/s)$
100
1000
10000
$T_e(eV)$
total
n'=2
n'=3
n'=4
n'=5
n'=6

Fig.8

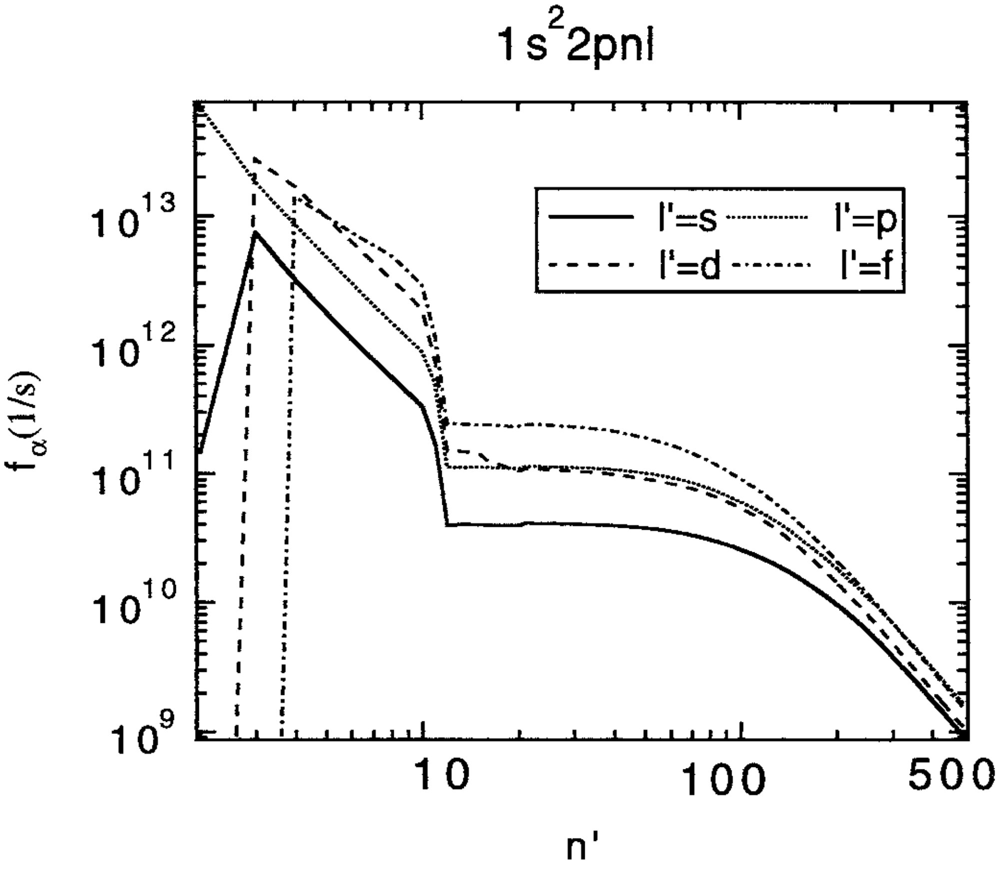
1s^{2}2pnl
l'=s
l'=p
l'=d
l'=f
f_α(1/s)
10^{13}
10^{12}
10^{11}
10^{10}
10^{9}
10
100
500
n'

Fig.9(a)

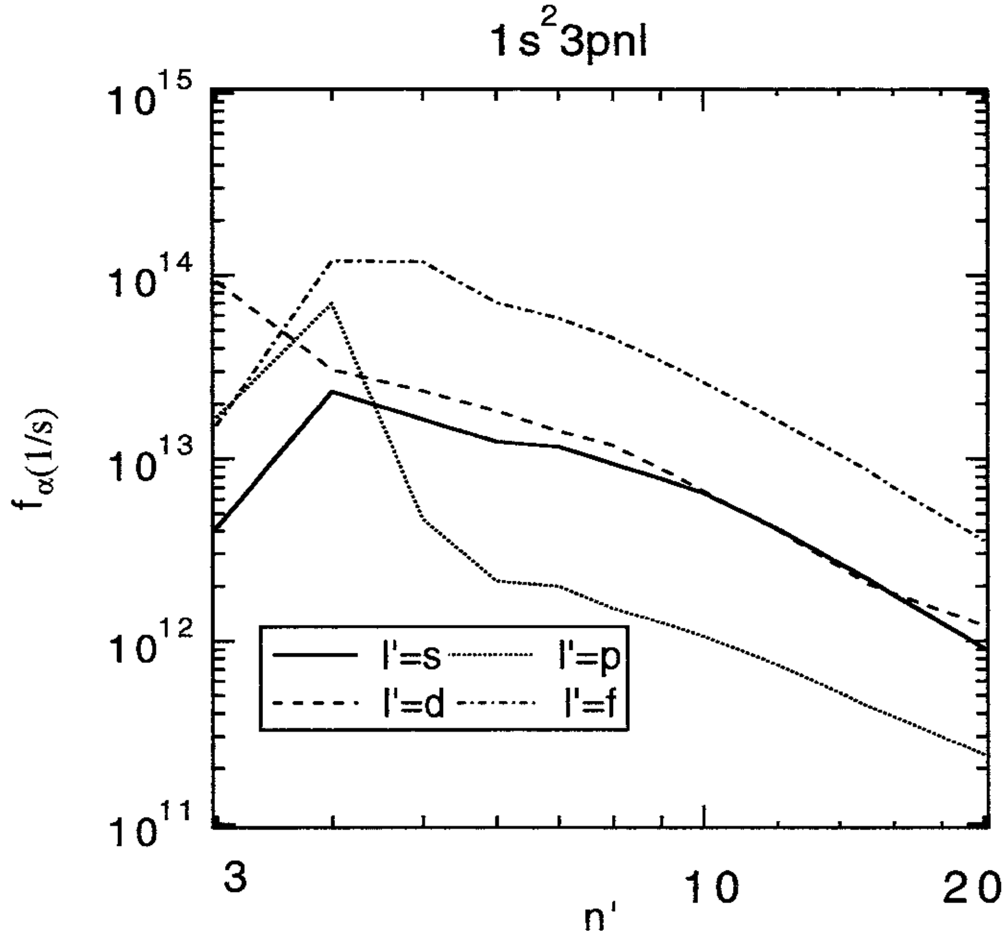
1s^{2}3pnl
10^{15}
10^{14}
10^{13}
10^{12}
10^{11}
f_α(1/s)
l'=s
l'=p
l'=d
l'=f
3
10
20
n'

Fig.9(b)

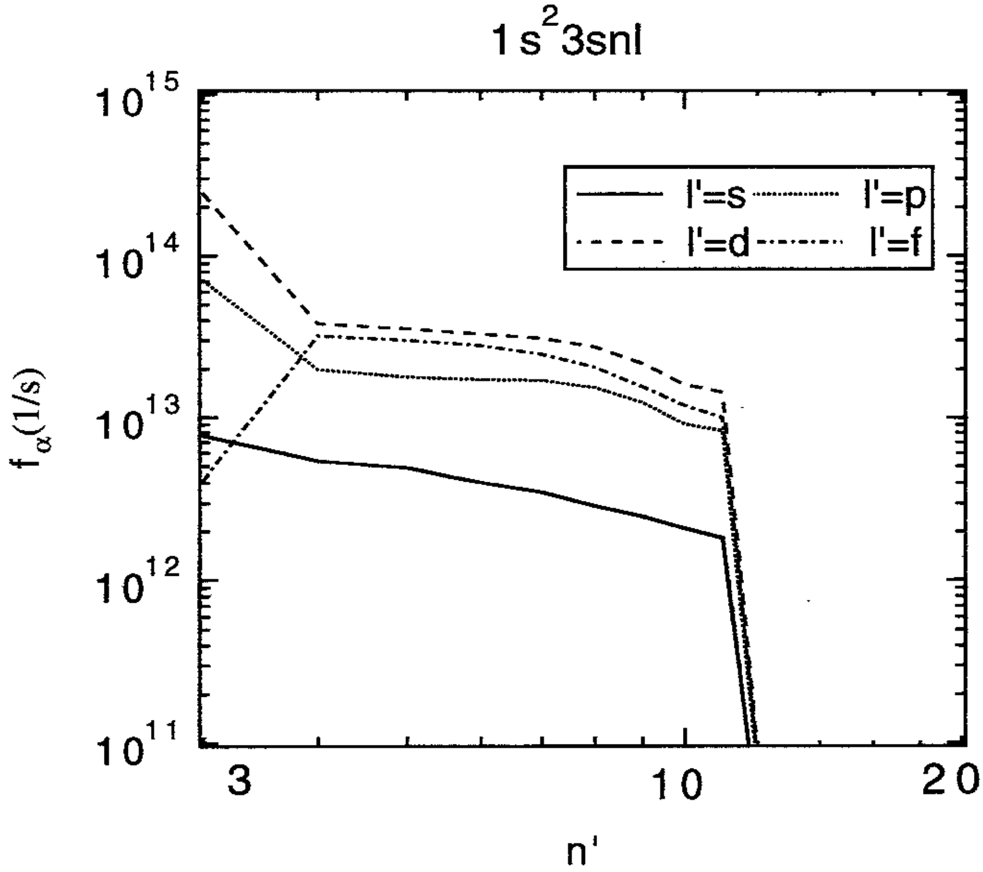

1s^{2}3snl
10^{15}
10^{14}
10^{13}
10^{12}
10^{11}
f_α(1/s)
l'=s
l'=p
l'=d
l'=f
3
10
20
n'

Fig.9(c)

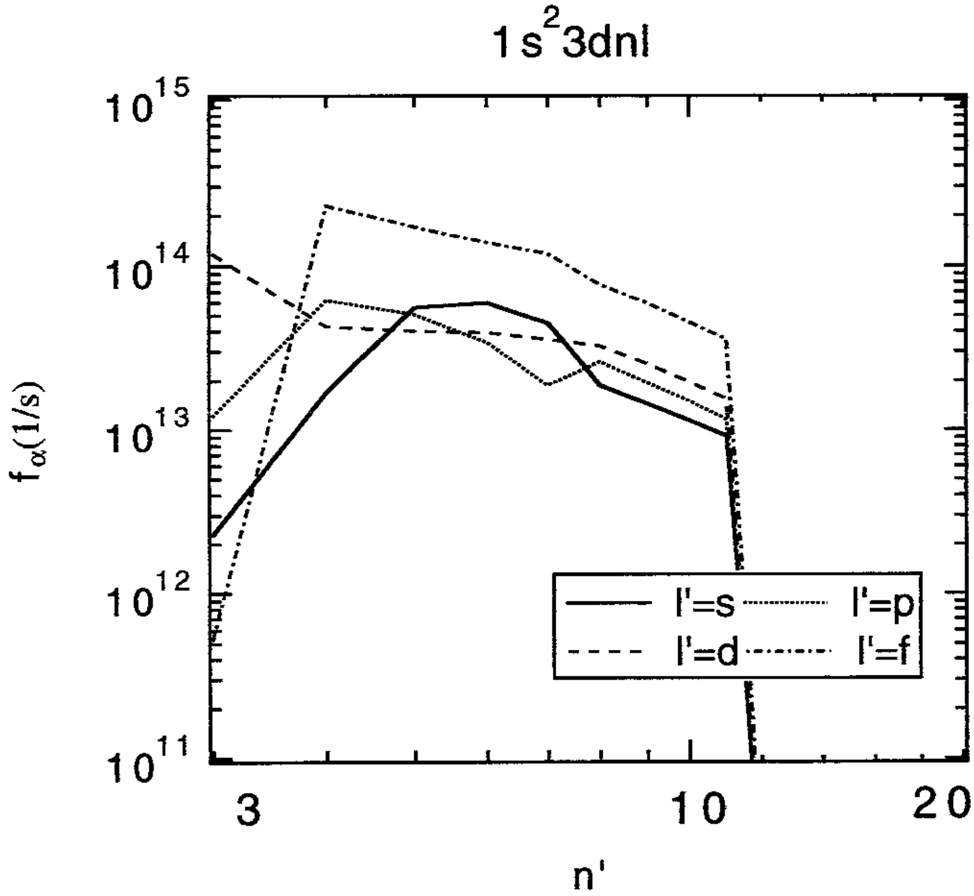

1s^{2}3dnl
10^{15}
10^{14}
10^{13}
10^{12}
10^{11}
f_α(1/s)
l'=s
l'=p
l'=d
l'=f
3
10
20
n'

Fig.9(d)

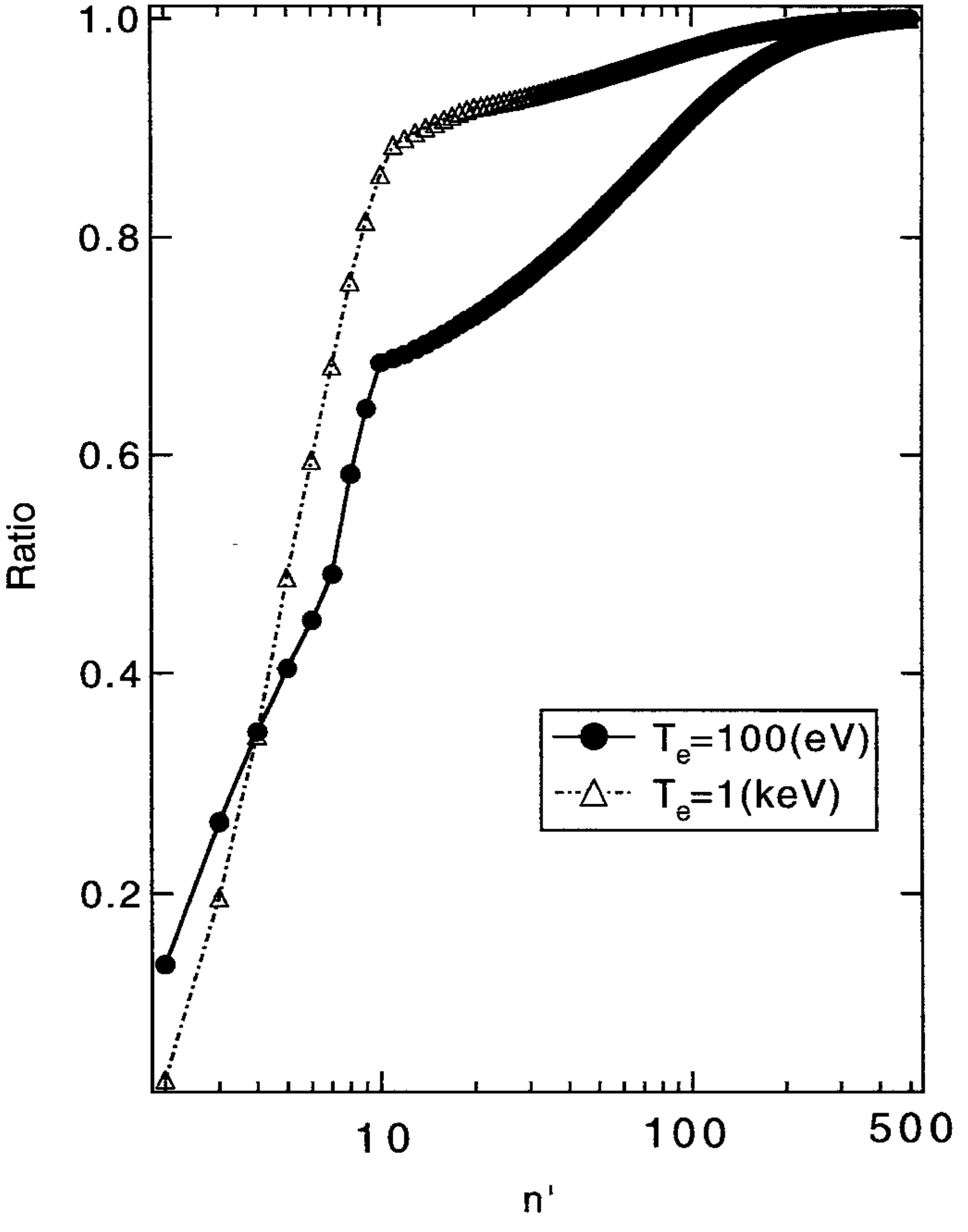

Fig.10

Publication List of NIFS-DATA Series

NIFS-DATA-1 Y. Yamamura, T. Takiguchi and H. Tawara,
Data Compilation of Angular Distributions of Sputtered Atoms;
Jan. 1990

NIFS-DATA-2 T. Kato, J. Lang and K. E. Berrington,
Intensity Ratios of Emission Lines from OV Ions for Temperature and Density Diagnostics ; Mar. 1990 [At Data and Nucl Data Tables 44(1990)133]

NIFS-DATA-3 T. Kaneko,
Partial Electronic Straggling Cross Sections of Atoms for Protons
;Mar. 1990

NIFS-DATA-4 T. Fujimoto, K. Sawada and K. Takahata,
Cross Section for Production of Excited Hydrogen Atoms Following Dissociative Excitation of Molecular Hydrogen by Electron Impact ; Mar. 1990

NIFS-DATA-5 H. Tawara,
Some Electron Detachment Data for H^- Ions in Collisions with Electrons, Ions, Atoms and Molecules –an Alternative Approach to High Energy Neutral Beam Production for Plasma Heating– ;
Apr. 1990

NIFS-DATA-6 H. Tawara, Y. Itikawa, H. Nishimura, H. Tanaka and Y. Nakamura,
Collision Data Involving Hydro-Carbon Molecules ; July 1990
[Supplement to Nucl. Fusion 2(1992)25]

NIFS-DATA-7 H.Tawara,
Bibliography on Electron Transfer Processes in Ion-Ion/Atom/Molecule Collisions –Updated 1990–; Aug. 1990

NIFS-DATA-8 U.I.Safronova, T.Kato, K.Masai, L.A.Vainshtein and A.S.Shlyapzeva,
Excitation Collision Strengths, Cross Sections and Rate Coefficients for OV, SiXI, FeXXIII, MoXXXIX by Electron Impact ($1s^22s^2$-$1s^22s2p$-$1s^22p^2$ Transitions) Dec.1990

NIFS-DATA-9 T.Kaneko,
Partial and Total Electronic Stopping Cross Sections of Atoms and Solids for Protons; Dec. 1990

NIFS-DATA-10 K.Shima, N.Kuno, M.Yamanouchi and H.Tawara,
Equilibrium Charge Fraction of Ions of Z=4-92 (0.02-6 MeV/u) and Z=4-20 (Up to 40 MeV/u) Emerging from a Carbon Foil; Jan.1991
[AT.Data and Nucl. Data Tables 51(1992)173]

NIFS-DATA-11 T. Kaneko, T. Nishihara, T. Taguchi, K. Nakagawa, M. Murakami, M. Hosono, S. Matsushita, K. Hayase, M.Moriya, Y.Matsukuma, K.Miura and Hiro Tawara,
Partial and Total Electronic StoppingCross Sections of Atoms for a Singly Charged Helium Ion: Part I;Mar. 1991

NIFS-DATA-12 Hiro Tawara,
Total and Partial Cross Sections of Electron Transfer Processes for Be^{q+} *and* B^{q+} *Ions in Collisions with H,* H_2 *and He Gas Targets - Status in 1991-;* June 1991

NIFS-DATA-13 T. Kaneko, M. Nishikori, N. Yamato, T. Fukushima, T. Fujikawa, S. Fujita, K. Miki, Y. Mitsunobu, K. Yasuhara, H. Yoshida and Hiro Tawara,
Partial and Total Electronic Stopping Cross Sections of Atoms for a Singly Charged Helium Ion : Part II; Aug. 1991

NIFS-DATA-14 T. Kato, K. Masai and M. Arnaud,
Comparison of Ionization Rate Coefficients of Ions from Hydrogen through Nickel ; Sep. 1991

NIFS-DATA-15 T. Kato, Y. Itikawa and K. Sakimoto,
Compilation of Excitation Cross Sections for He Atoms by Electron Impact; Mar. 1992

NIFS-DATA-16 T. Fujimoto, F. Koike, K. Sakimoto, R. Okasaka, K. Kawasaki, K. Takiyama, T. Oda and T. Kato,
Atomic Processes Relevant to Polarization Plasma Spectroscopy ; Apr. 1992

NIFS-DATA-17 H. Tawara,
Electron Stripping Cross Sections for Light Impurity Ions in Colliding with Atomic Hydrogens Relevant to Fusion Research; Apr. 1992

NIFS-DATA-18 T. Kato,
Electron Impact Excitation Cross Sections and Effective Collision Strengths of N Atom and N-Like Ions -A Review of Available Data and Recommendations- ; Sep. 1992

NIFS-DATA-19 Hiro Tawara,
Atomic and Molecular Data for H_2O, *CO &* CO_2 *Relevant to Edge Plasma Impurities*, Oct. 1992

NIFS-DATA-20 Hiro. Tawara,
Bibliography on Electron Transfer Processes in Ion-Ion/Atom/Molecule Collisions -Updated 1993-; Apr. 1993

NIFS-DATA-21 J. Dubau and T. Kato, *Dielectronic Recombination Rate Coefficients to the Excited States of C I from C II;* Aug. 1994

NIFS-DATA-22 T. Kawamura, T. Ono, Y. Yamamura, *Simulation Calculations of Physical Sputtering and Reflection Coefficient of Plasma-Irradiated Carbon Surface;* Aug. 1994

NIFS-DATA-23 Y. Yamamura and H. Tawara, *Energy Dependence of Ion-Induced Sputtering Yields from Monoatomic Solids at Normal Incidence;* Mar. 1995

NIFS-DATA-24 T. Kato, U. Safronova, A. Shlyaptseva, M. Cornille, J. Dubau, *Comparison of the Satellite Lines of H-like and He-like Spectra;* Apr. 1995

NIFS-DATA-25 H. Tawara, *Roles of Atomic and Molecular Processes in Fusion Plasma Researches - from the cradle (plasma production) to the grave (after-burning) -;* May 1995

NIFS-DATA-26 N. Toshima and H. Tawara *Excitation, Ionization, and Electron Capture Cross Sections of Atomic Hydrogen in Collisions with Multiply Charged Ions;* July 1995

NIFS-DATA-27 V.P. Shevelko, H. Tawara and E.Salzborn, *Multiple-Ionization Cross Sections of Atoms and Positive Ions by Electron Impact;* July 1995

NIFS-DATA-28 V.P. Shevelko and H. Tawara, *Cross Sections for Electron-Impact Induced Transitions Between Excited States in He: n, n'=2,3 and 4;* Aug. 1995

NIFS-DATA-29 U.I. Safronova, M.S. Safronova and T. Kato, *Cross Sections and Rate Coefficients for Excitation of* $\Delta n = 1$ *Transitions in Li-like Ions with* $6<Z<42$*;* Sep. 1995

NIFS-DATA-30 T. Nishikawa, T. Kawachi, K. Nishihara and T. Fujimoto, *Recommended Atomic Data for Collisional-Radiative Model of Li-like Ions and Gain Calculation for Li-like Al Ions in the Recombining Plasma;* Sep. 1995

NIFS-DATA-31 Y. Yamamura, K. Sakaoka and H. Tawara, *Computer Simulation and Data Compilation of Sputtering Yield by Hydrogen Isotopes (*$^{1}H^{+}$, $^{2}D^{+}$, $^{3}T^{+}$*) and Helium (*$^{4}He^{+}$*) Ion Impact from Monatomic Solids at Normal Incidence;* Oct. 1995

NIFS-DATA-32 T. Kato, U. Safronova and M. Ohira,
Dielectronic Recombination Rate Coefficients to the Excited States of CII from CIII; Feb. 1996

NIFS-DATA-33 K.J. Snowdon and H. Tawara,
Low Energy Molecule-Surface Interaction Processes of Relevance to Next-Generation Fusion Devices; Mar. 1996

NIFS-DATA-34 T. Ono, T. Kawamura, K. Ishii and Y. Yamamura,
Sputtering Yield Formula for B_4C Irradiated with Monoenergetic Ions at Normal Incidence; Apr. 1996

NIFS-DATA-35 I. Murakami, T. Kato and J. Dubau,
UV and X-Ray Spectral Lines of Be-Like Fe Ion for Plasma Diagnostics; Apr. 1996

NIFS-DATA-36 K. Moribayashi and T. Kato,
Dielectronic Recombination of Be-like Fe Ion; Apr. 1996